



Recent Developments on Beam Dynamics and Wake Field Simulations at TEMF

Wolfgang Ackermann and Erion Gjonaj

Institut für Theorie Elektromagnetischer Felder (TEMF)

Technische Universität Darmstadt

Joint DESY and University of Hamburg Accelerator Physics Seminar

December 18, 2007, DESY, Hamburg

Technische Universität Darmstadt, Fachbereich Elektrotechnik und Informationstechnik
Schlossgartenstraße 8, 64289 Darmstadt, Germany - URL: www.TEMF.de



- **Wakefield Computations**
 - PBCI
 - Wakefield Simulations at TEMF
- **Self-Consistent PIC Simulations**
 - Higher Order Finite Elements
 - Current Work
- **V-Code**
 - Basic principle based on the moment approach
 - Implementation using symbolic algebra transformation



Motivation for improved wakefield codes

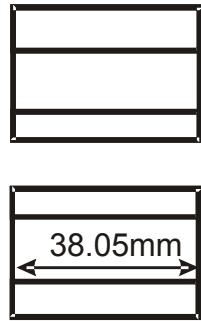
1. A new generation of LINACs with ultra-short electron bunches
 - *bunch size for ILC: 300 μm*
 - *bunch size for LCLS: 20 μm*
2. Geometry of tapers, collimators... far from rotational
 - *8 rectangular collimators at ILC-ESA in the design process*
 - *30 rectangular-to-round transitions in the undulator of LCLS*
3. Many (semi-) analytical approximations become invalid
 - *based on rotationally symmetric geometry*
 - *low frequency assumptions (Yokoya, Stupakov)*



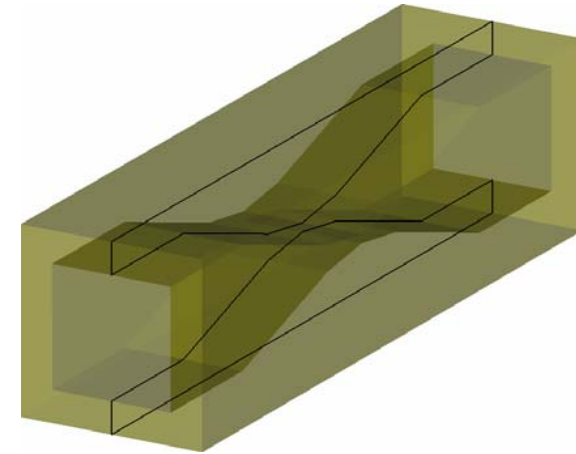
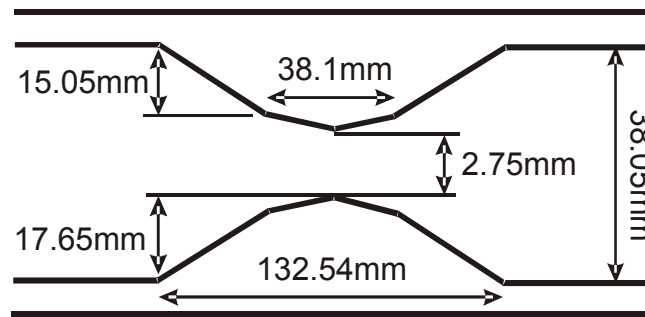
Wakefield Computations



beam view

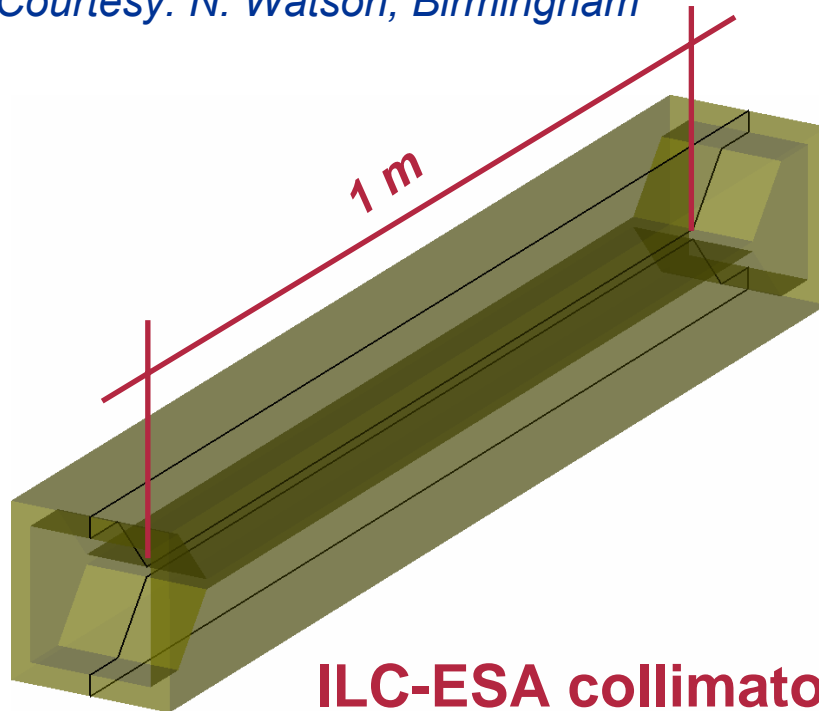


side view



ILC-ESA collimator #8

Courtesy: N. Watson, Birmingham

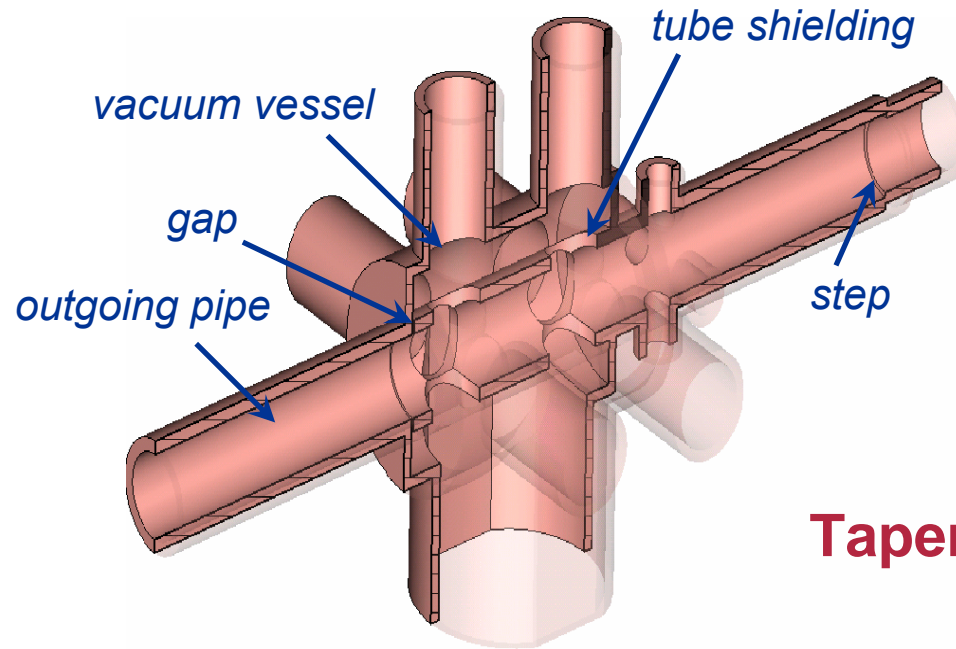


ILC-ESA collimator #3

<i>bunch length</i>	<i>300μm</i>
<i>collimator length</i>	<i>~1.2m</i>
<i>catch-up distance</i>	<i>~2.4m</i>



Wakefield Computations

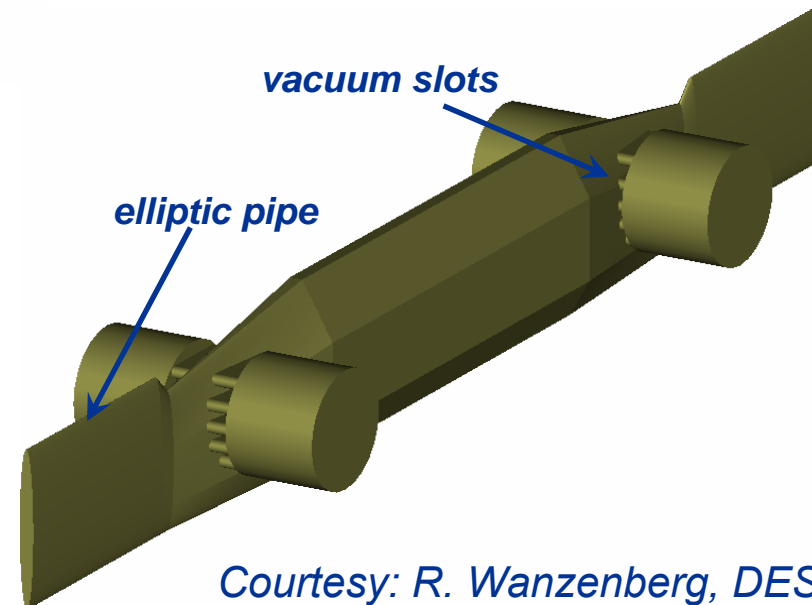
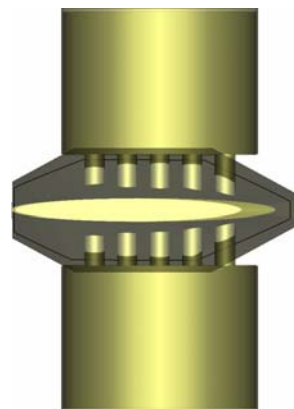


PITZ diagnostics double cross

<i>bunch length</i>	2.5mm
<i>bunch width</i>	2.5mm
<i>structure length</i>	325mm

Tapered transition @PETRA III

<i>bunch length</i>	1cm
<i>taper length</i>	50cm



Courtesy: R. Wanzenberg, DESY



There is an actual demand for:

1. Wake field simulations in arbitrary 3D-geometry
3D-codes
2. Utilizing large computational resources
parallelized codes
3. Specialized algorithms for long accelerator structures
moving window – dispersion free codes



An (incomplete) survey of available codes

	<i>Dimensions</i>	<i>Nondispersive</i>	<i>Parallelized</i>	<i>Moving window</i>	
1980	BCI / TBCI	2.5D	No	No	Yes
20 years	NOVO	2.5D	Yes	No	No
	ABCI	2.5D	No	No	Yes
	MAFIA	2.5/3D	No	No	Yes
2002	GdfidL	3D	No	Yes	No
	Tau3P	3D	No	Yes	No
5 years	ECHO	2.5/3D	Yes	No	Yes
	CST	3D	No	No	No
	PBCI	3D	Yes	Yes	Yes
2007	NEKCEM	3D	No	Yes	No

1980

20 years

2002

5 years

2007

Time

Based on the FIT discretization

$$\oint_{\partial A} \vec{E} \cdot d\vec{s} = -\frac{\partial}{\partial t} \iint_A \mu \vec{H} \cdot d\vec{A}$$

$$\oint_{\partial A} \vec{H} \cdot d\vec{s} = \iint_A \left(\frac{\partial}{\partial t} \varepsilon \vec{E} + \vec{J} \right) \cdot d\vec{A}$$

$$\iiint_{\partial V} \mu \vec{H} \cdot d\vec{A} = 0$$

$$\iiint_{\partial V} \varepsilon \vec{E} \cdot d\vec{A} = \iiint_V \rho dV$$



$$\mathbf{C} \hat{\mathbf{e}} = -\frac{d}{dt} \mathbf{M}_\mu \hat{\mathbf{h}}$$

$$\mathbf{C} \hat{\mathbf{h}} = \frac{d}{dt} \mathbf{M}_\varepsilon \hat{\mathbf{e}} + \hat{\mathbf{j}}$$

$$\tilde{\mathbf{S}} \mathbf{M}_\varepsilon \hat{\mathbf{e}} = \mathbf{q}$$

$$\mathbf{S} \mathbf{M}_\mu \hat{\mathbf{h}} = 0$$

A moving window algorithm is not directly applicable:

- *Stability limit $\Delta t < \Delta x / c$*
- *Longitudinal dynamics has numerical dispersion*

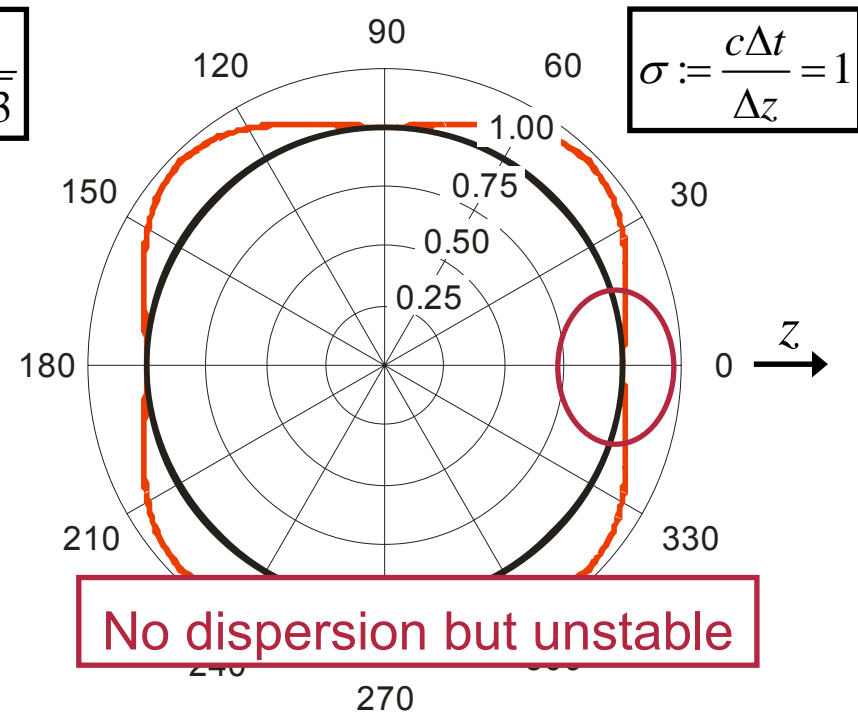
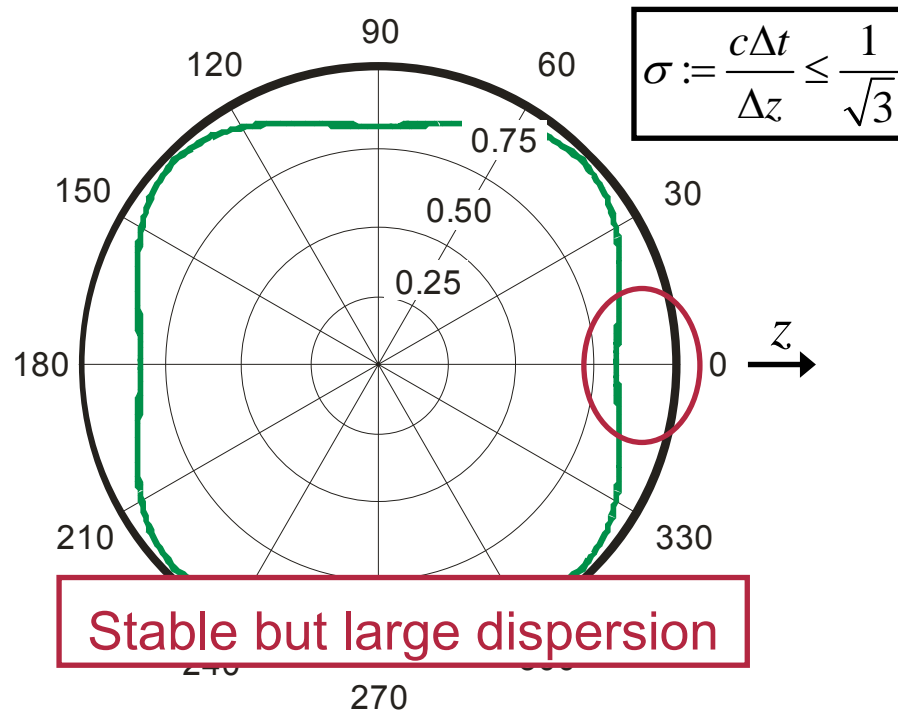
Important works of I. Zagorodnov on TE/TM splitting for the ECHO code



Using the conventional leapfrog time integration

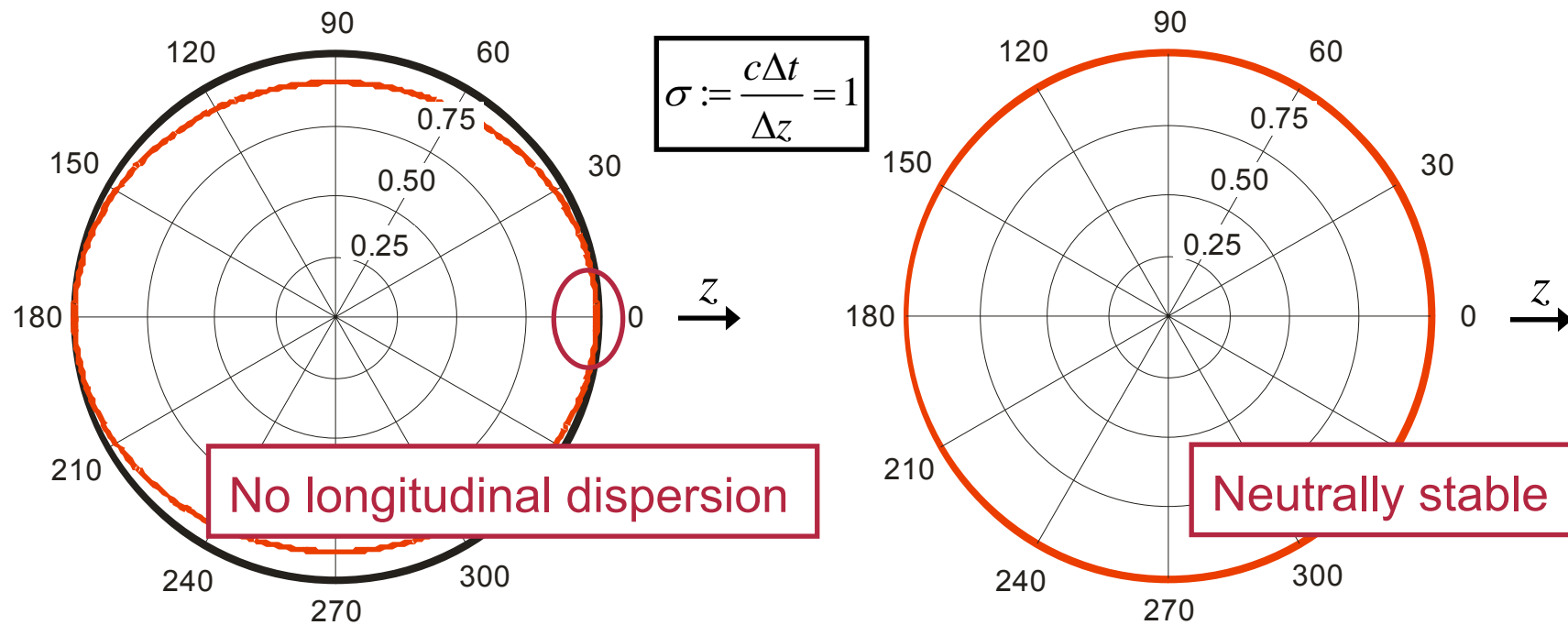
$$\begin{pmatrix} \widehat{\mathbf{e}}^{n+1/2} \\ \widehat{\mathbf{h}}^{n+1} \end{pmatrix} = \begin{pmatrix} \mathbf{1} & \Delta t \mathbf{M}_\varepsilon^{-1} \mathbf{C}^T \\ -\Delta t \mathbf{M}_\mu^{-1} \mathbf{C} & \mathbf{1} - \Delta t^2 \mathbf{M}_\mu^{-1} \mathbf{C} \mathbf{M}_\varepsilon^{-1} \mathbf{C}^T \end{pmatrix} \begin{pmatrix} \widehat{\mathbf{e}}^{n-1/2} \\ \widehat{\mathbf{h}}^n \end{pmatrix} - \begin{pmatrix} \Delta t \mathbf{M}_\varepsilon^{-1} \widehat{\mathbf{j}}^n \\ \mathbf{0} \end{pmatrix}$$

Behavior of numerical phase velocity vs. propagation angle



Using a split-operator method (LT)

Behavior of numerical phase velocity vs. propagation angle

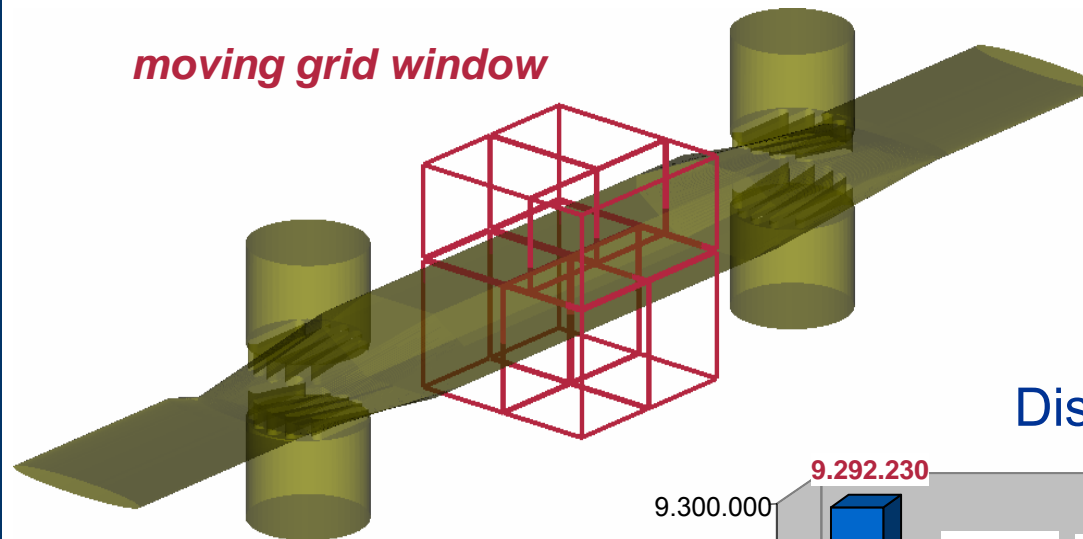


Note: The elimination of longitudinal dispersion does not necessarily improve accuracy. “Splitting error” may become important.

Non-split algorithms are currently under investigation.



Example: Tapered transition for PETRA III

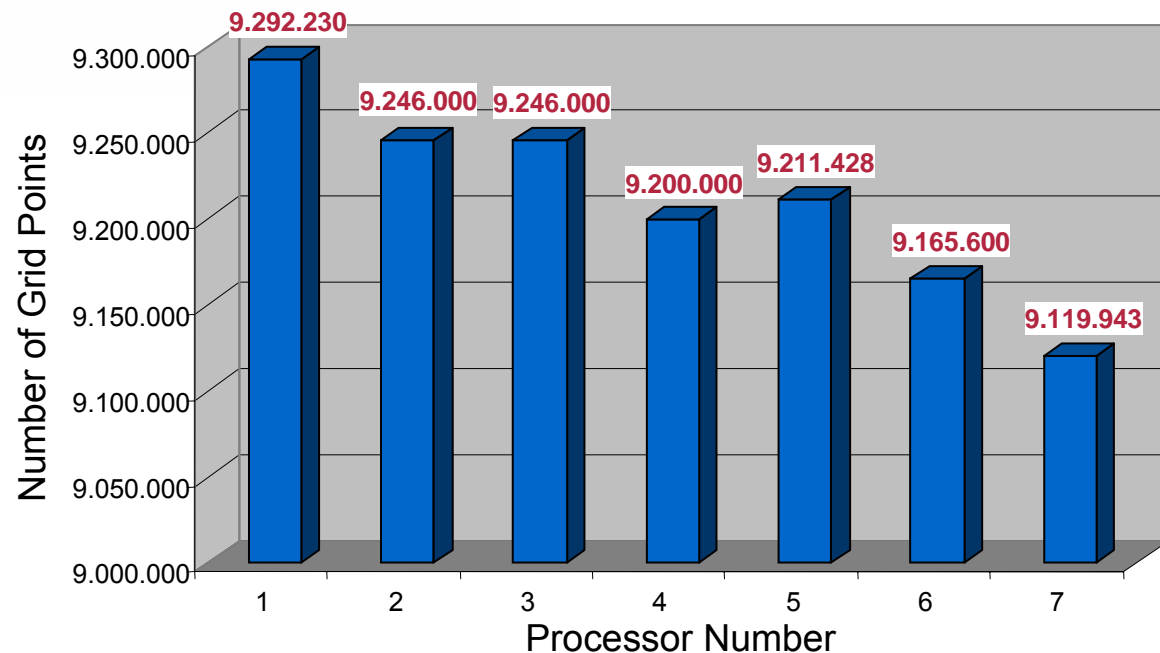


moving grid window

Domain partitioning pattern
for 7 processors

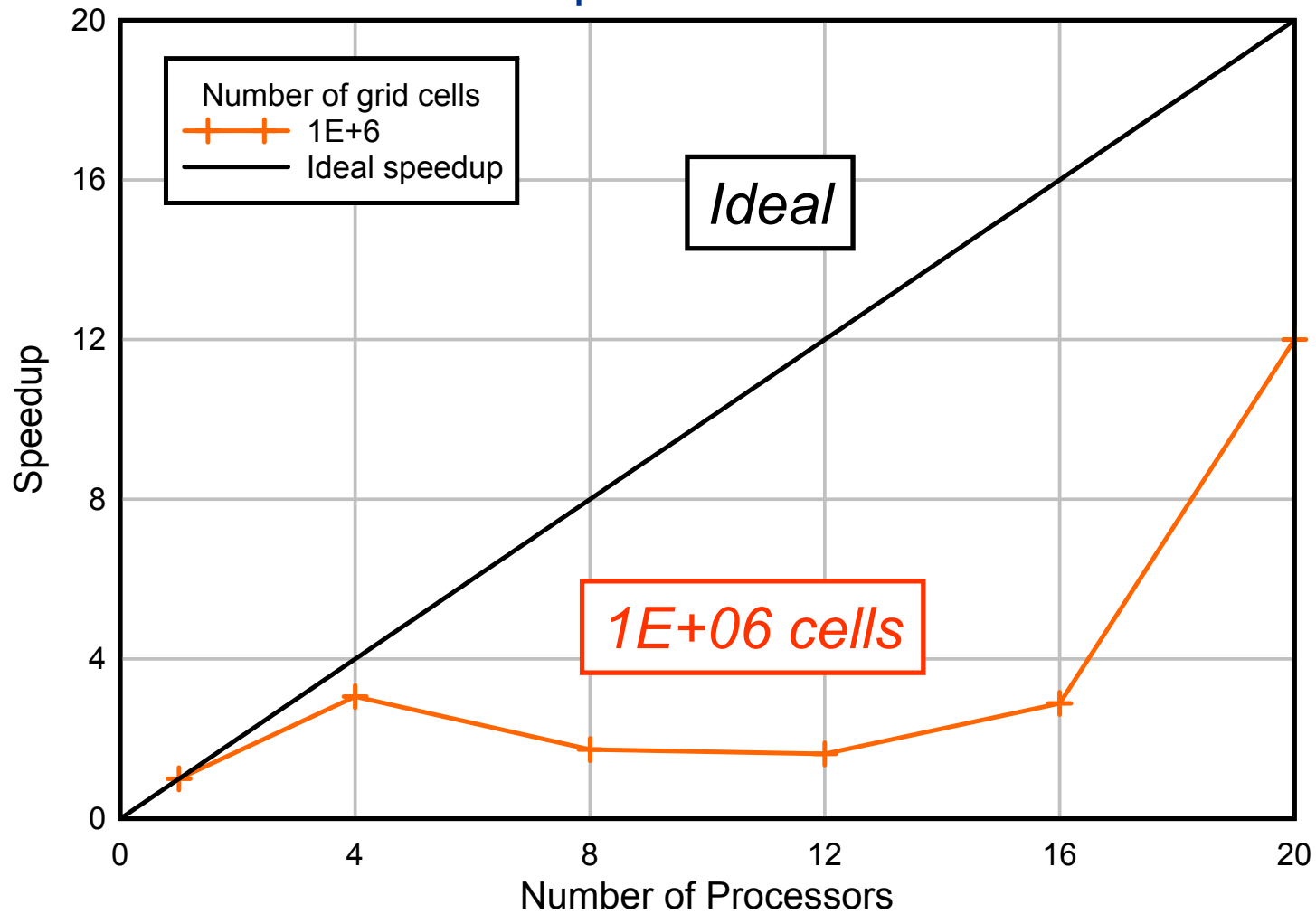
Distribution of grid points

	Grid points
Total	64.481.201
Min	9.119.943
Max	9.292.230
Dev.	< 1.0%



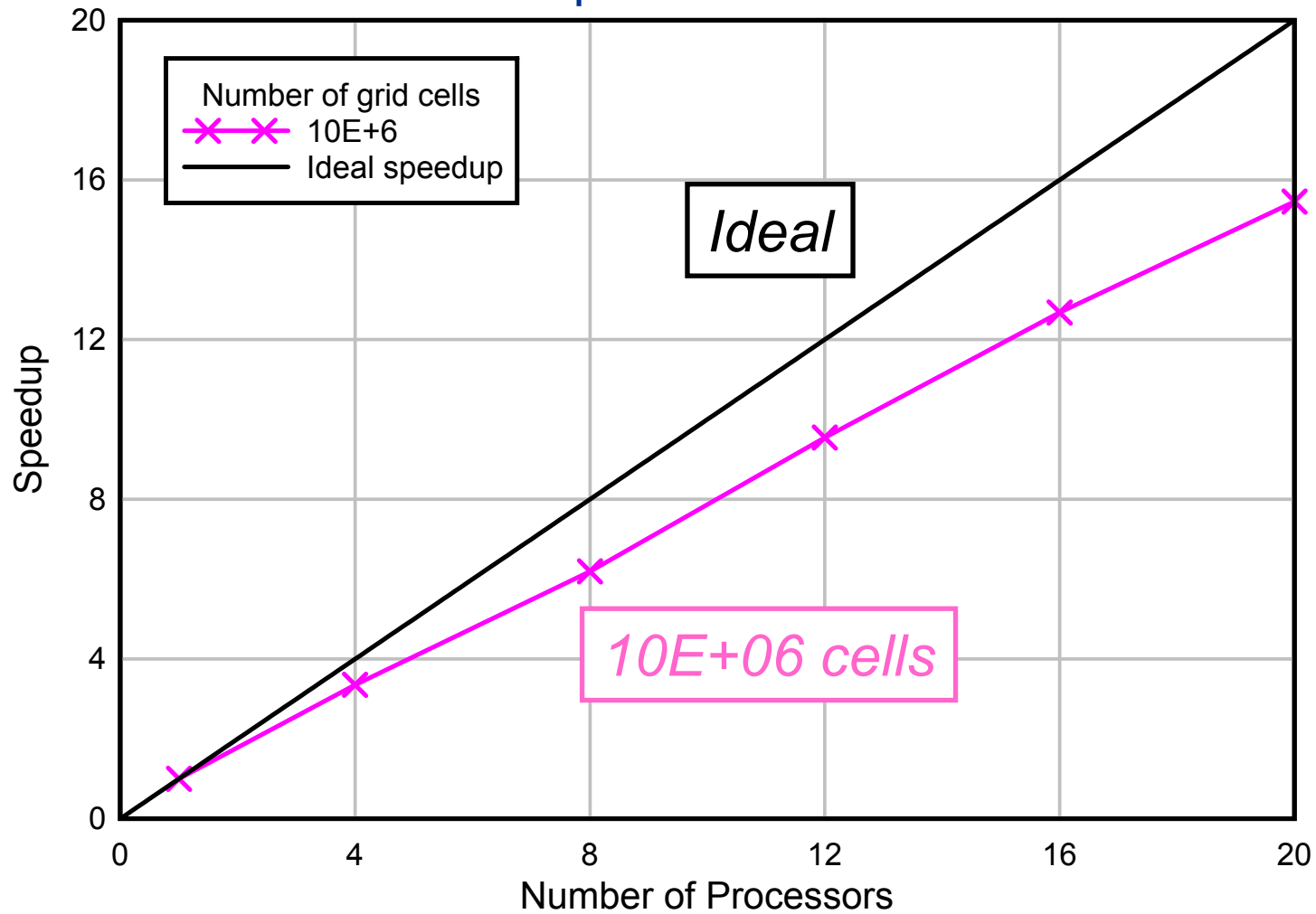


Parallel performance tests



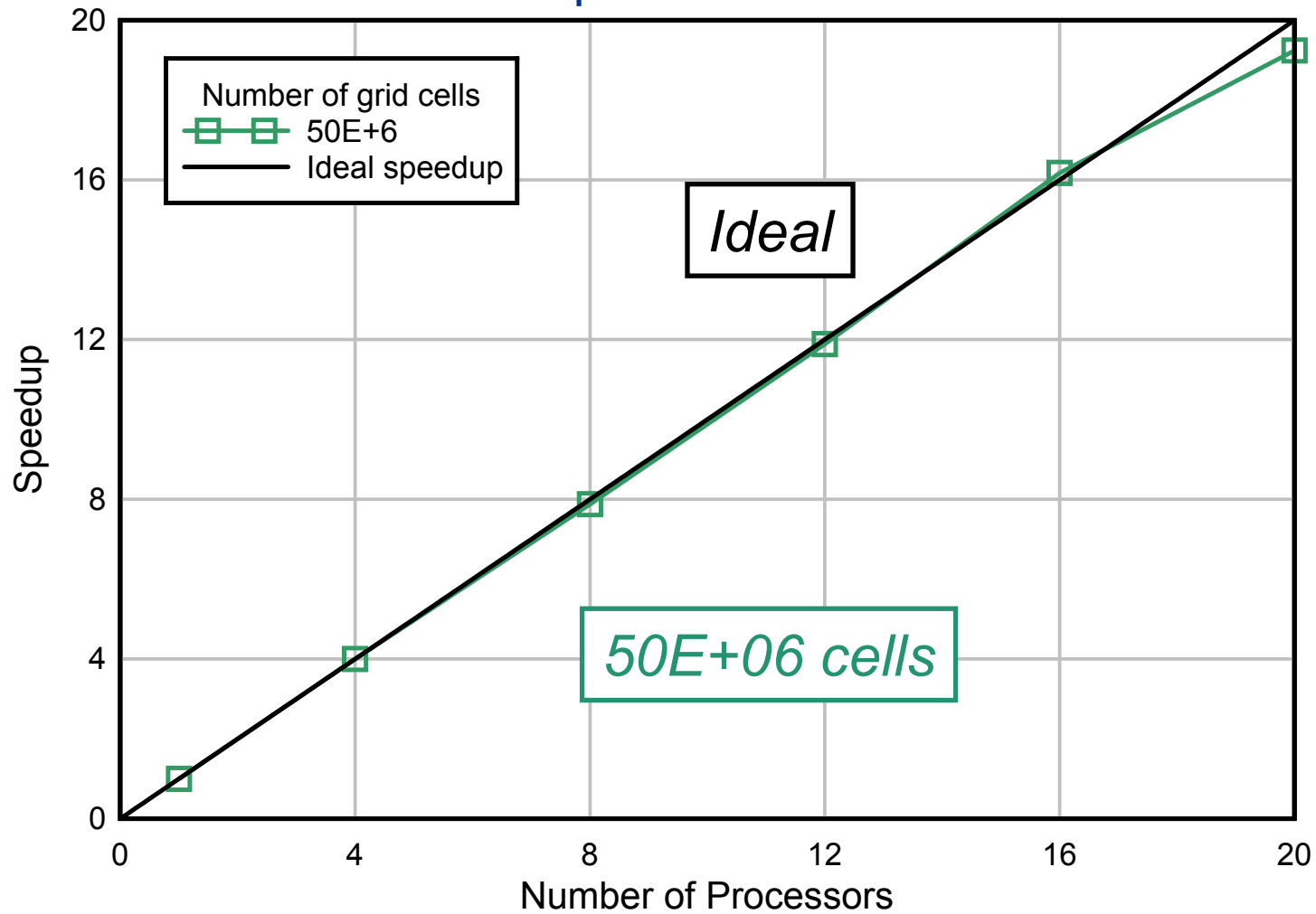


Parallel performance tests



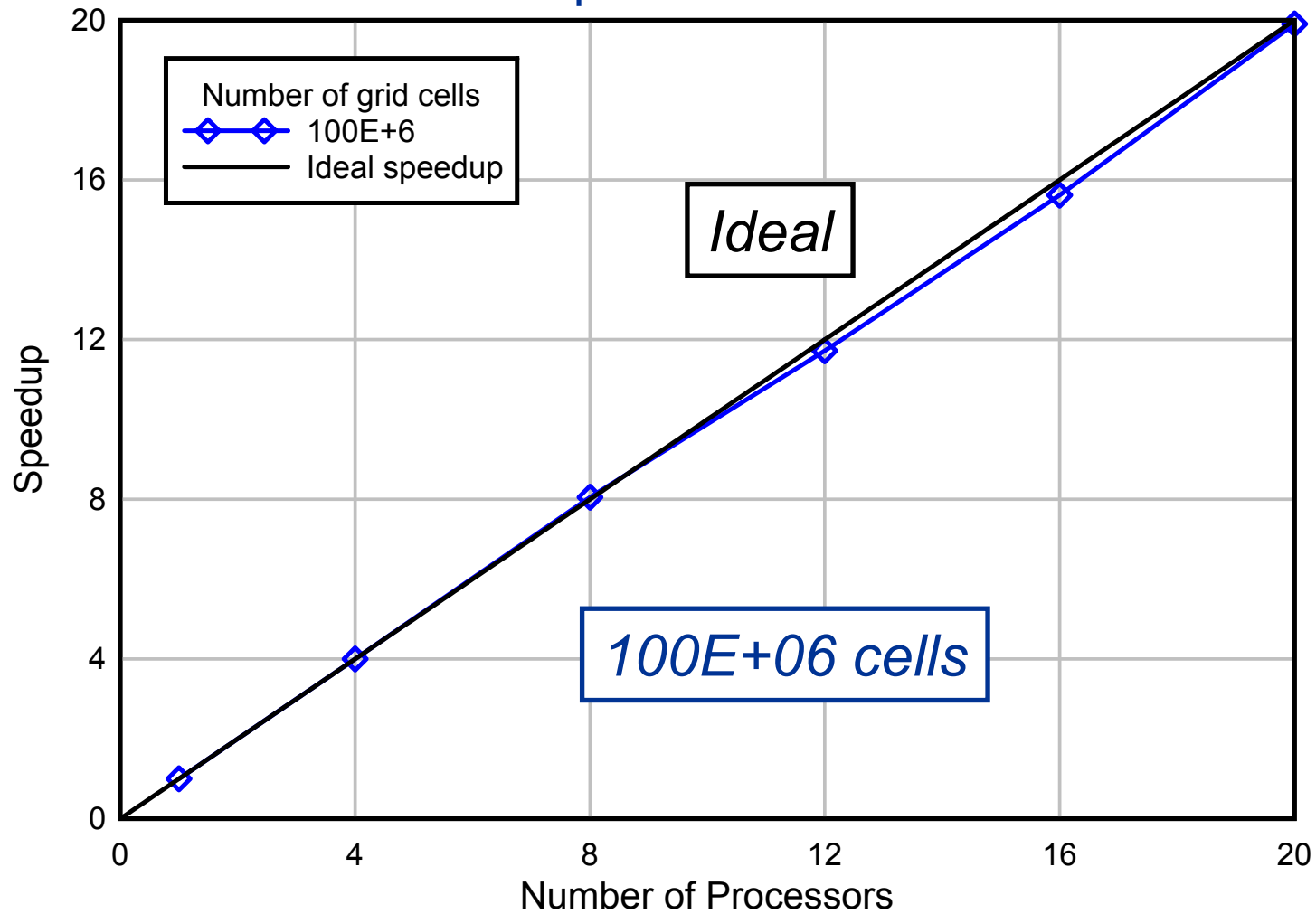


Parallel performance tests



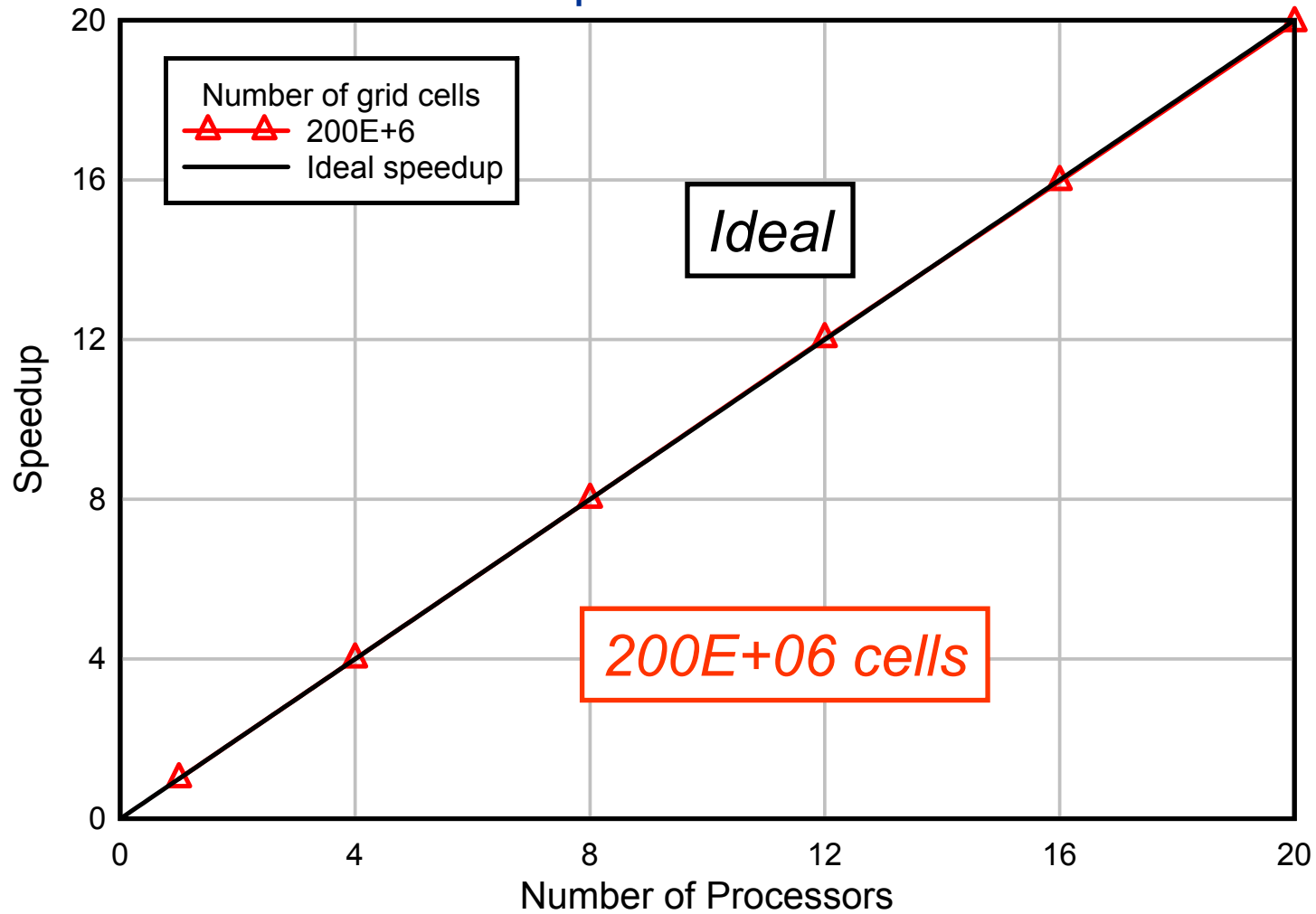


Parallel performance tests



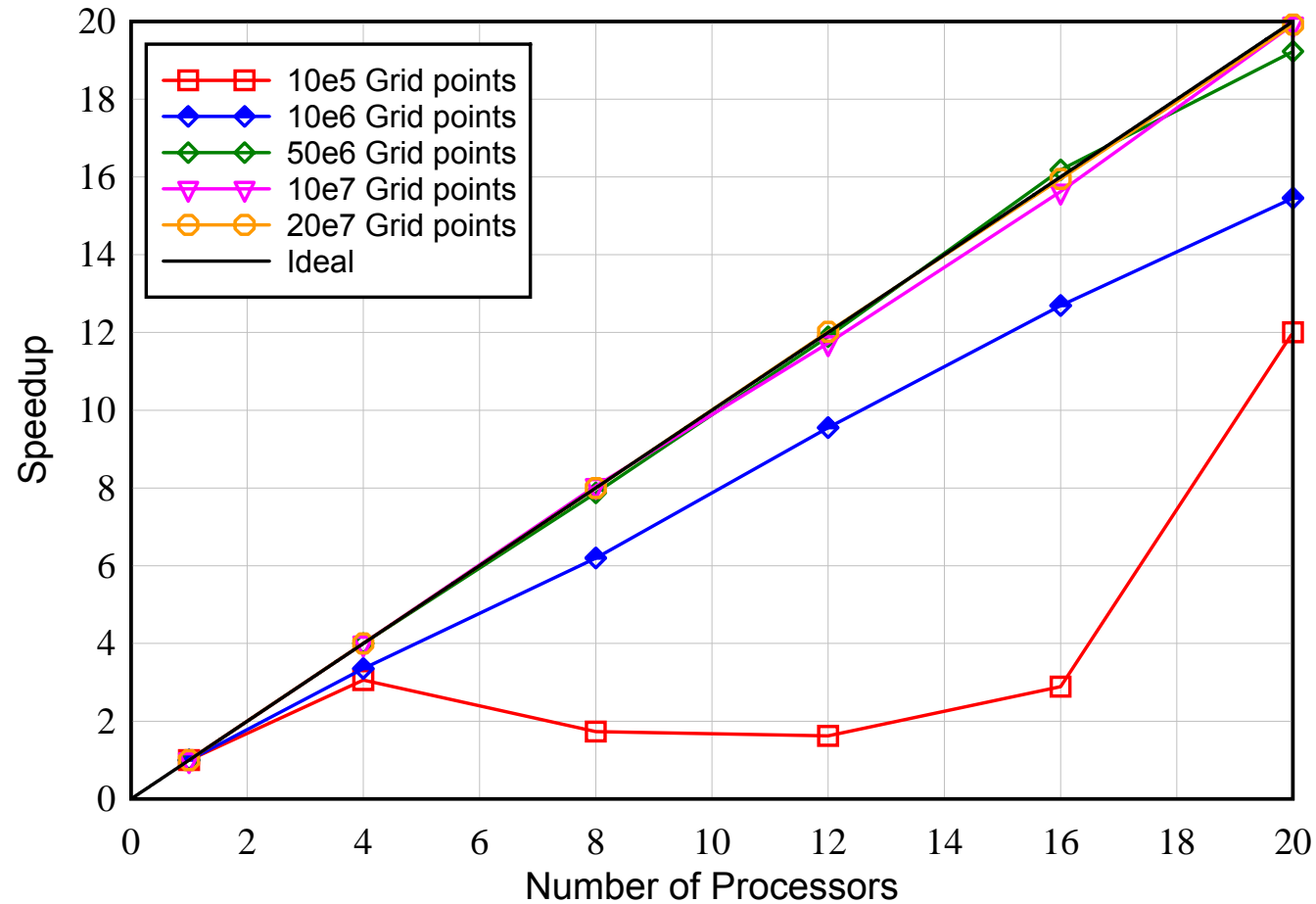


Parallel performance tests





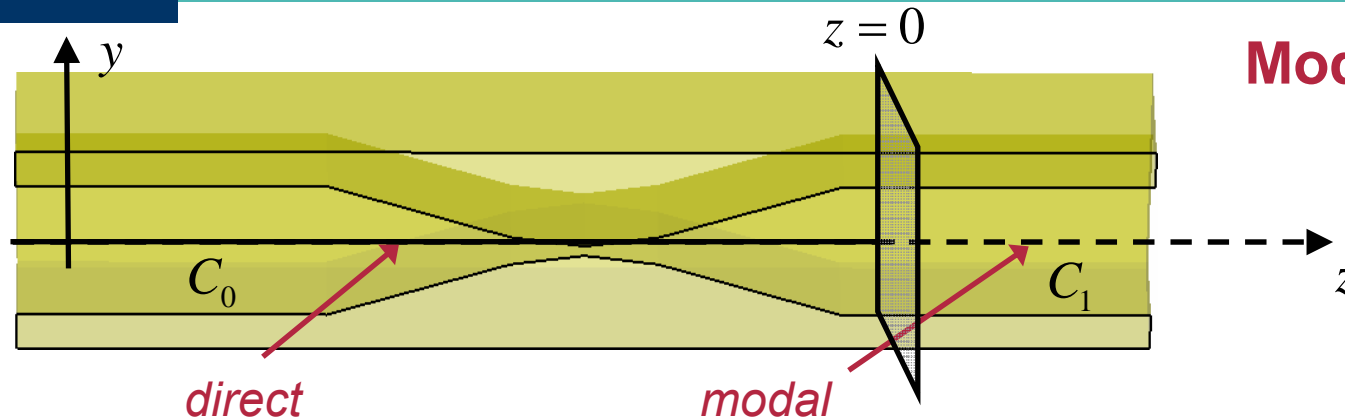
Parallel performance tests



TEMF Cluster: on 20 INTEL CPUs @ 3.4GHz, 8GB RAM, 1Gbit/s Ethernet Network



Modal Termination of Pipes



$$W_z(s) = -\frac{1}{Q} \int_{-\infty}^{\infty} dz E_z(z, t = \frac{z+s}{c}) = -\frac{1}{Q} \int_{C_0} dz E_z(z, t = \frac{z+s}{c}) - \frac{1}{Q} \sum_n e_z^n(x, y) W_n(s)$$

$$\int_0^{\infty} dz E_z(x, y, z, t = (z+s)/c) = \int_0^{\infty} dz \left[\int_{-\infty}^{\infty} d\omega \sum_n C_n(\omega) e_z^n(x, y) e^{ik_n(\omega)z} e^{-i\omega \frac{z+s}{c}} \right] =$$

$$= \sum_n e_z^n(x, y) \int_{-\infty}^{\infty} d\omega C_n(\omega) \frac{1}{i(\omega/c - k_{z,n}(\omega))} e^{-i(\omega/c)s}$$

spectral coefficient of n-th (TM) mode

n-th (TM) mode contribution

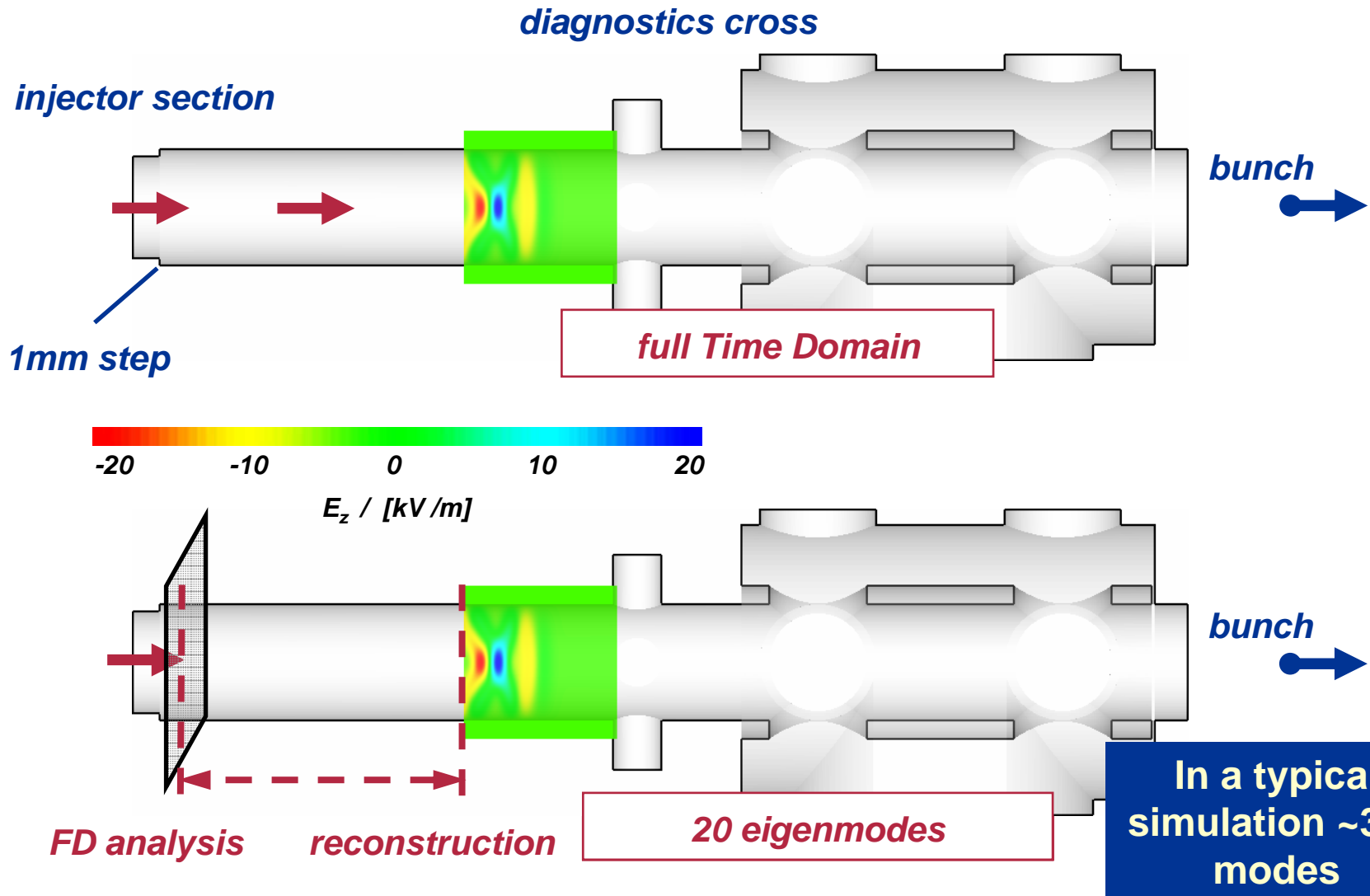
Indirect methods for wake potential integration, I. Zagorodnov et al, PRSTAB 9, '06
 Eigenmode expansion method in the indirect calculation of wake potential in 3D in structures, X. Dong et al, ICAP'06



Modal Termination of Pipes



Using modal reconstruction in long intermediate pipes

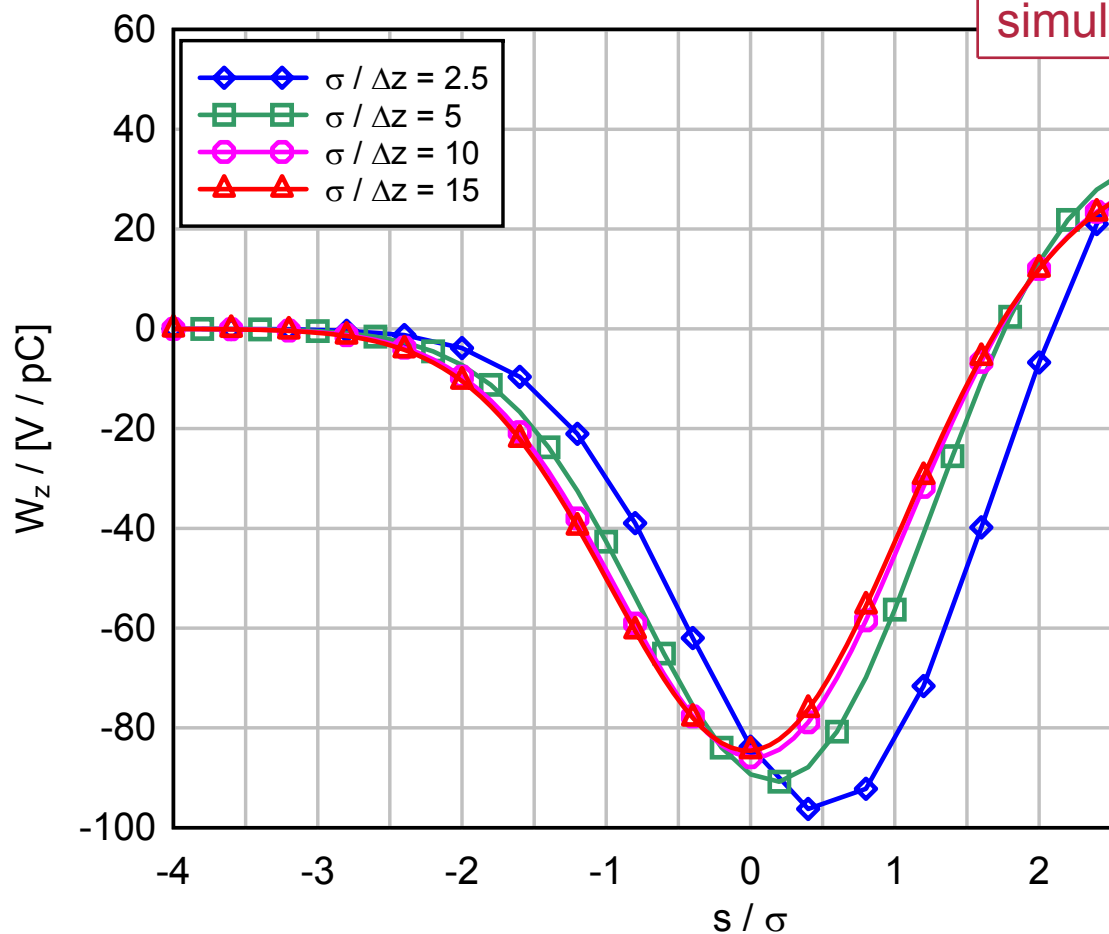




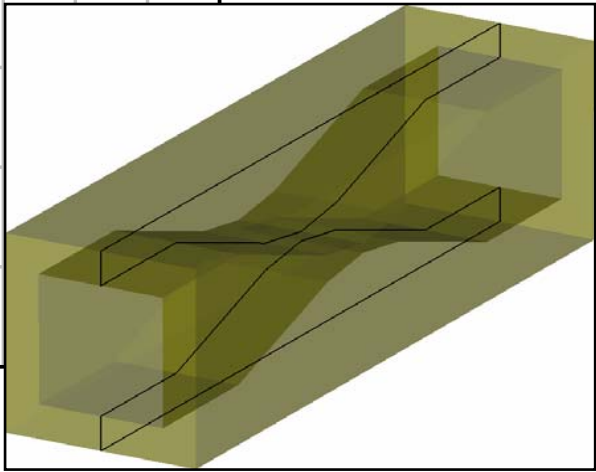
ILC-ESA collimator #8

bunch size	300 μ m
no. of grid points	~450M
no. of processors	24
simulation time	85hrs

Convergence vs. grid step



**Moving window:
3 mm length**

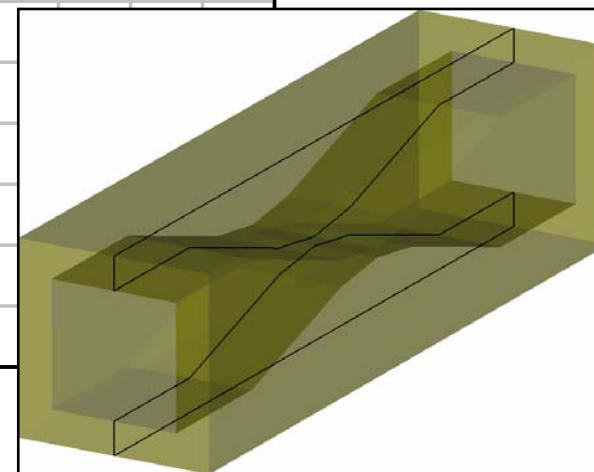
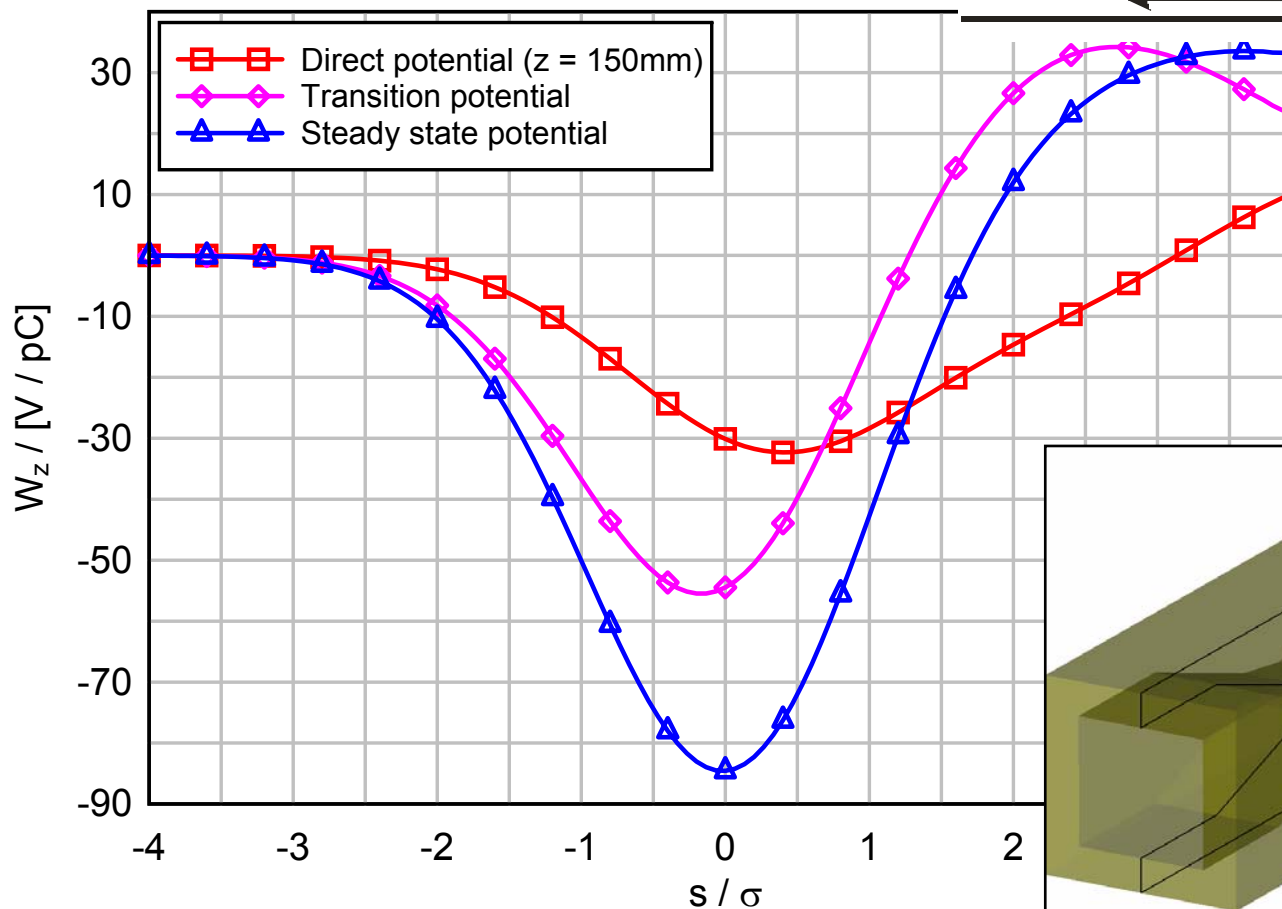
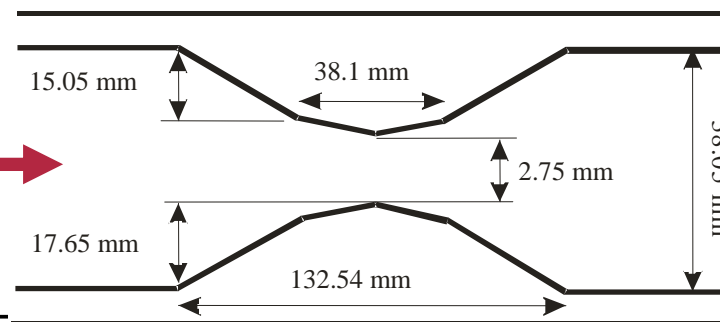




ILC-ESA collimator #8

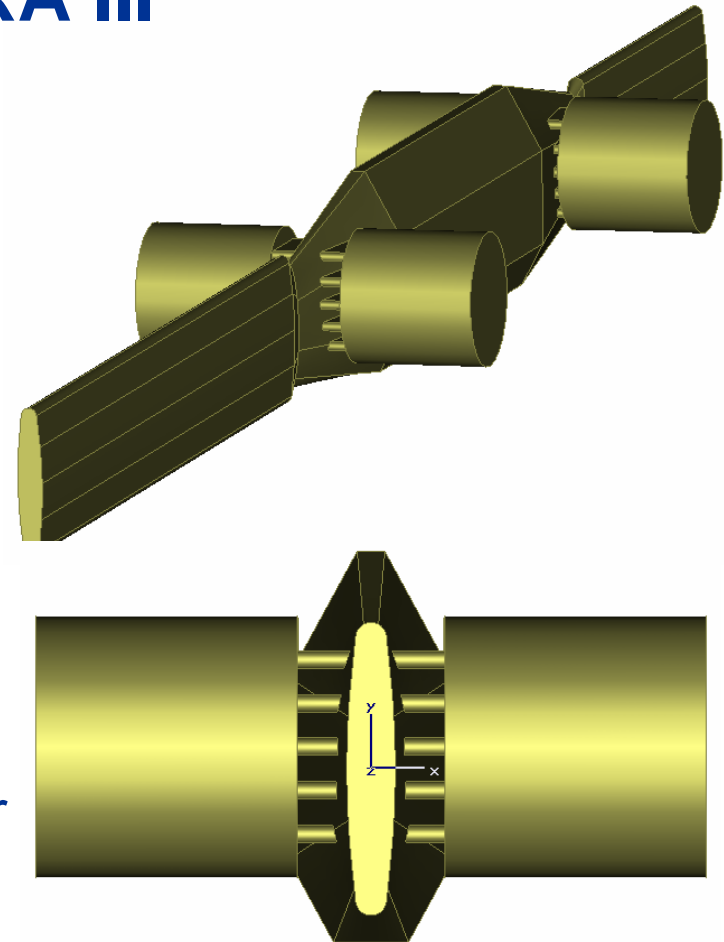
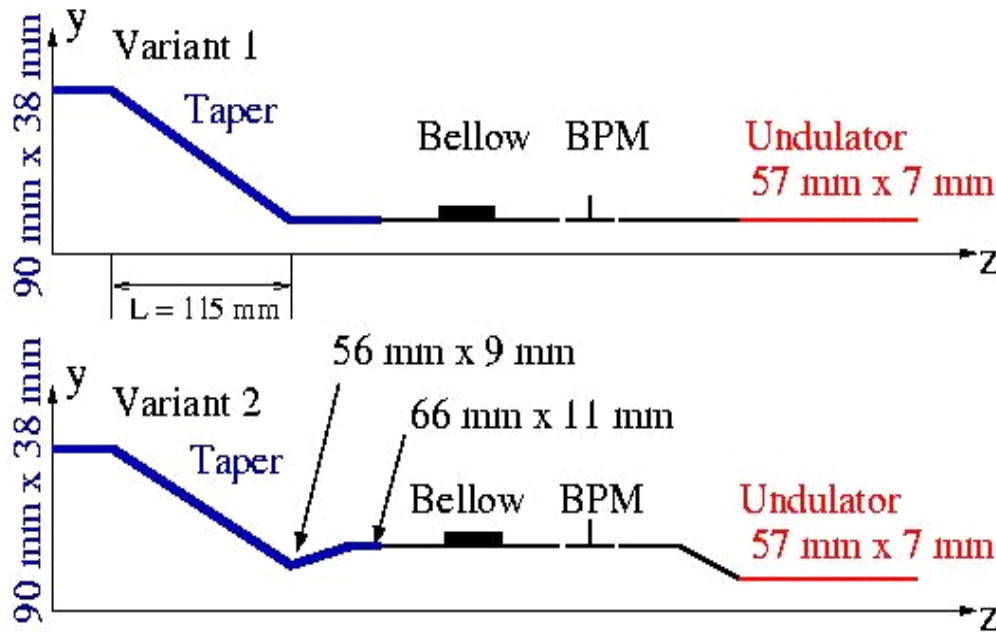
Direct vs. transition wakes

bunch →





Tapered Transitions for PETRA III

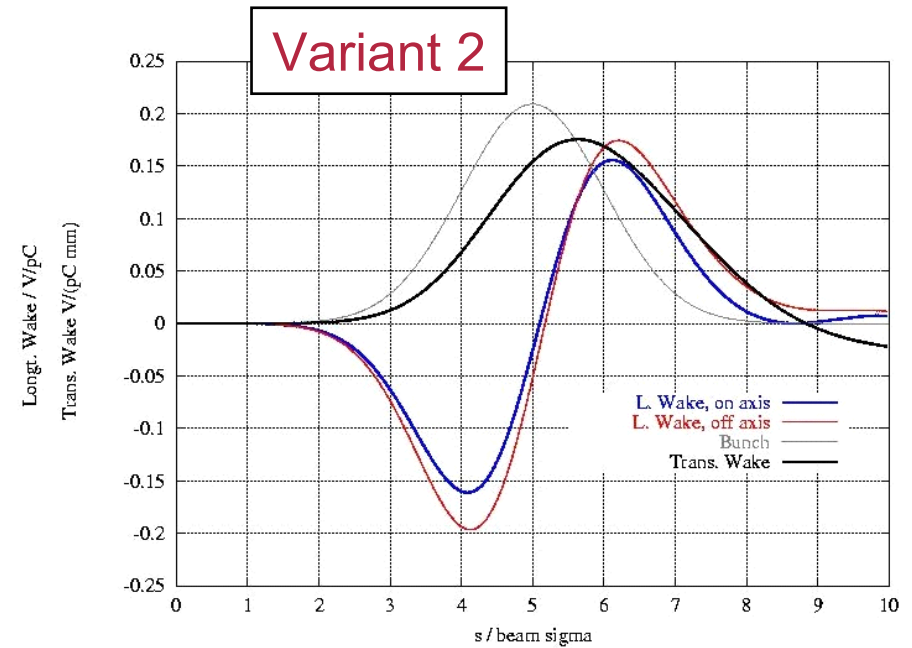
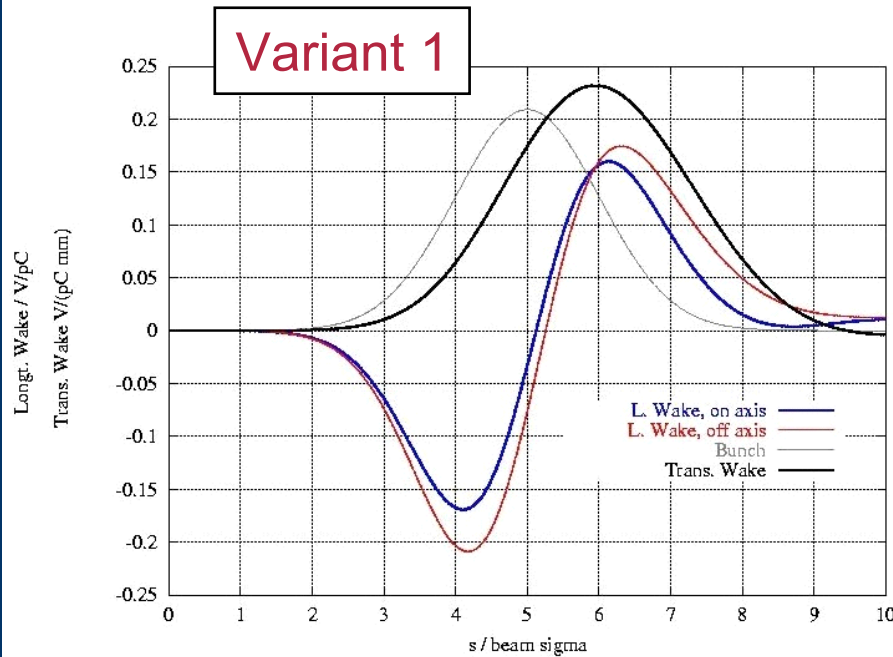


The two variants of the vacuum-to-undulator tapered transition

“Wake Computations for Undulator Vacuum Chambers of PETRA III”, R. Wanzenberg et al, PAC’07



Tapered Transition for PETRA III

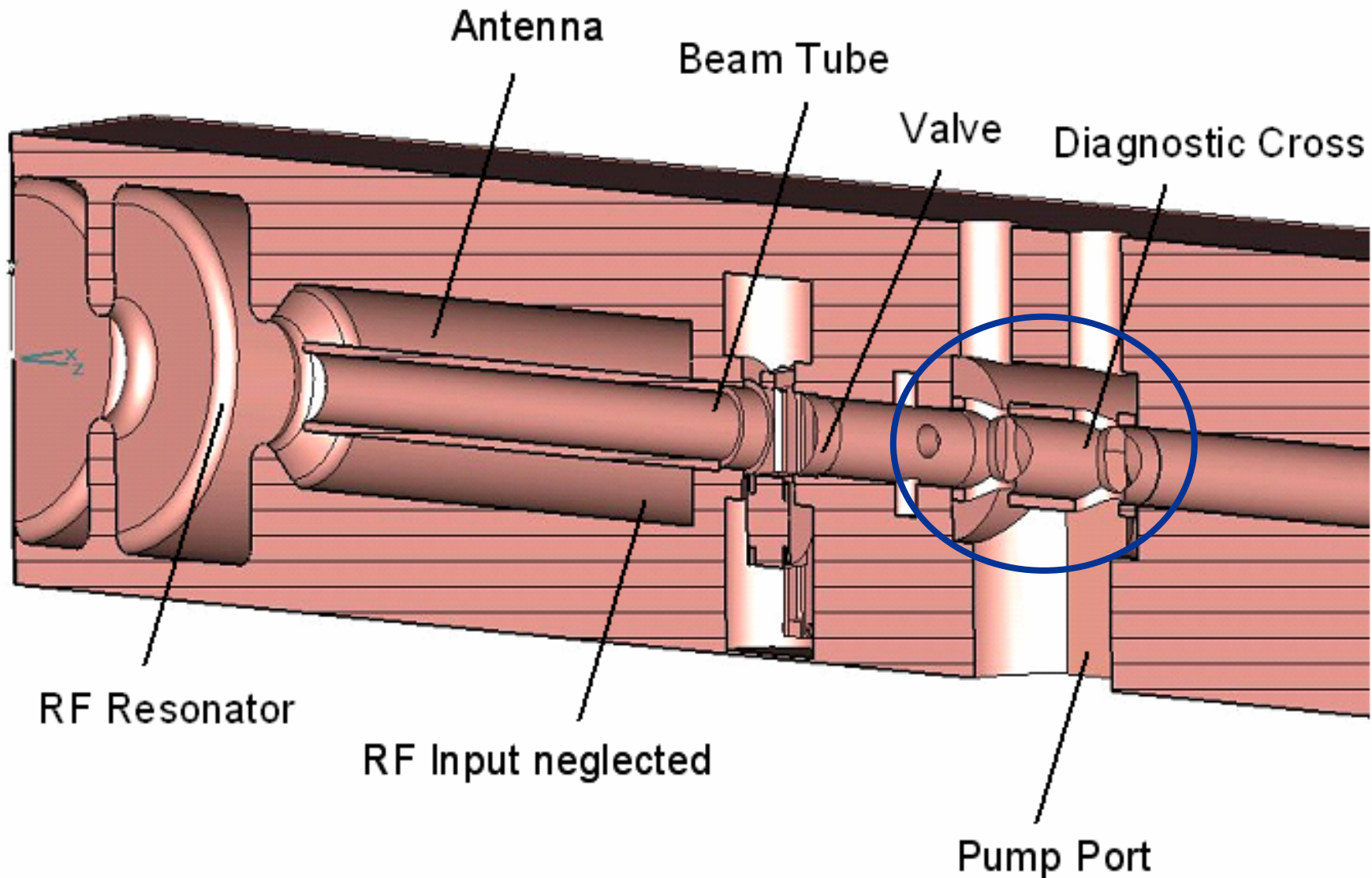


Variant / Code	$k_{ } / (V/nC)$	$k_{ }(1) / (V/pC m)$	$k_{\perp} / (V/pC m)$
Variant1 / MAFIA	-7.4	-6.8	138.6
Variant1 / PBCI	-7.1	-4.8	75.6
Variant2 / PBCI	-5.2	-4.6	62.8

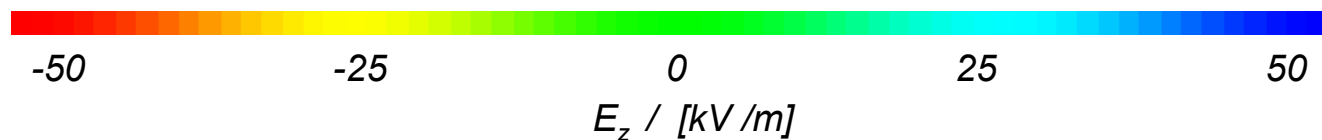
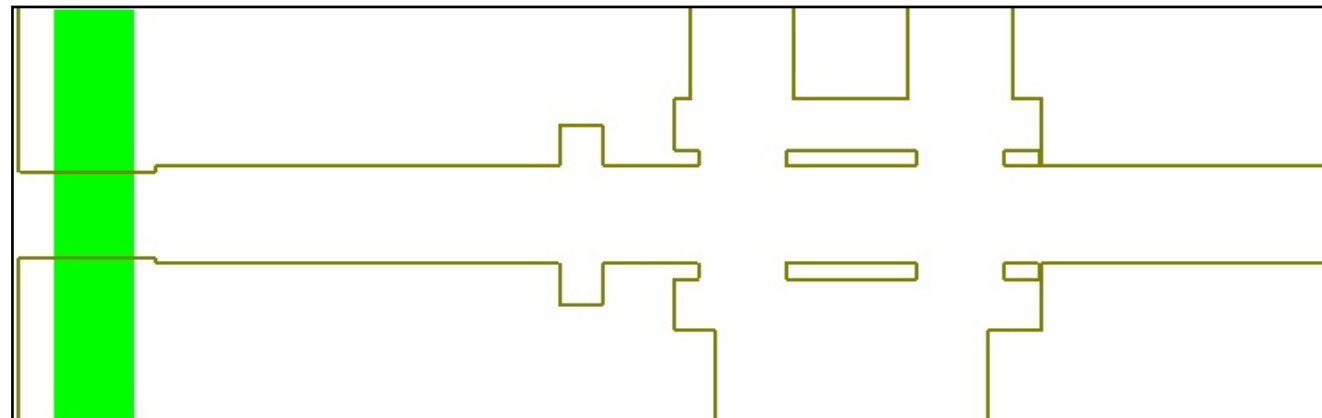
factor ~1.8 higher than PBCI due to insufficient resolution



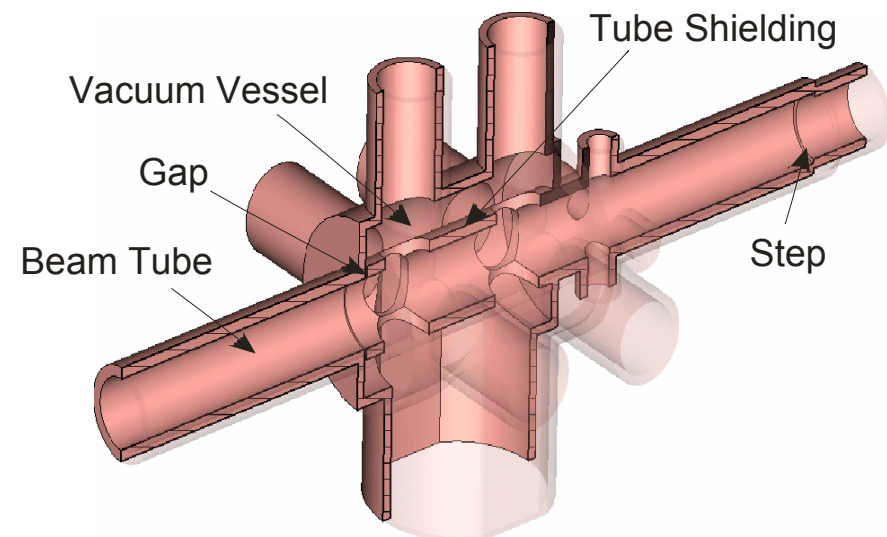
PITZ diagnostics double cross



PITZ diagnostics double cross



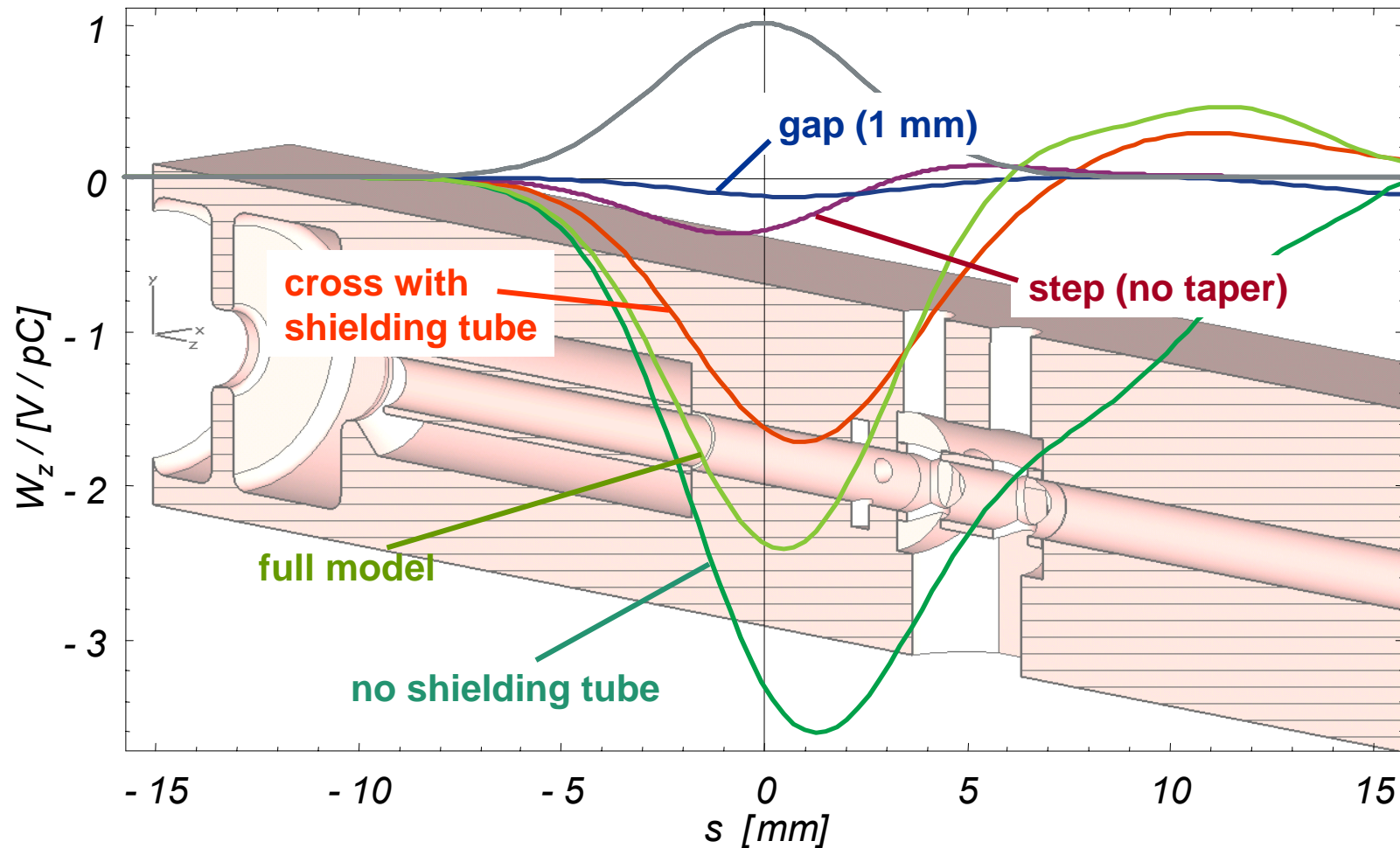
bunch size	2.5mm
$\sigma / \Delta z$	30
no. of grid points	$\sim 500e6$
no. of processors	24
simulation time	32hrs





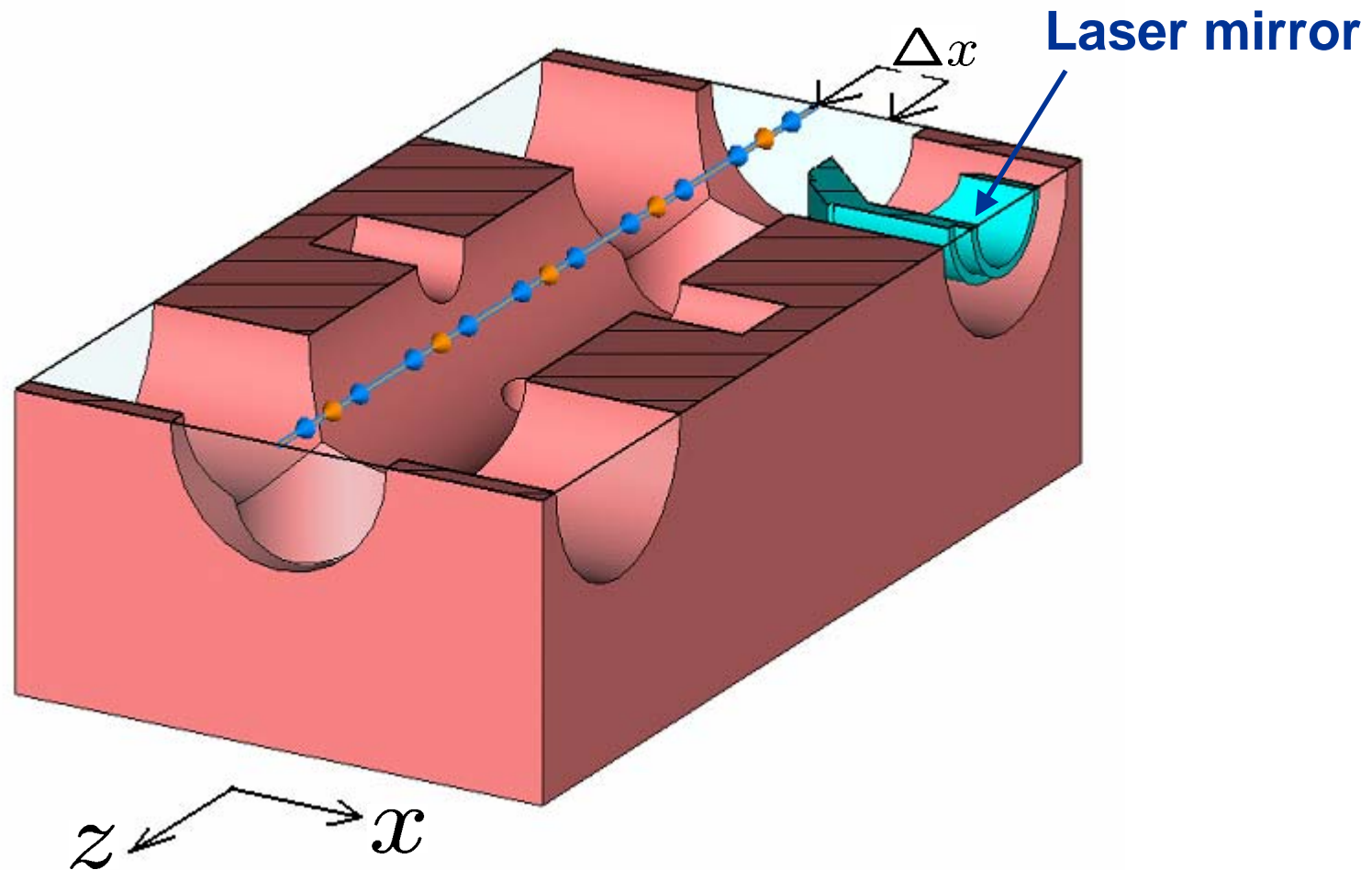
PITZ diagnostics double cross

Wake field impact of the single components





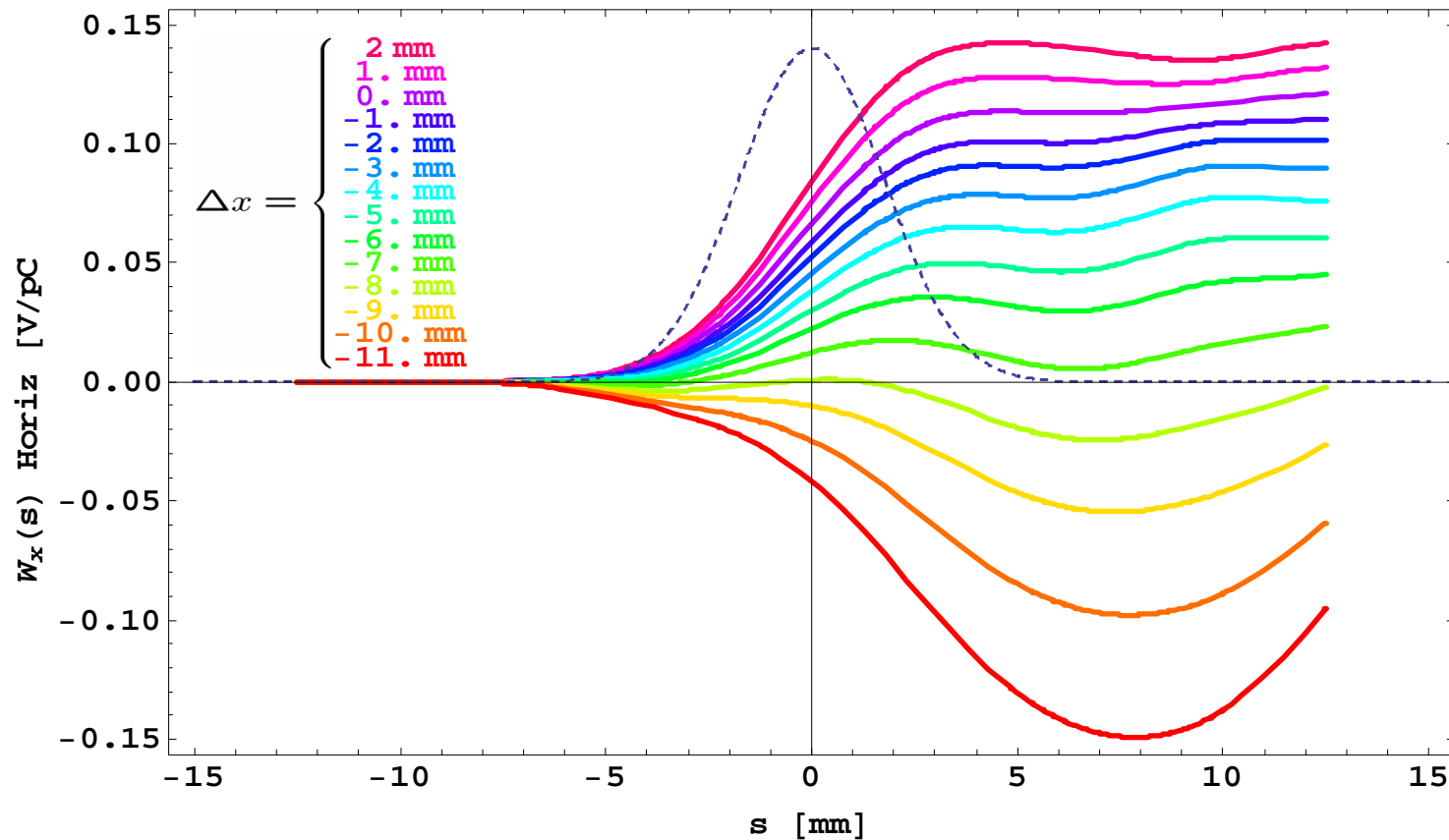
PITZ diagnostics double cross

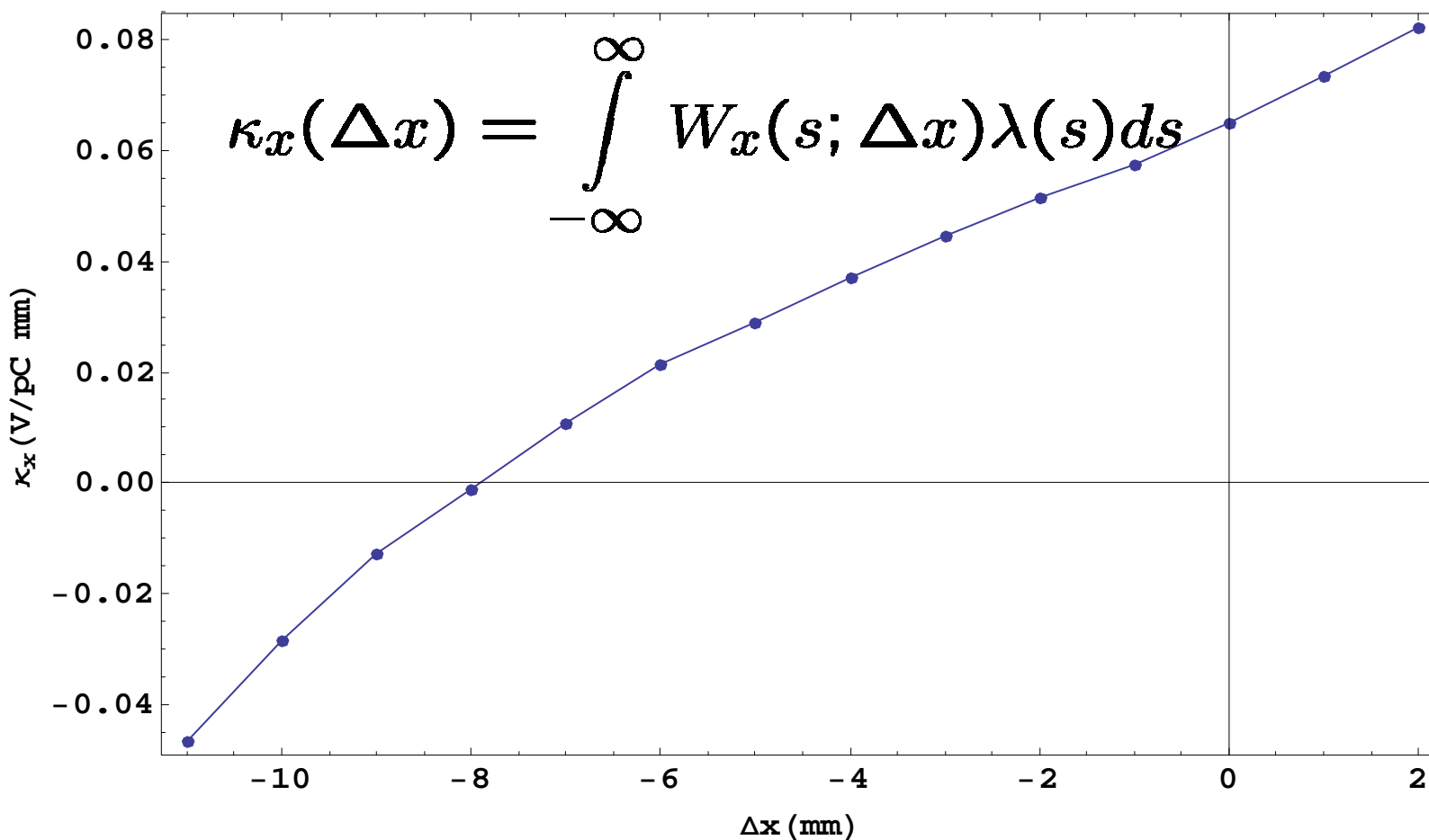




PITZ diagnostics double cross

Transversal wake potentials for different beam offsets

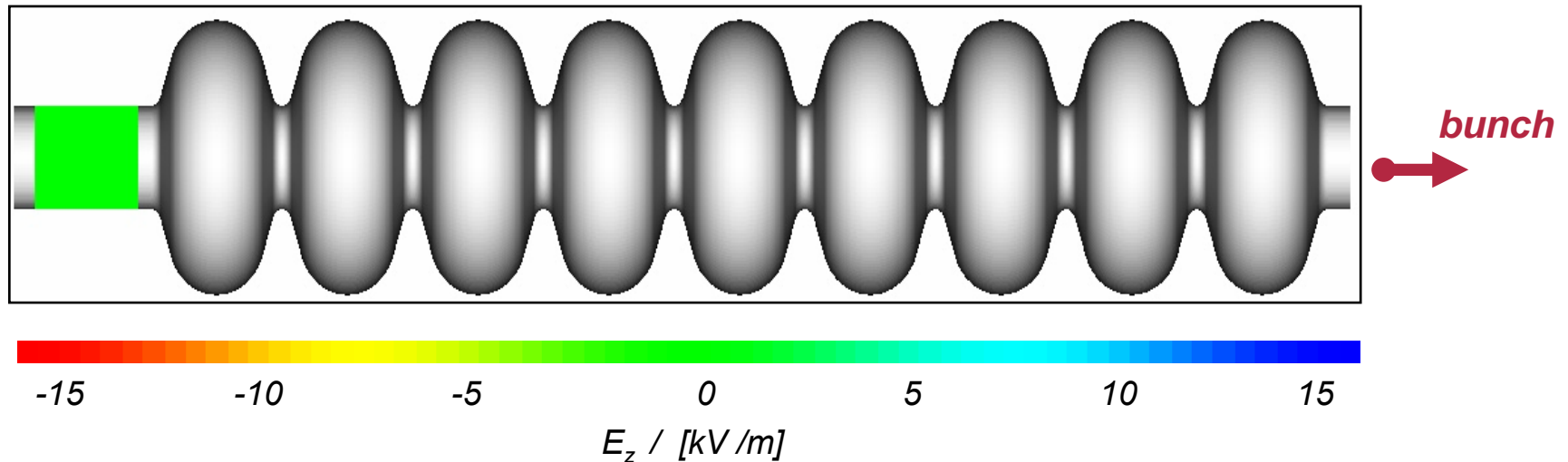




„Optimal“ offset at 8mm from tube axes



TESLA 9-cell cavity

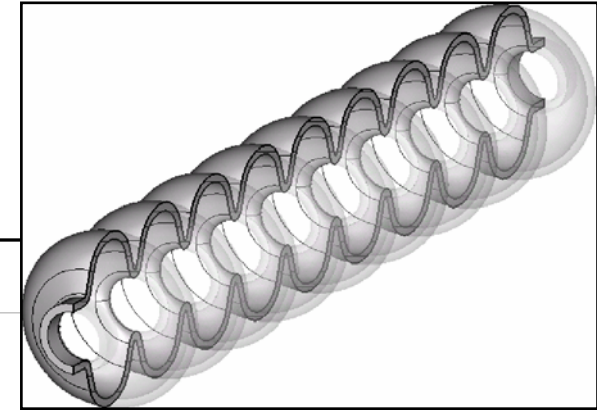
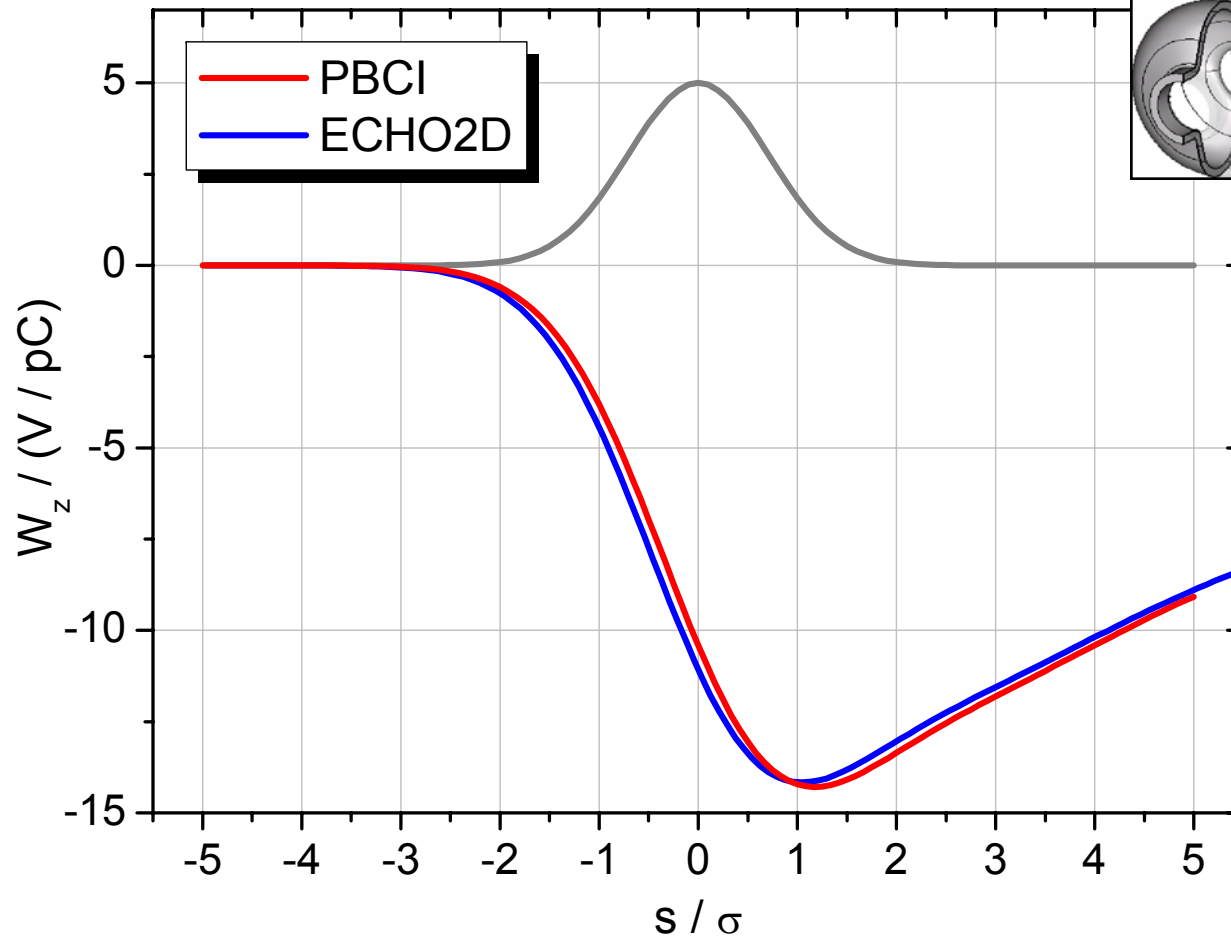


bunch length	1mm
bunch charge	1nC
cavity length	~1m
no. of grid points	~760M
no. of processor cores	408
simulation time	~40hrs



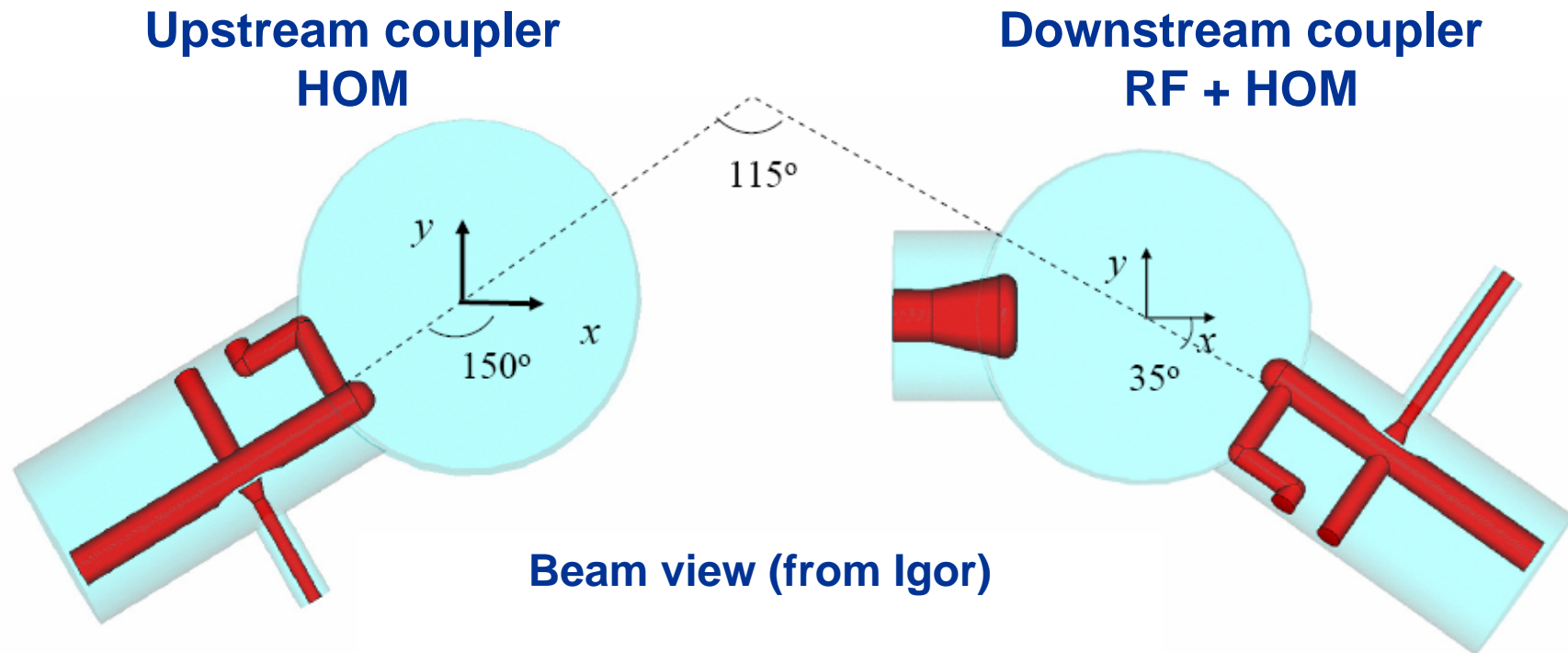
TESLA 9-cell cavity

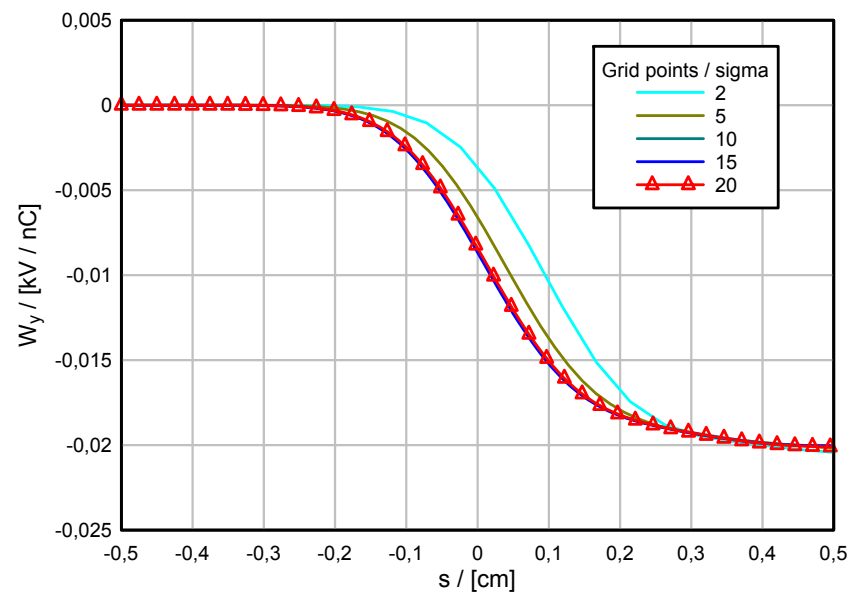
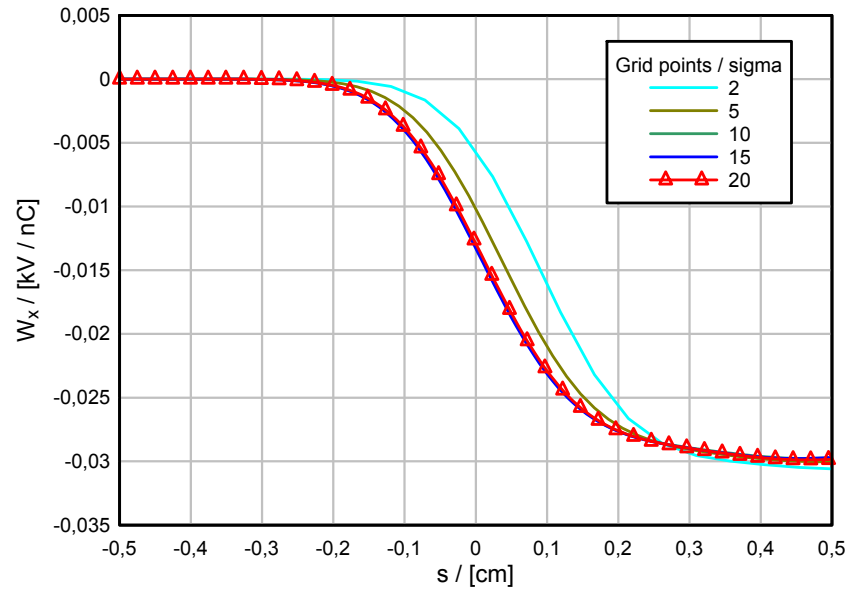
Longitudinal wake potential



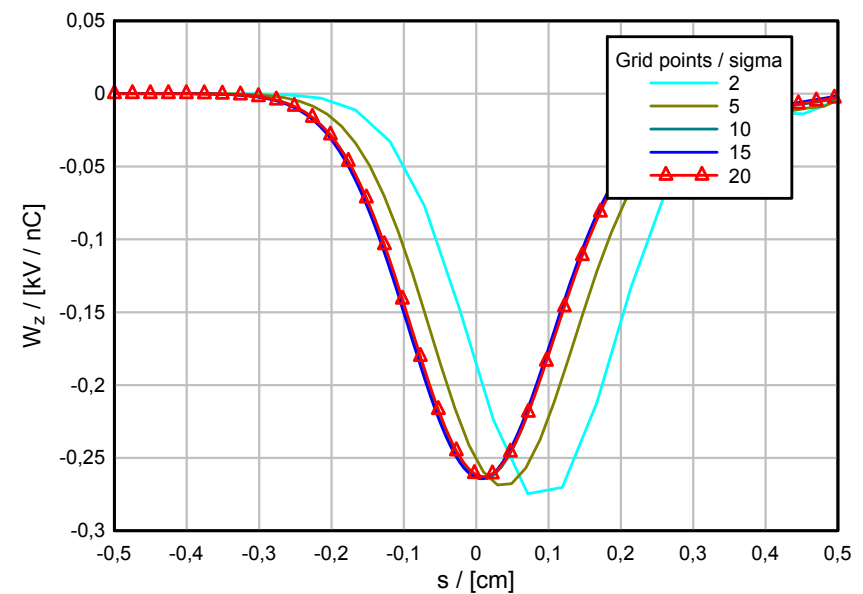
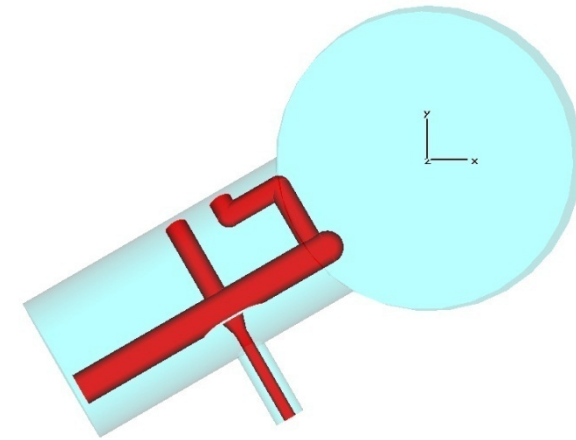


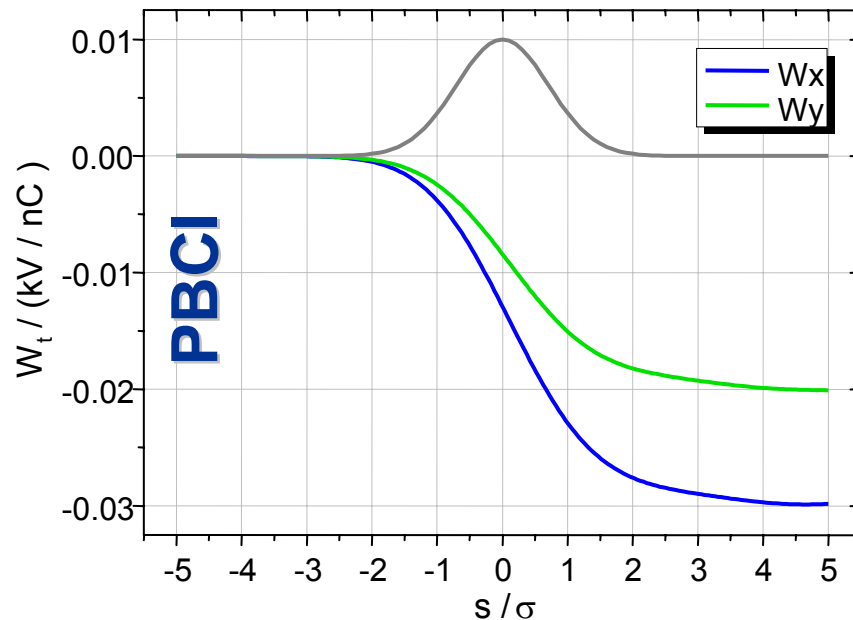
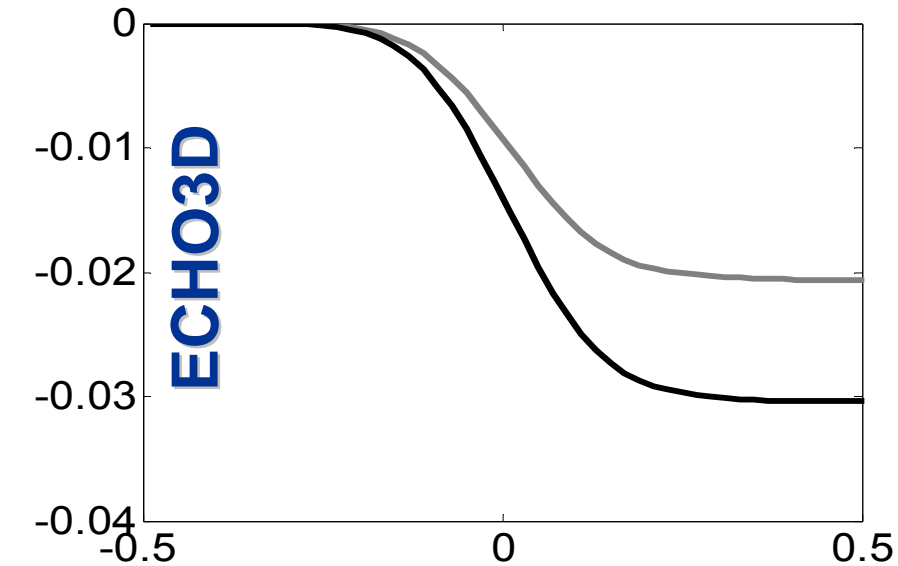
HOM / HOM-RF coupler (present DESY design)



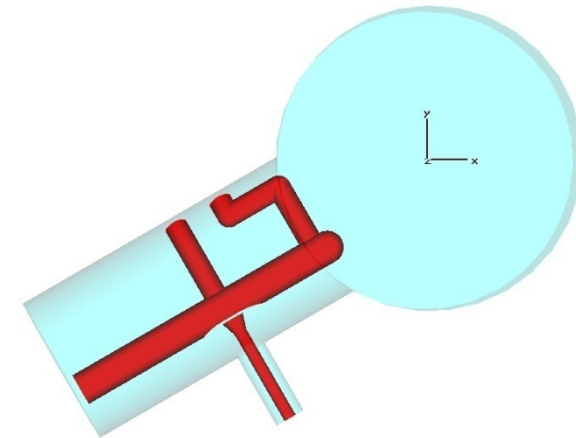


Upstream coupler

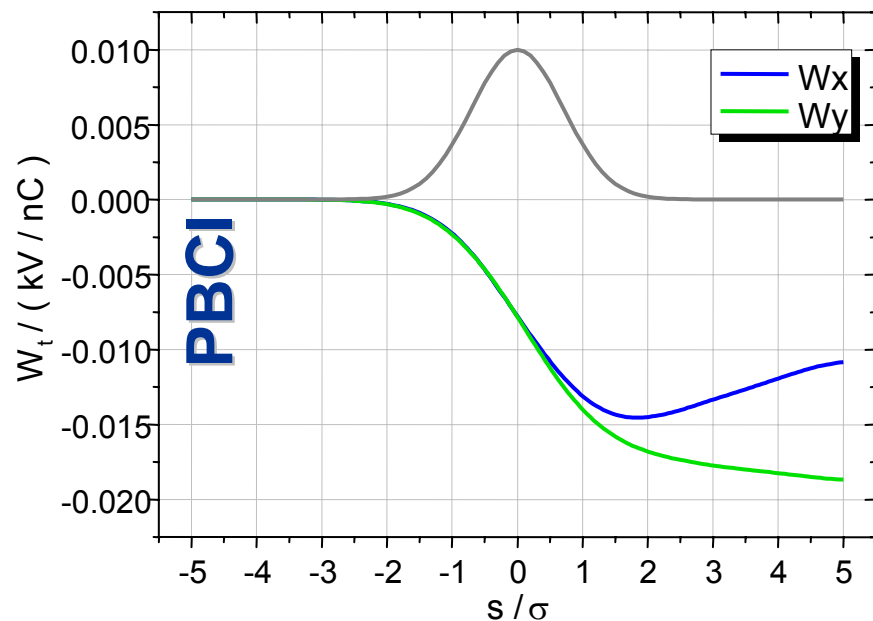
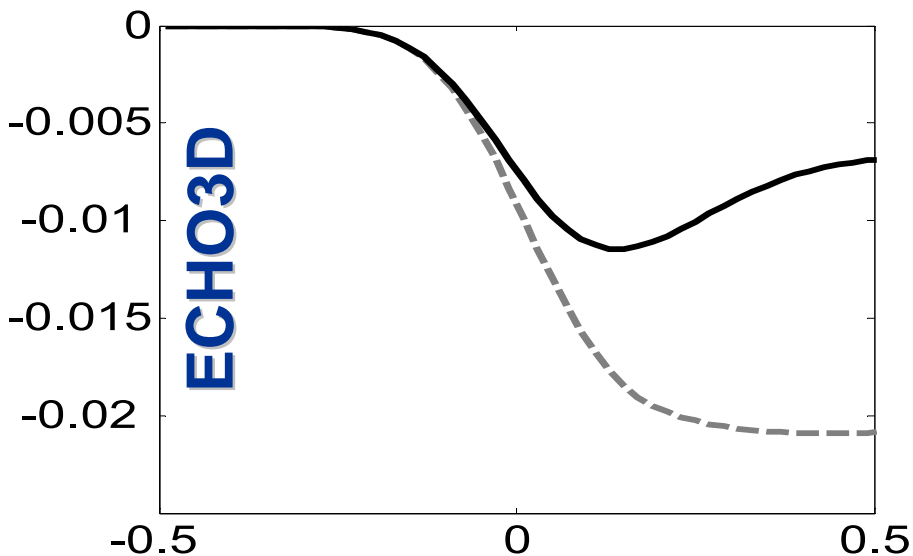




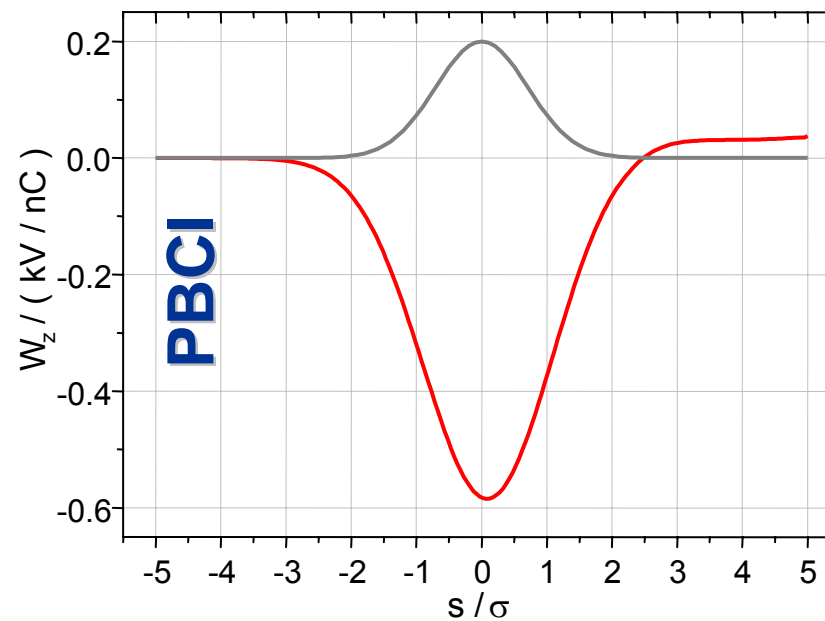
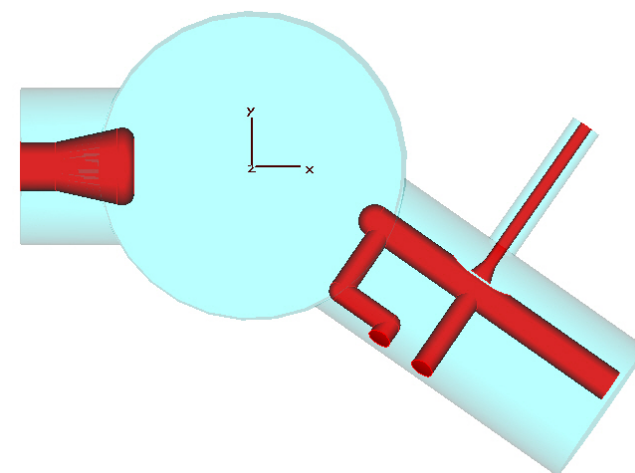
Upstream coupler



bunch length	1mm
coupler length	60mm
bunch charge	1nC
grid points (max)	~650M
processor cores	408
simulation time	~24hrs

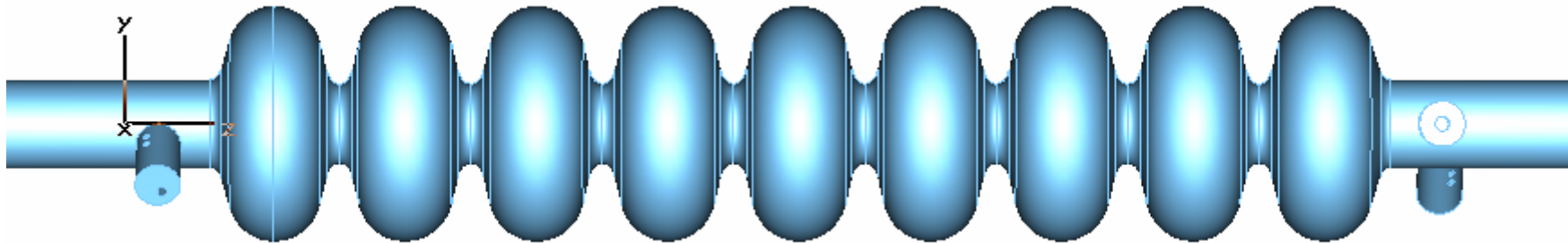


Downstream coupler

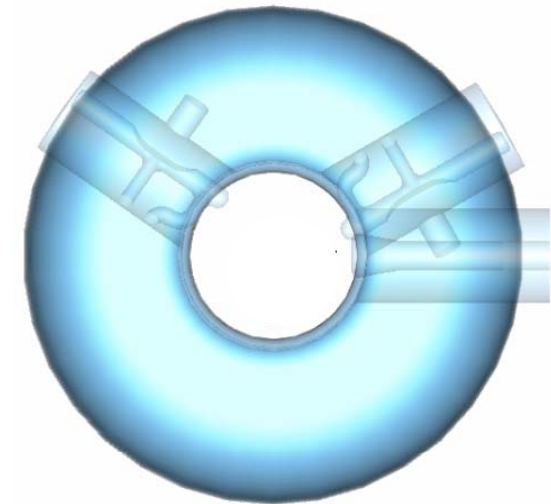
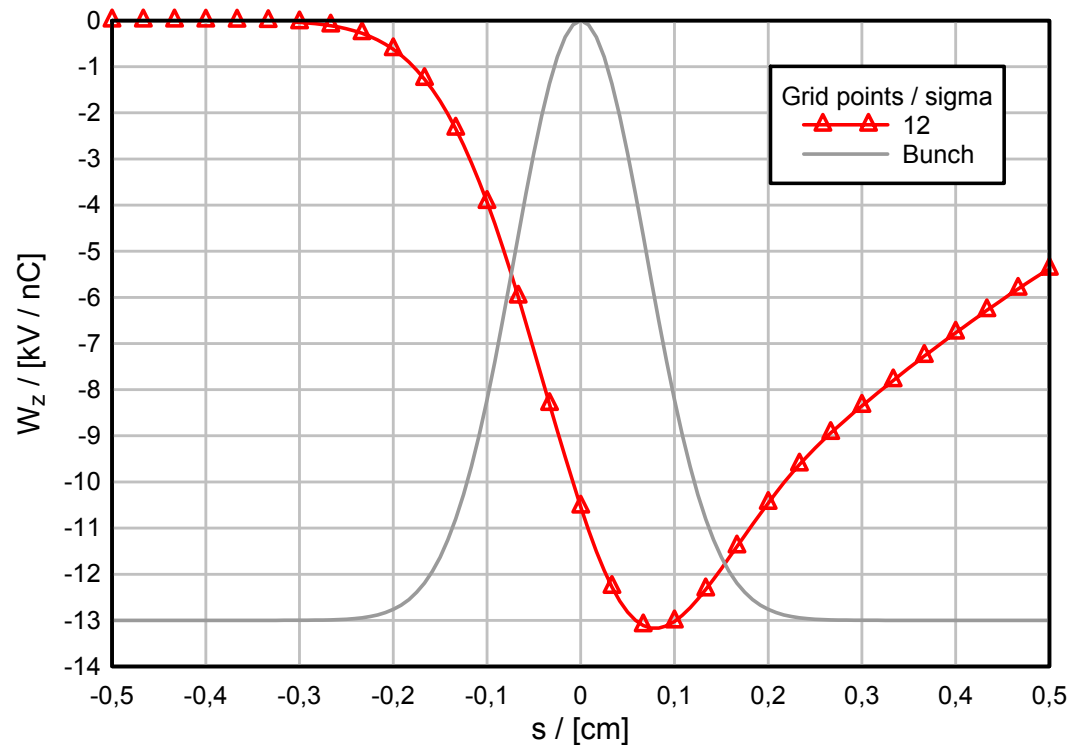




Present DESY Design



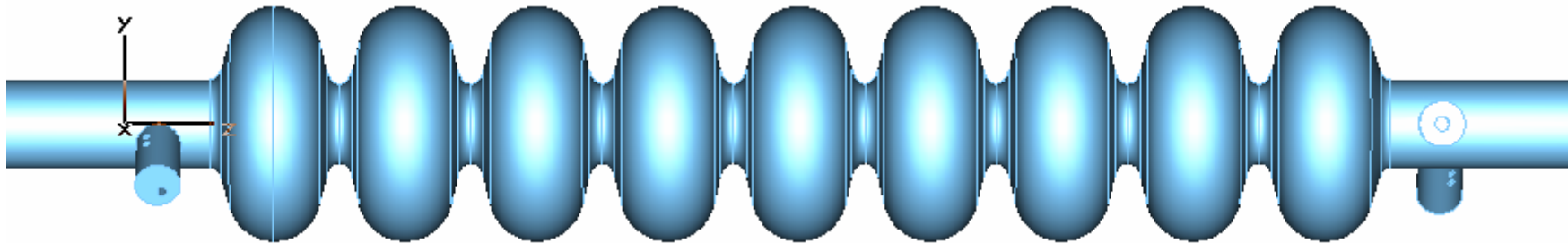
Longitudinal wake potential



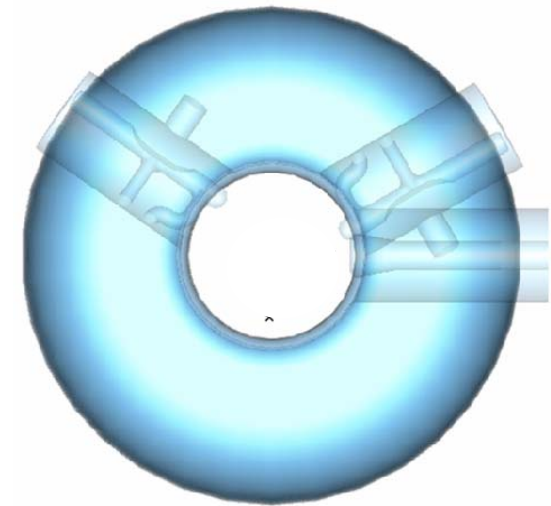
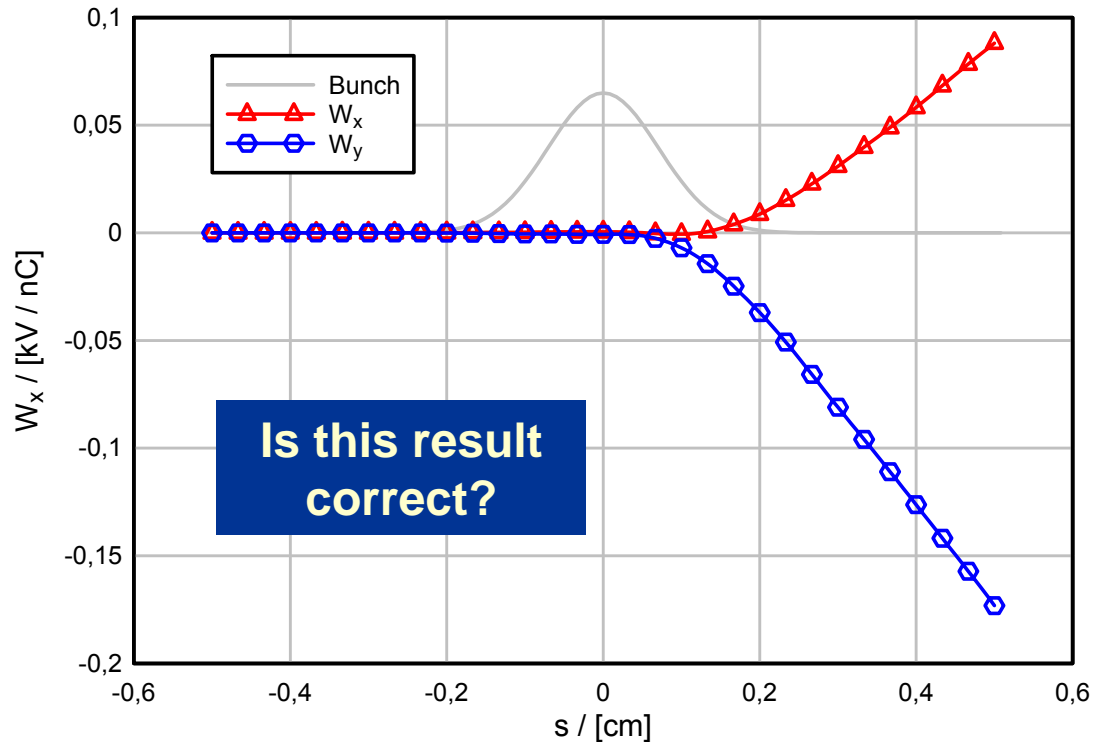
Beam view



Present DESY Design



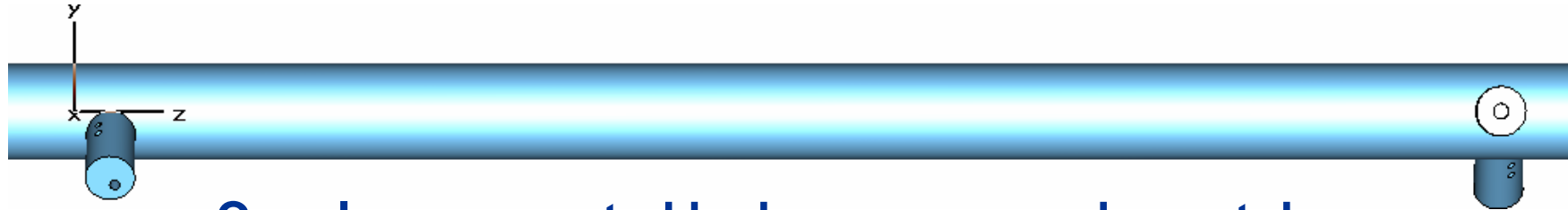
Transversal wake potentials



Beam view

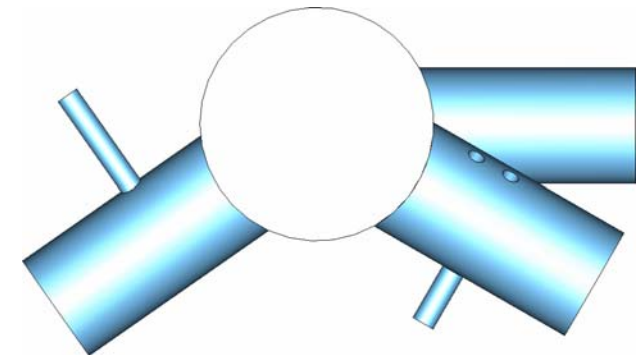
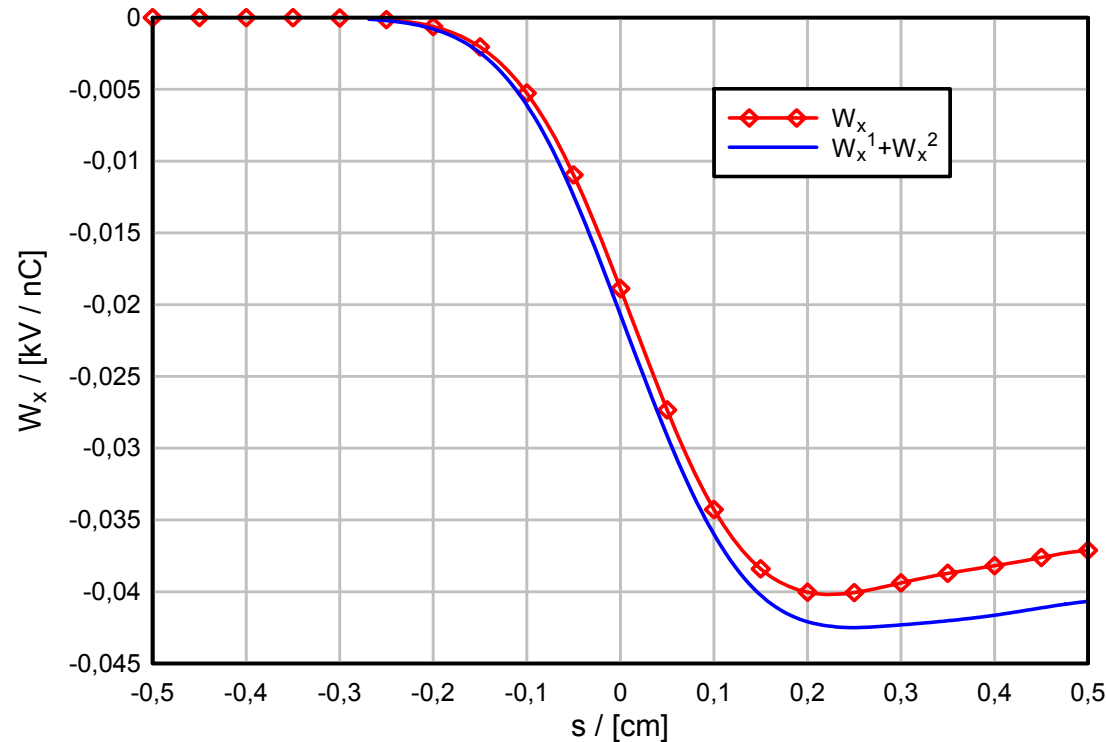


Simplified „Design“



Couplers connected by homogeneous beam tube

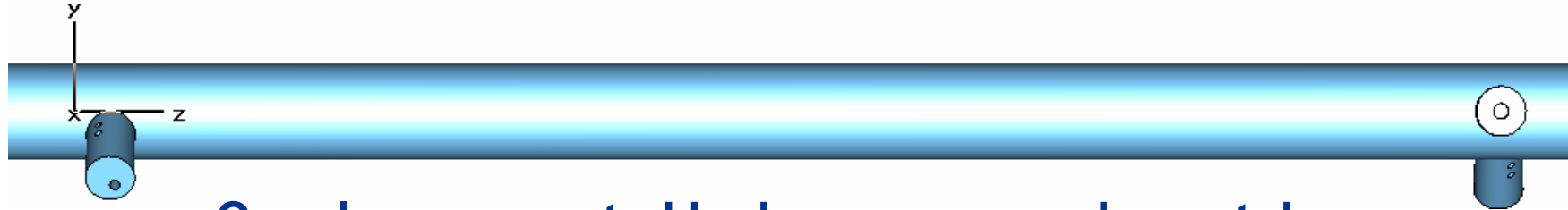
Transversal wake potentials



Beam view

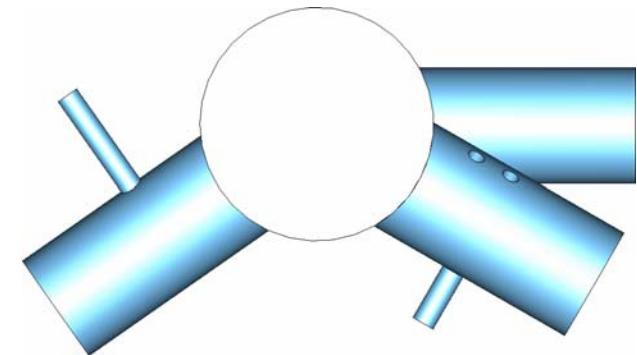
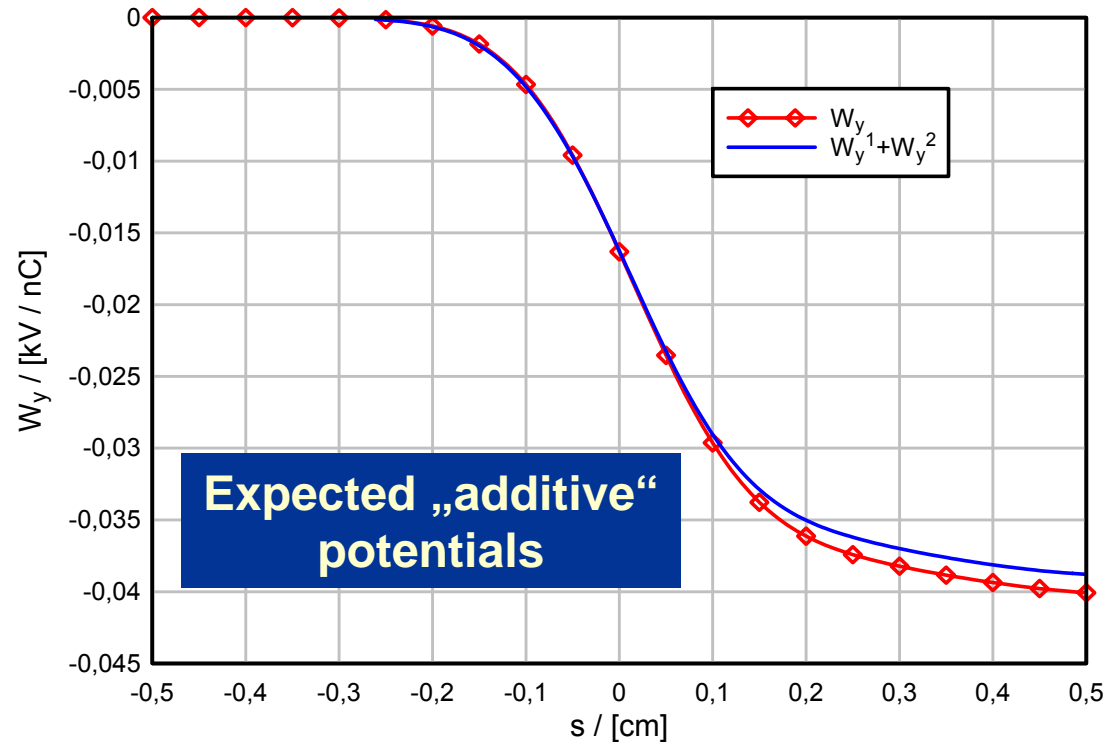


Simplified „Design“



Couplers connected by homogeneous beam tube

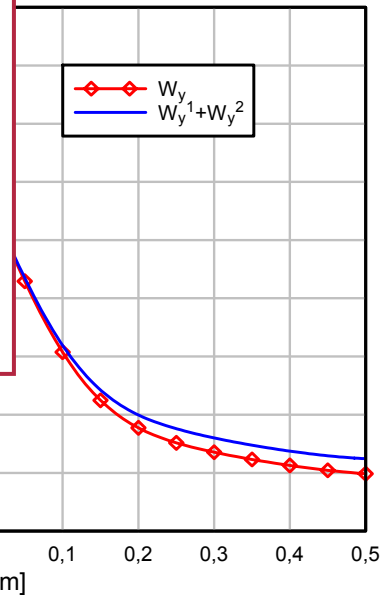
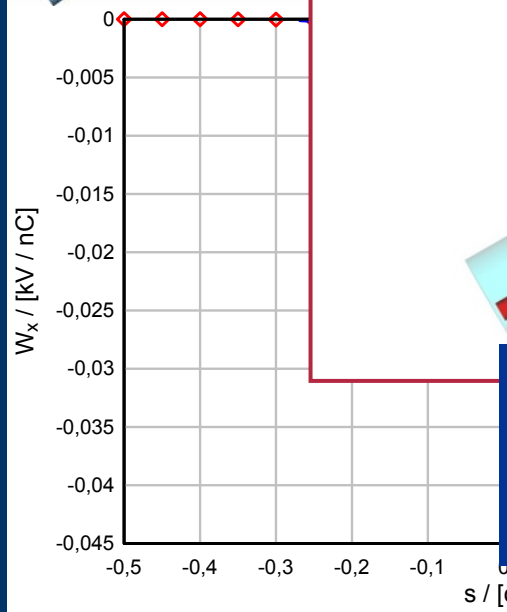
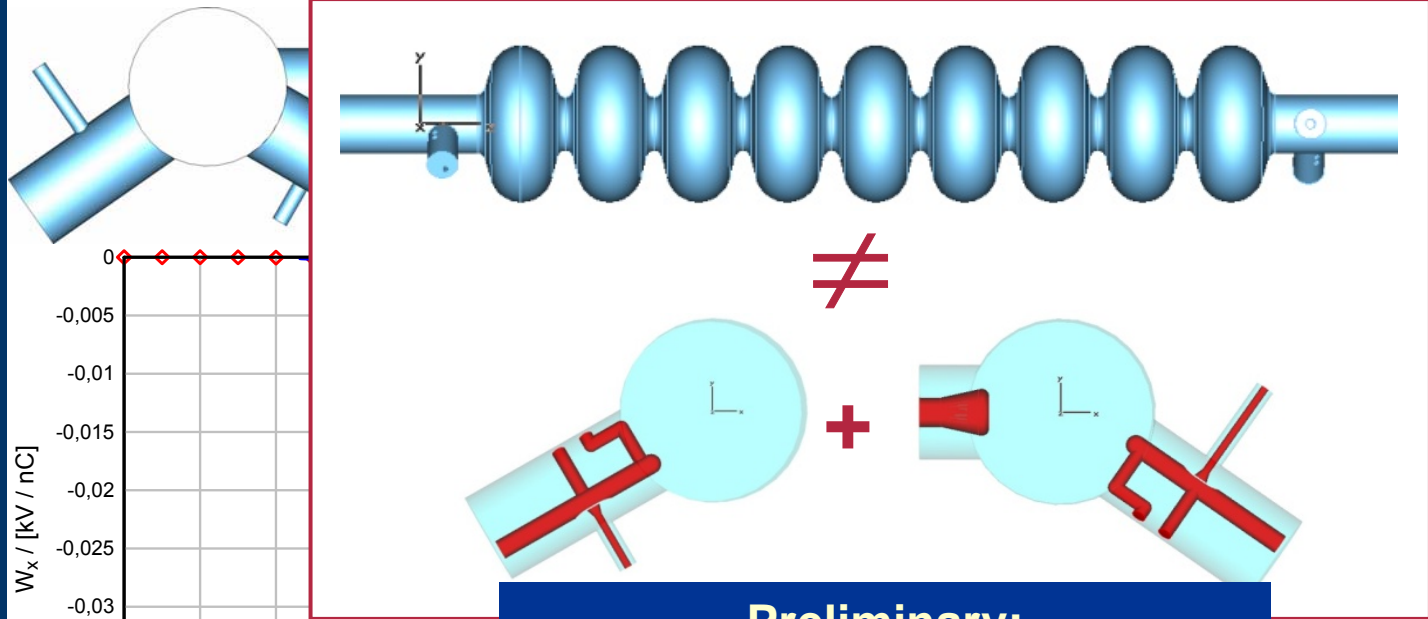
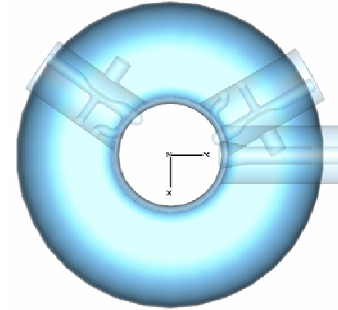
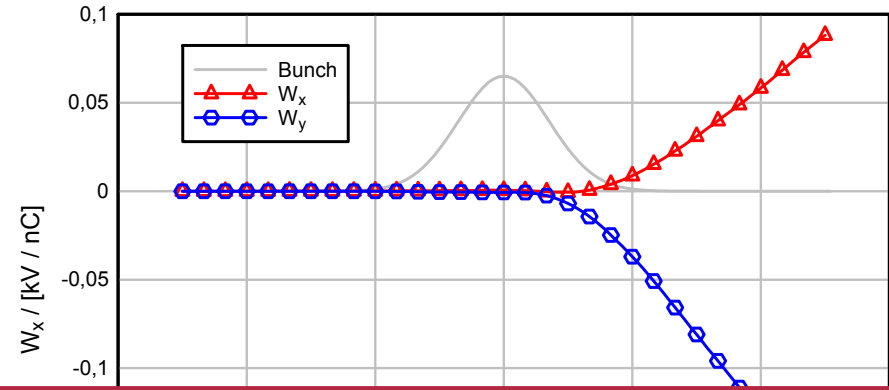
Transversal wake potentials



Beam view



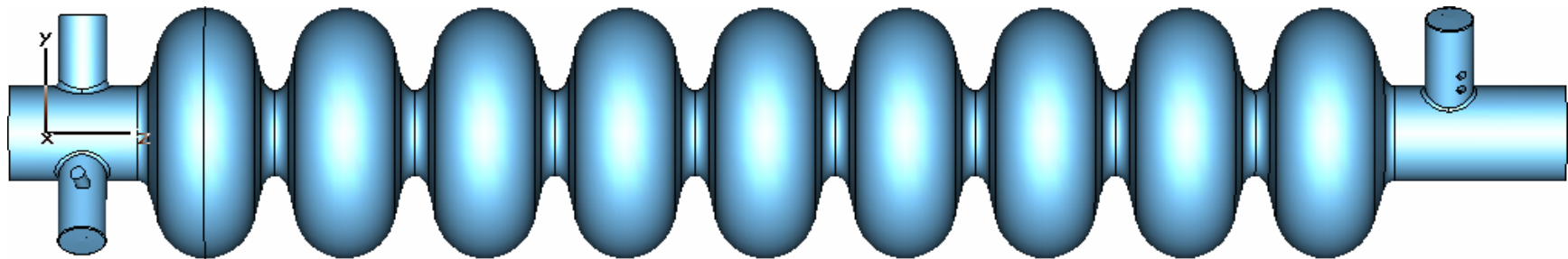
TESLA / HOM coupler



**Preliminary:
Transversal wakes are affected
by the cryomodule?**

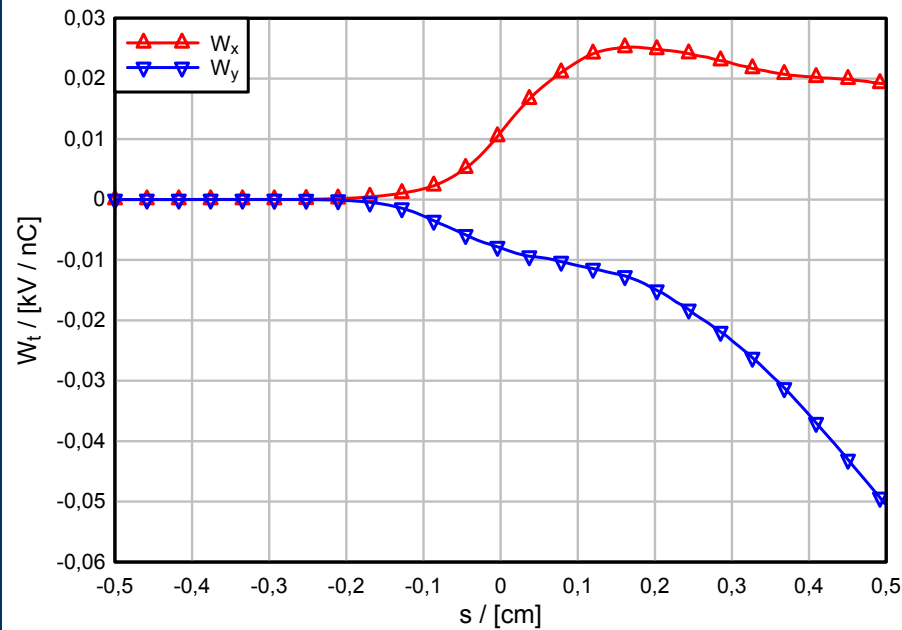


FNAL Design

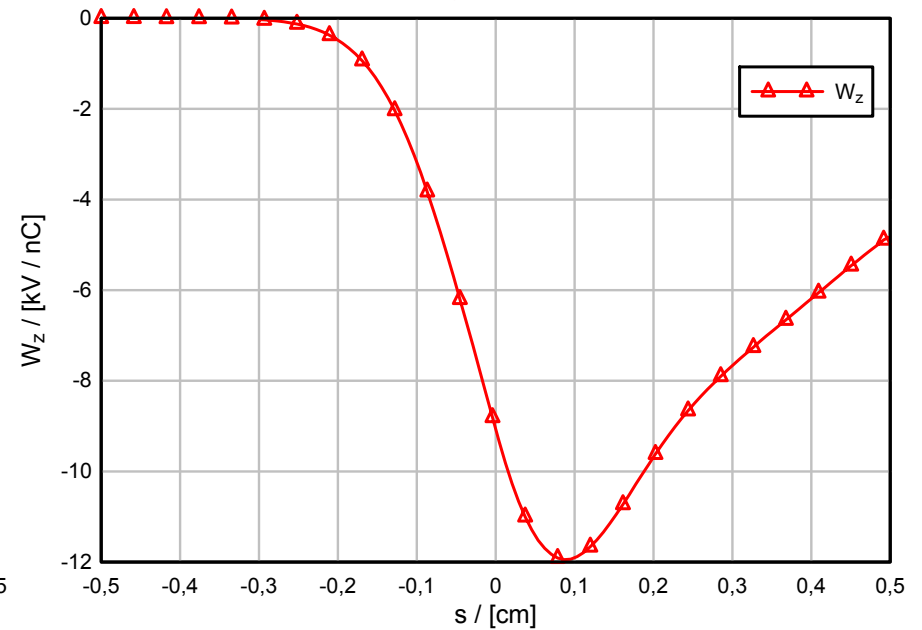


couplers are interchanged

Transversal



Longitudinal





Current / future work on wakefield codes at TEMF

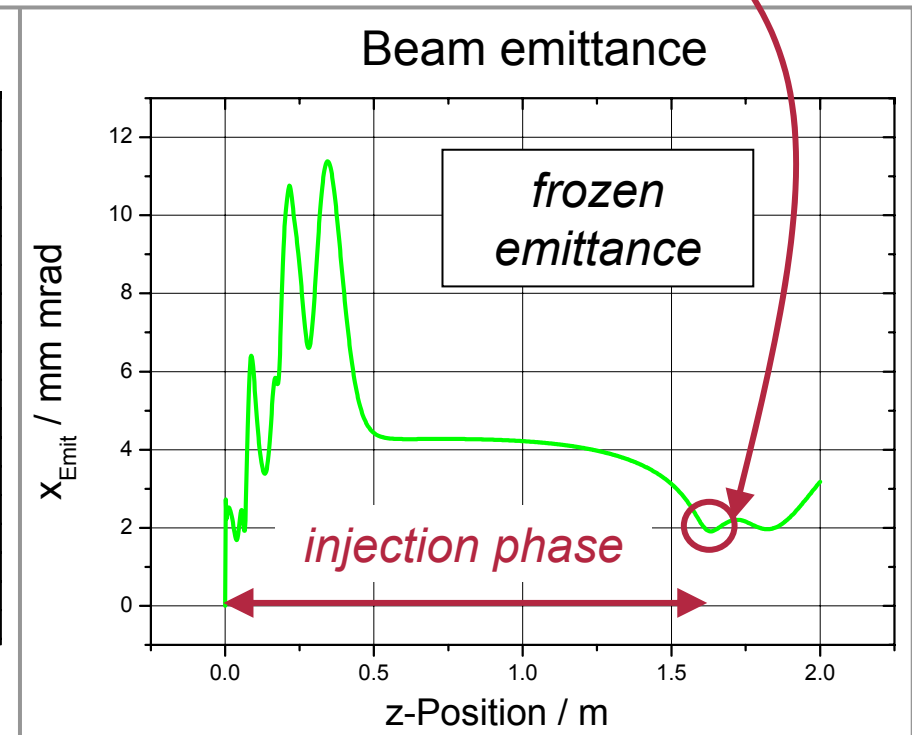
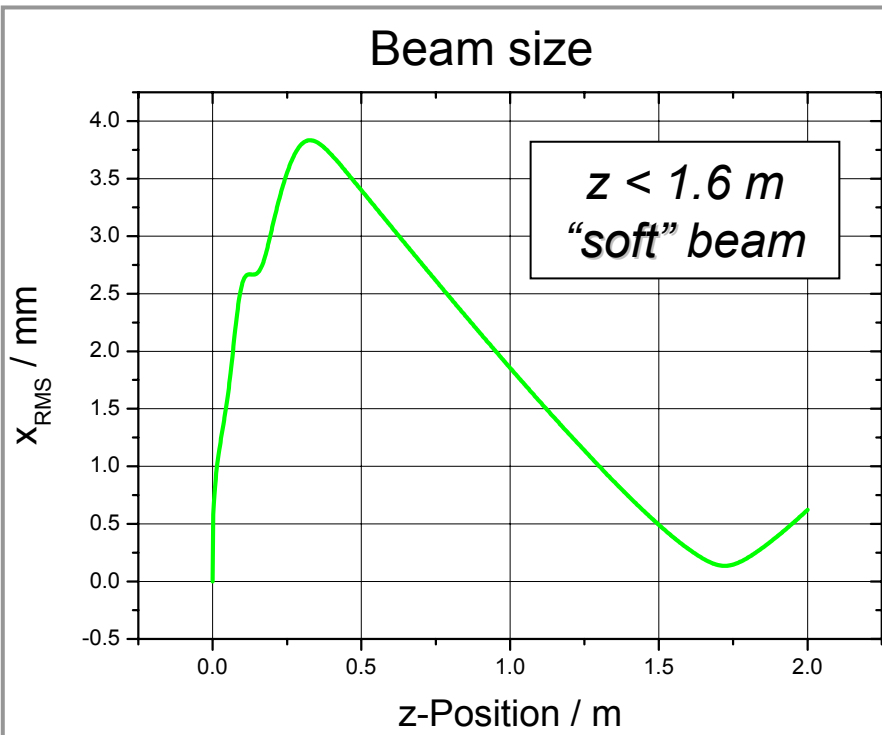
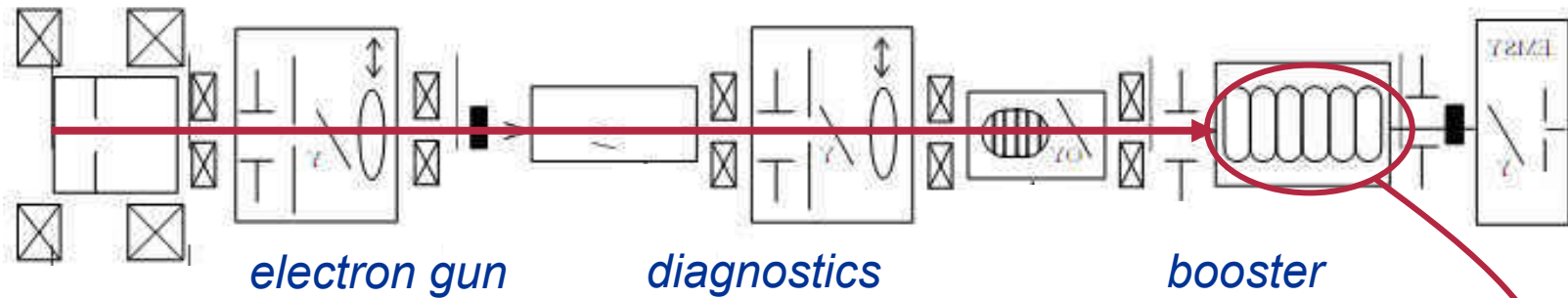
1. Non-split algorithms for moving windows: A new finite volume based algorithm is available.
2. Implementation of impedance boundary conditions for resistivity wakes.
3. Handling of long (super-periodic) structures with a modal approach



Self-Consistent Simulations

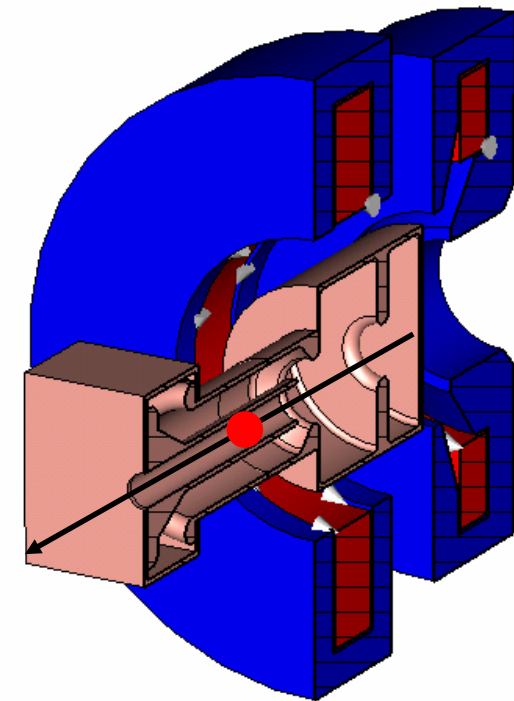
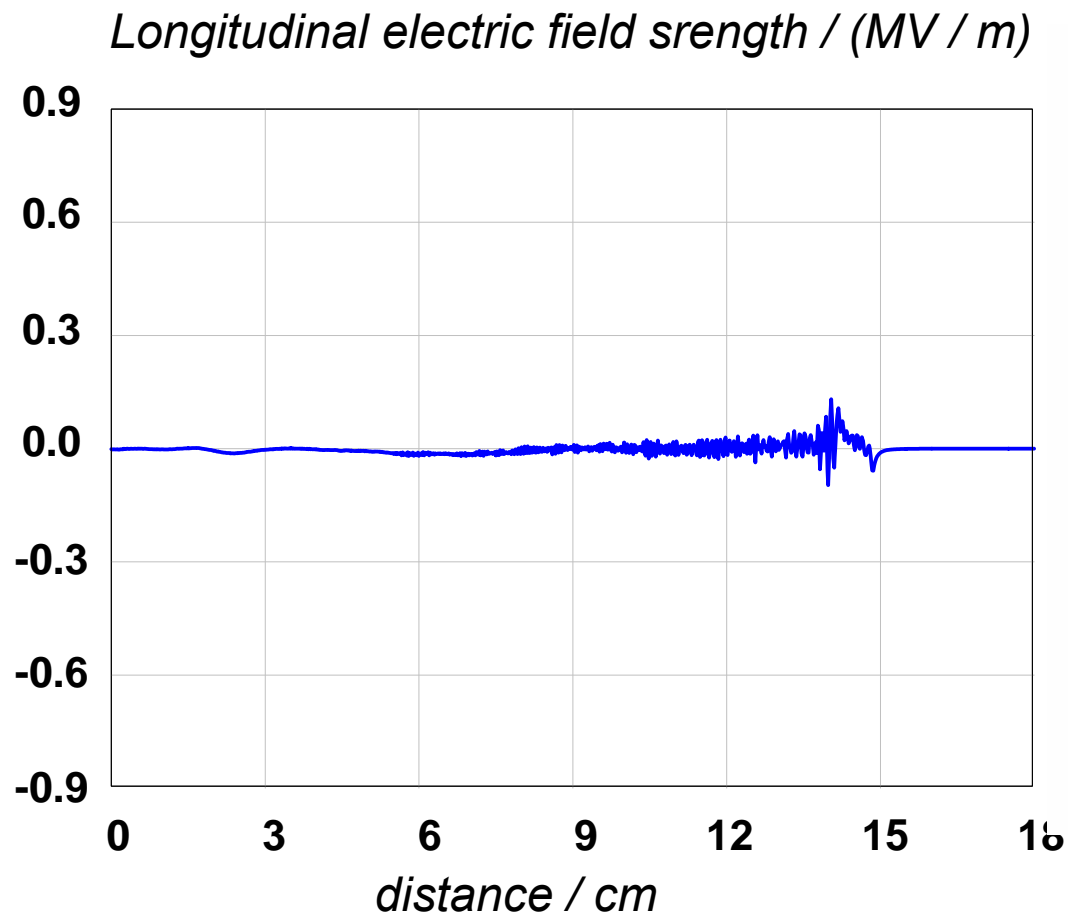


The European X-Ray Laser Project XFEL at DESY, Hamburg





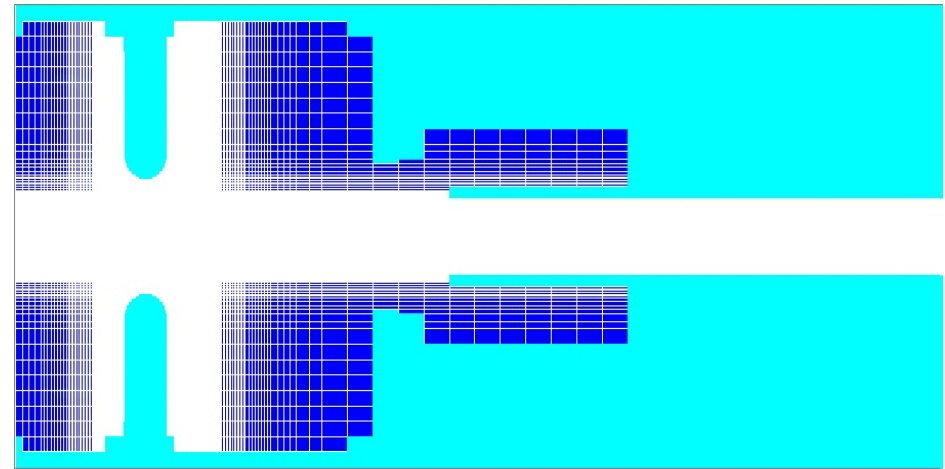
HF-Noise in PIC Simulations (PITZ Gun)



Numerical approaches for time domain simulations

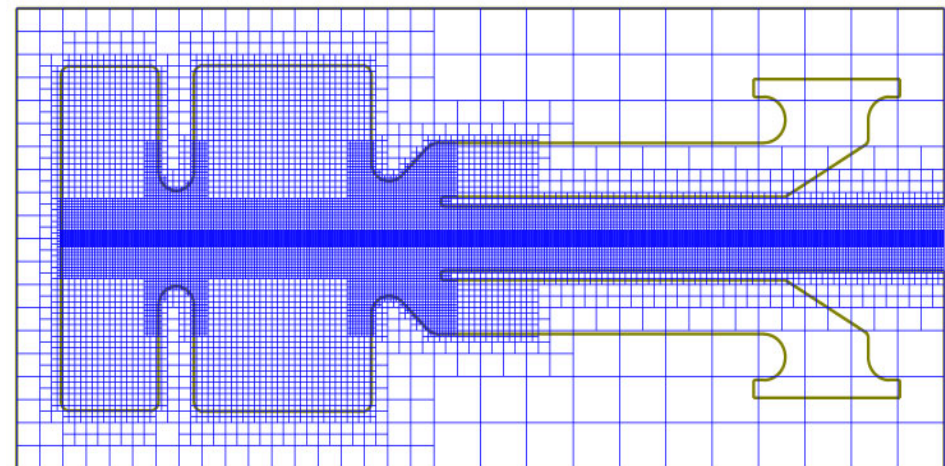
Time-adaptive mesh refinement

- “On the fly”-discretization of bunch and structure



Higher order FEM on unstructured grids

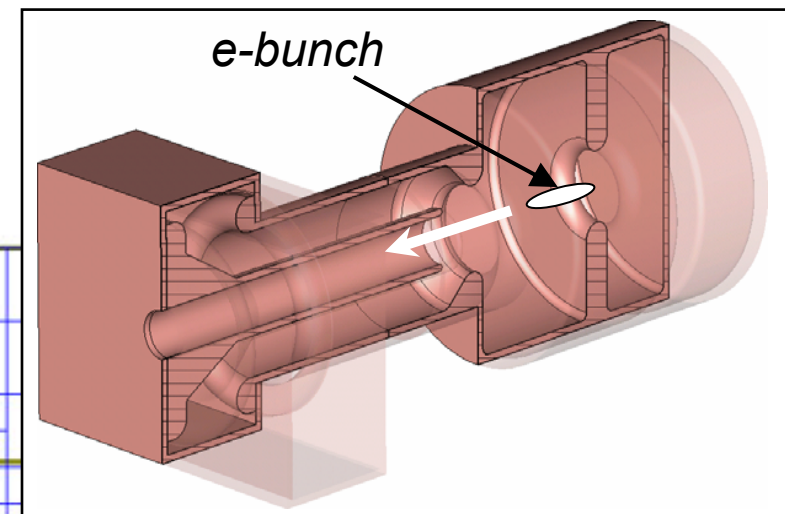
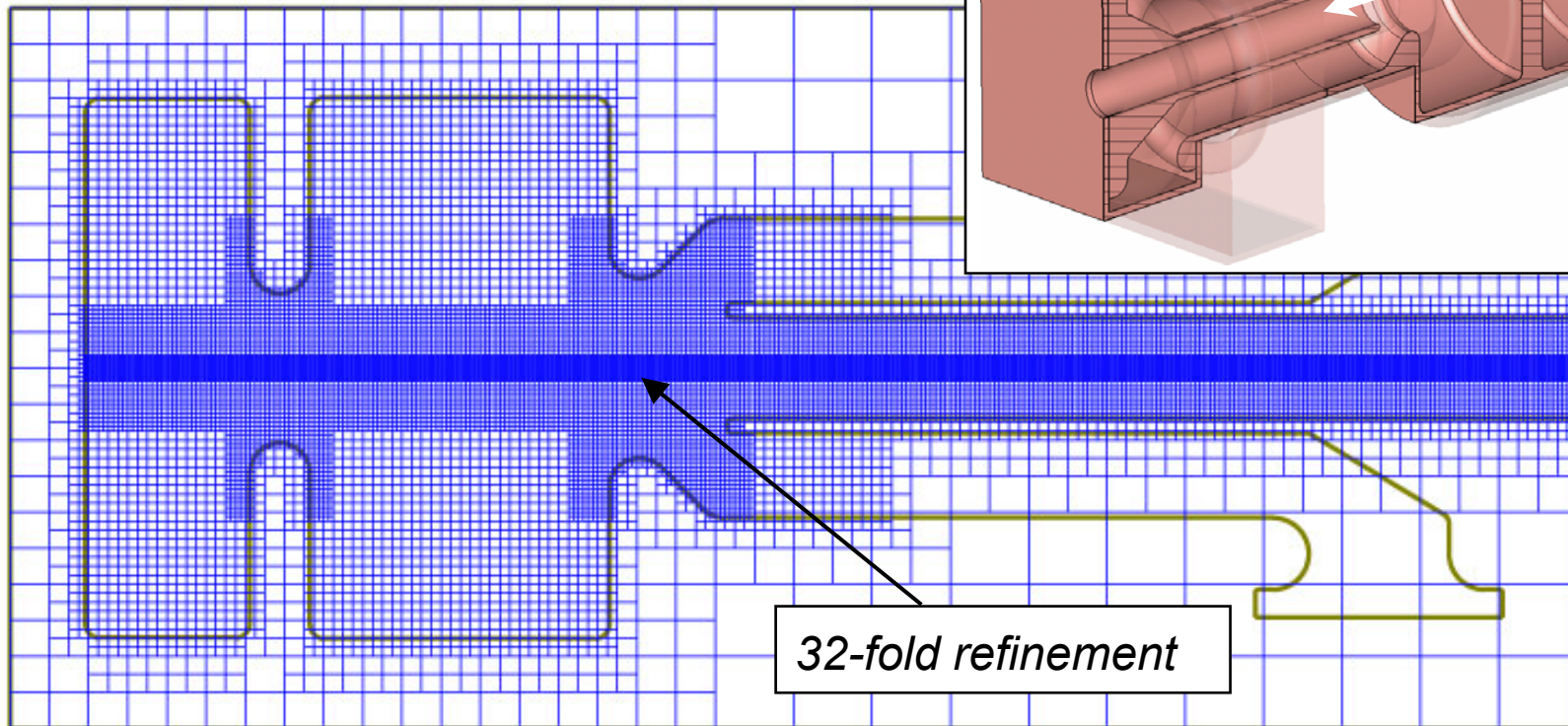
- Accuracy
- Local mesh refinement





Examples of local mesh refinement

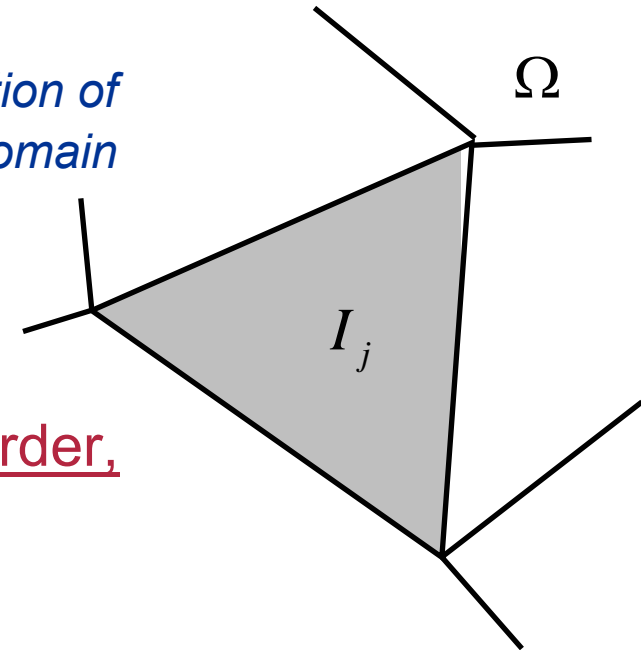
Discretization of the RF PITZ gun



The DG-FEM formulation for Maxwell Equations

$$\begin{cases} \frac{\partial \varepsilon \mathbf{E}}{\partial t} - \nabla \times \mathbf{H} = 0 \\ \frac{\partial \mu \mathbf{H}}{\partial t} + \nabla \times \mathbf{E} = 0 \end{cases}$$

*Discretization of
computational domain*



Approximate field components with high order, piecewise polynomial basis functions.

$$E_x(\mathbf{r}, t) \approx \bar{E}_x(\mathbf{r}, t) = \sum_{j,p} E_{j;p}^x(t) \varphi_{j;p}(\mathbf{r})$$

$$E_y(\mathbf{r}, t) \approx \bar{E}_y(\mathbf{r}, t) = \sum_{j,p} E_{j;p}^y(t) \varphi_{j;p}(\mathbf{r})$$

\vdots

$$H_z(\mathbf{r}, t) \approx \bar{H}_z(\mathbf{r}, t) = \sum_{j,p} H_{j;p}^z(t) \varphi_{j;p}(\mathbf{r})$$

$$\bar{\mathbf{E}}(\mathbf{r}, t) = \sum_{j,p} \mathbf{E}_{j;p}(t) \varphi_{j;p}(\mathbf{r})$$

$$\bar{\mathbf{H}}(\mathbf{r}, t) = \sum_{j,p} \mathbf{H}_{j;p}(t) \varphi_{j;p}(\mathbf{r})$$

Test approximate equations (e.g., Ampere's law)

$$\int_{I_i} d^3 \mathbf{r} \frac{\partial \varepsilon \bar{\mathbf{E}}}{\partial t} \varphi - \int_{I_i} d^3 \mathbf{r} \nabla \times \bar{\mathbf{H}} \varphi = \int_{I_i} d^3 \mathbf{r} \frac{\partial \varepsilon \bar{\mathbf{E}}}{\partial t} \varphi - \int_{I_i} d^3 \mathbf{r} \nabla \times (\bar{\mathbf{H}} \varphi) + \int_{I_i} d^3 \mathbf{r} (\nabla \varphi) \times \bar{\mathbf{H}} = 0$$

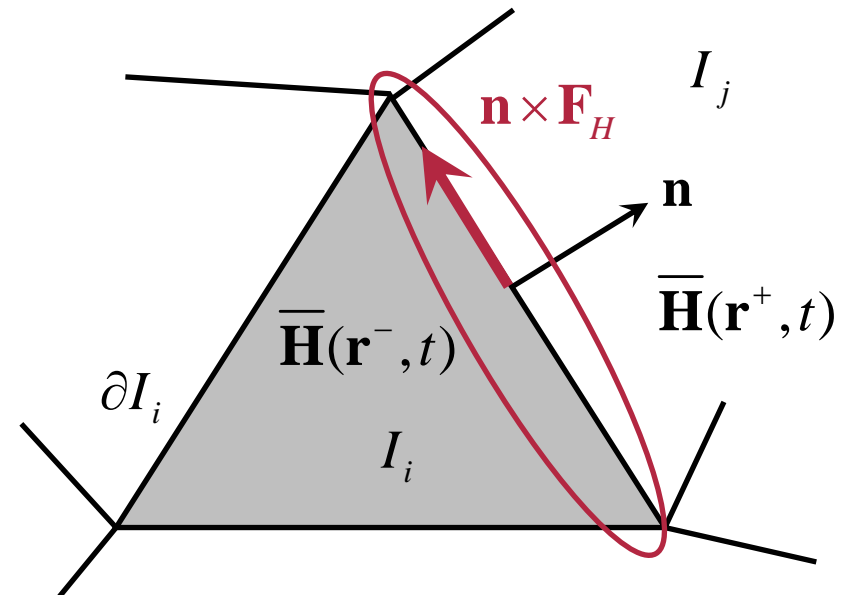
$$\Rightarrow \int_{I_i} d^3 \mathbf{r} \frac{\partial \varepsilon \bar{\mathbf{E}}}{\partial t} \varphi - \int_{\partial I_i} d^2 \mathbf{r} (\mathbf{n} \times \mathbf{F}_H) \varphi + \int_{I_i} d^3 \mathbf{r} (\nabla \varphi) \times \bar{\mathbf{H}} = 0$$

numerical flux

Ansatz: centered flux for tangential fields at element boundaries:

$$\mathbf{n} \times \mathbf{F}_E = \frac{1}{2} \mathbf{n} \times [\bar{\mathbf{E}}(\mathbf{r}^-, t) + \bar{\mathbf{E}}(\mathbf{r}^+, t)],$$

$$\mathbf{n} \times \mathbf{F}_H = \frac{1}{2} \mathbf{n} \times [\bar{\mathbf{H}}(\mathbf{r}^-, t) + \bar{\mathbf{H}}(\mathbf{r}^+, t)]$$





Matrix representation of semidiscrete equations

$$\frac{d}{dt} \begin{pmatrix} \mathbf{M}_\varepsilon \mathbf{e} \\ \mathbf{M}_\mu \mathbf{h} \end{pmatrix} + \begin{pmatrix} 0 & -\mathbf{C} \\ \mathbf{C}^T & 0 \end{pmatrix} \begin{pmatrix} \mathbf{e} \\ \mathbf{h} \end{pmatrix} = \begin{pmatrix} 0 \\ 0 \end{pmatrix}$$

semidiscrete DG formulation

skew-symmetric

$$\mathbf{e} = \begin{pmatrix} \mathbf{e}_x \\ \mathbf{e}_y \\ \mathbf{e}_z \end{pmatrix}, \quad \mathbf{h} = \begin{pmatrix} \mathbf{h}_x \\ \mathbf{h}_y \\ \mathbf{h}_z \end{pmatrix}$$

Recovers FDTD for piecewise constant basis functions, on Cartesian grids

symmetric, positive, (block-) diagonal

symmetric: $\mathbf{C}^T = \mathbf{C}$

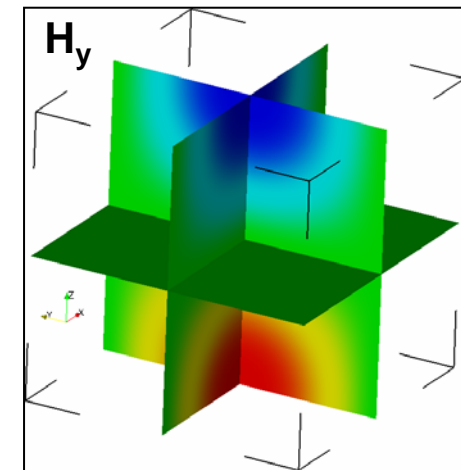
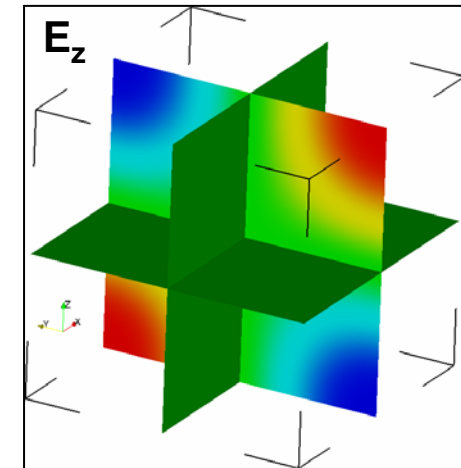
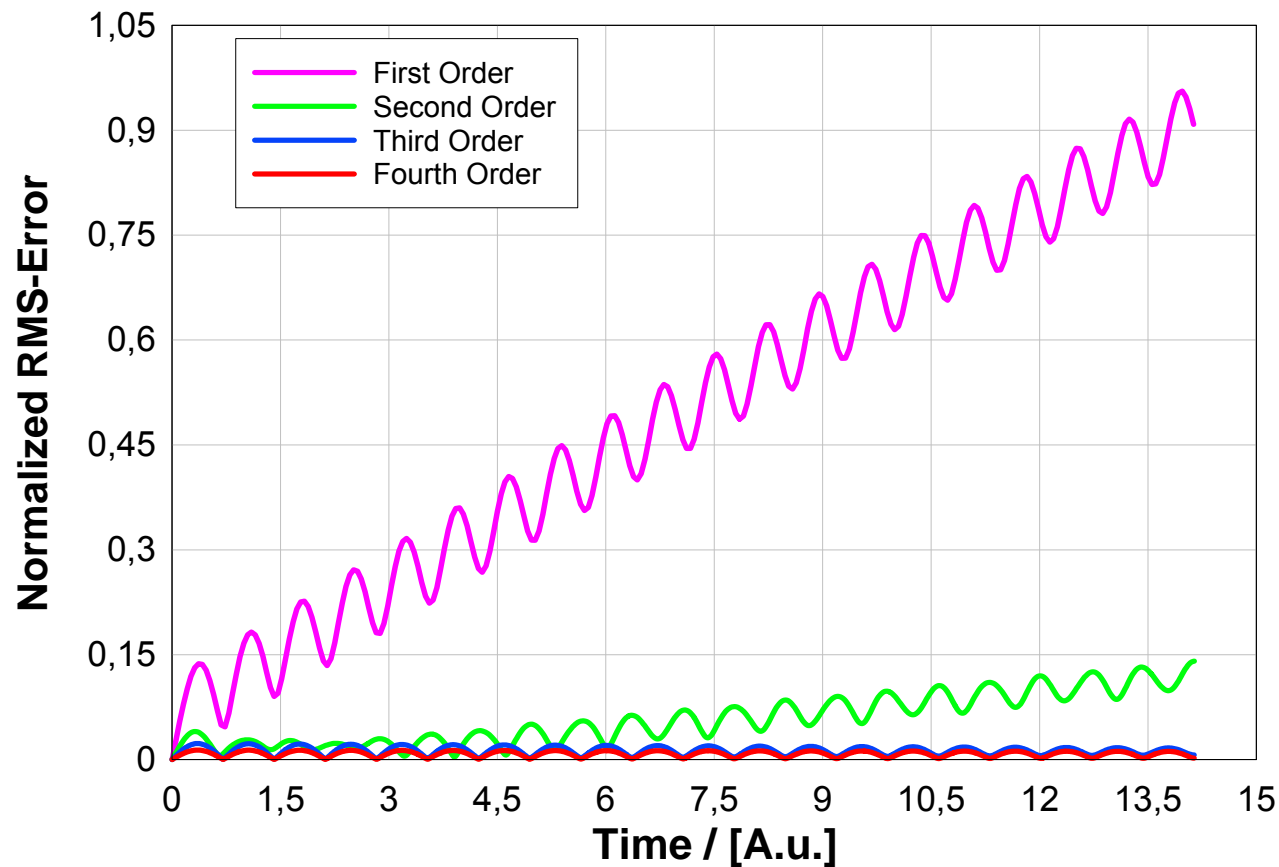
$$\mathbf{M}_\varepsilon = \begin{pmatrix} \mathbf{M}_{\varepsilon_x} & 0 & 0 \\ 0 & \mathbf{M}_{\varepsilon_y} & 0 \\ 0 & 0 & \mathbf{M}_{\varepsilon_z} \end{pmatrix},$$

$$\mathbf{M}_\mu = \begin{pmatrix} \mathbf{M}_{\mu_x} & 0 & 0 \\ 0 & \mathbf{M}_{\mu_y} & 0 \\ 0 & 0 & \mathbf{M}_{\mu_z} \end{pmatrix},$$

$$\mathbf{C} = \begin{pmatrix} 0 & -\mathbf{P}_z & \mathbf{P}_y \\ \mathbf{P}_z & 0 & -\mathbf{P}_x \\ -\mathbf{P}_y & \mathbf{P}_x & 0 \end{pmatrix}$$

Periodic solution in resonator box

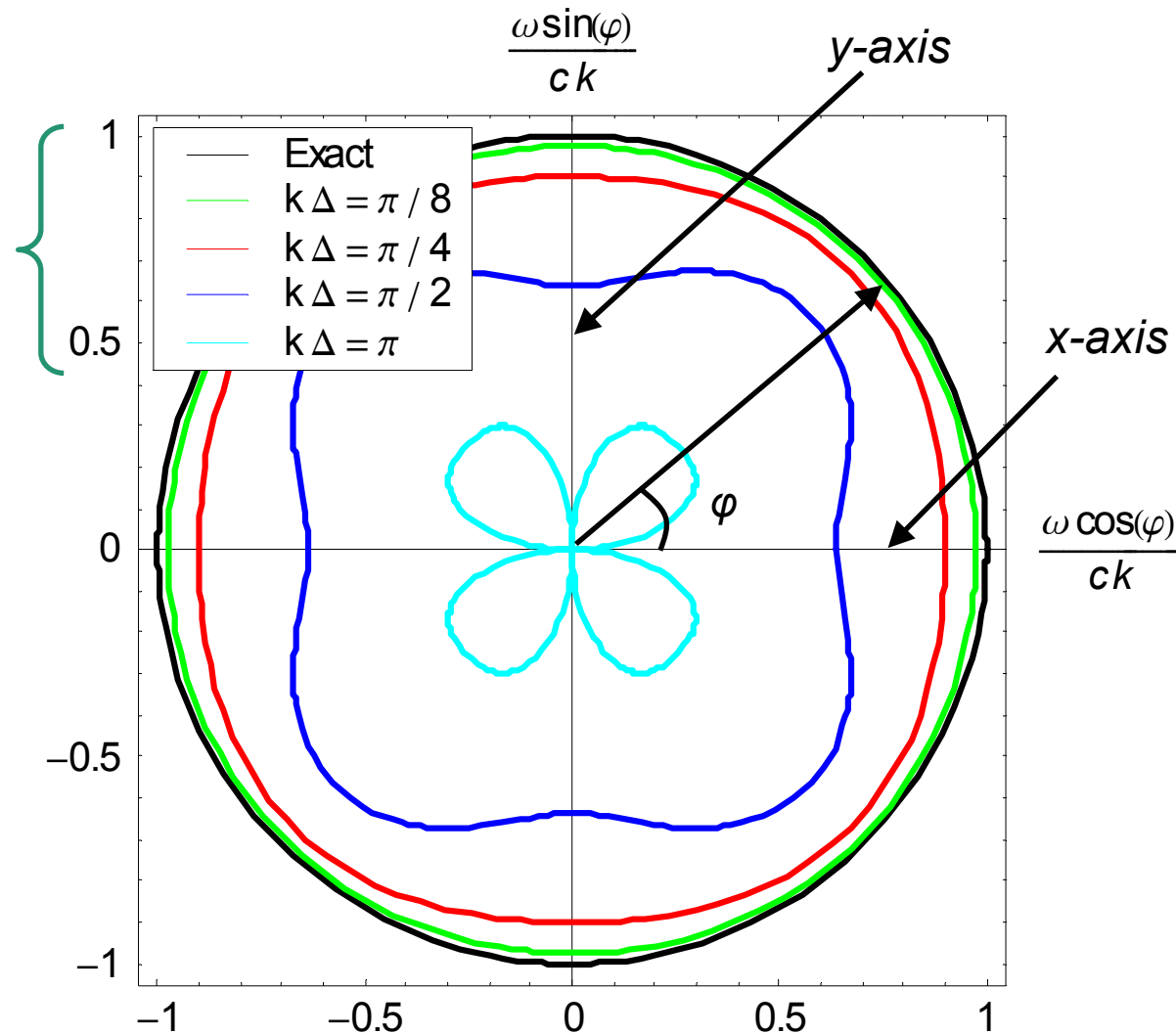
Dispersion error for EM_{111} mode





Dispersion analysis. The $P^0 \times P^0 \times P^0$ -case

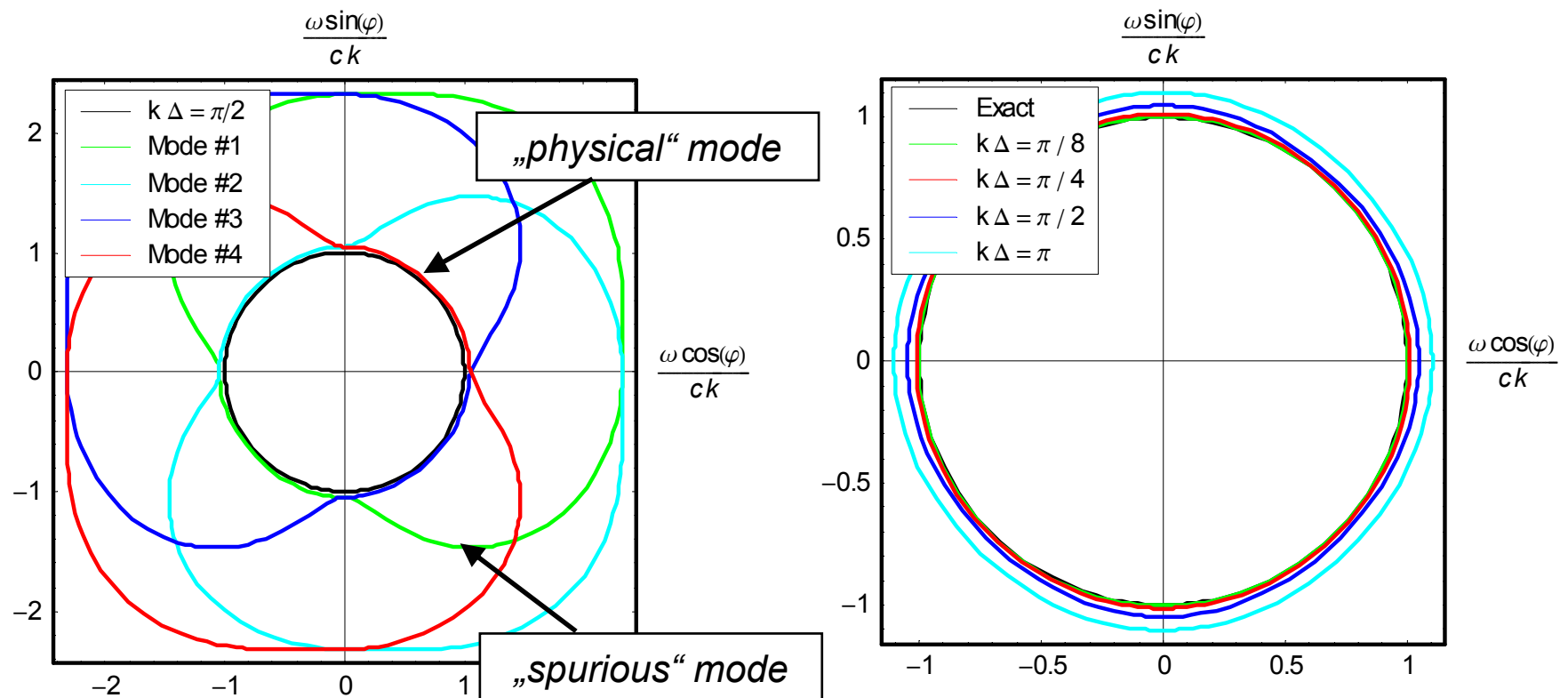
*~ grid points
/ wave length*





Dispersion analysis. The $P^1 \times P^1 \times P^1$ -case

Dispersion curves in the xy -plane





The Problem of Charge Conservation

Define a (consistent) divergence operator as: $\mathbf{S} = (\mathbf{P}_x \quad \mathbf{P}_y \quad \mathbf{P}_z)$

Continuity equations for electric and magnetic charges:

$$\frac{d}{dt}(\mathbf{S} \square \mathbf{d}) = \frac{d}{dt}(\mathbf{S} \square \mathbf{M}_\varepsilon \mathbf{e}) = \frac{d}{dt}(\mathbf{S} \square \mathbf{C} \mathbf{h}) \stackrel{?}{=} 0 \quad (\text{source free case})$$

$$\frac{d}{dt}(\mathbf{S} \square \mathbf{b}) = \frac{d}{dt}(\mathbf{S} \square \mathbf{M}_\mu \mathbf{h}) = -\frac{d}{dt}(\mathbf{S} \square \mathbf{C} \mathbf{e}) \stackrel{?}{=} 0$$

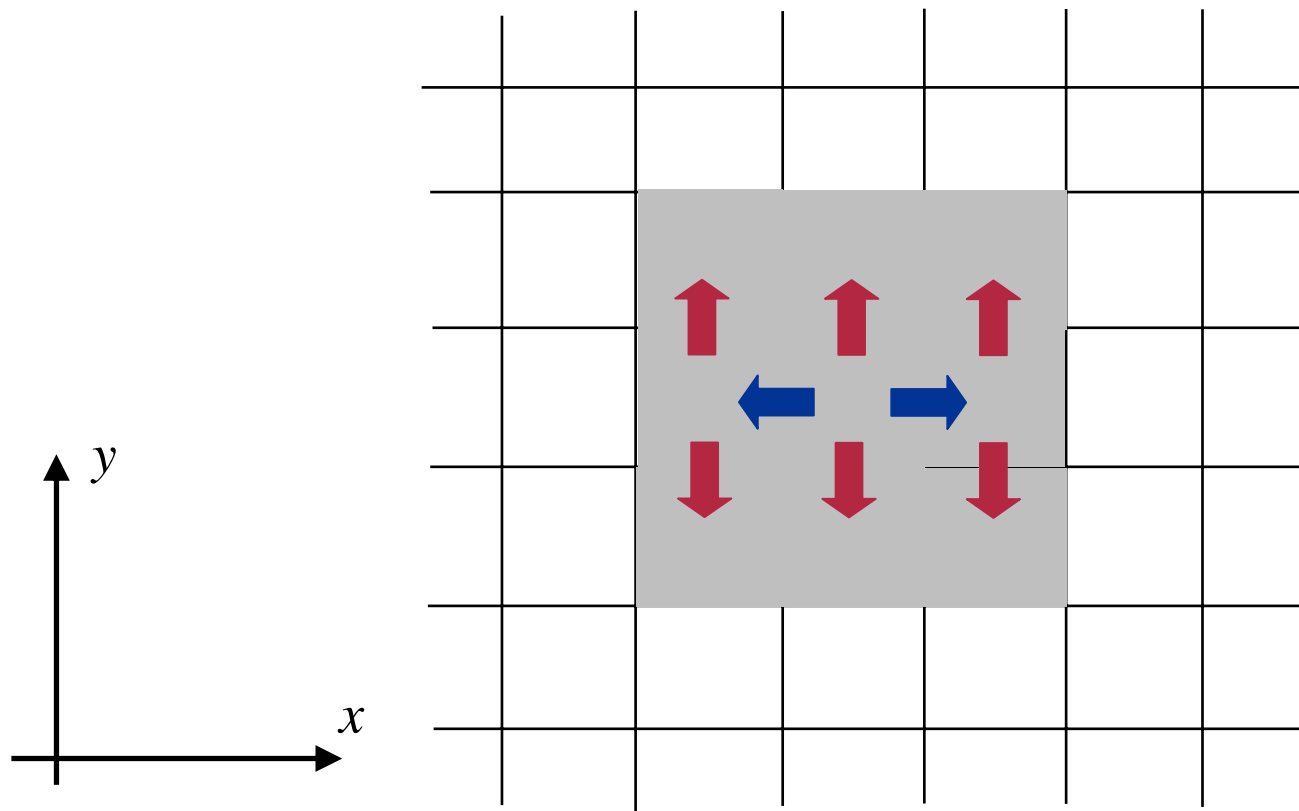
Sufficient and necessary conditions for charge conservation:

1. $\mathbf{S} \square \mathbf{C} = 0$
2. $[\mathbf{P}_x, \mathbf{P}_y] = [\mathbf{P}_x, \mathbf{P}_z] = [\mathbf{P}_y, \mathbf{P}_z] = 0$ pairwise commuting derivatives



The tensor product case

*Domain of influence of product
derivative operators*

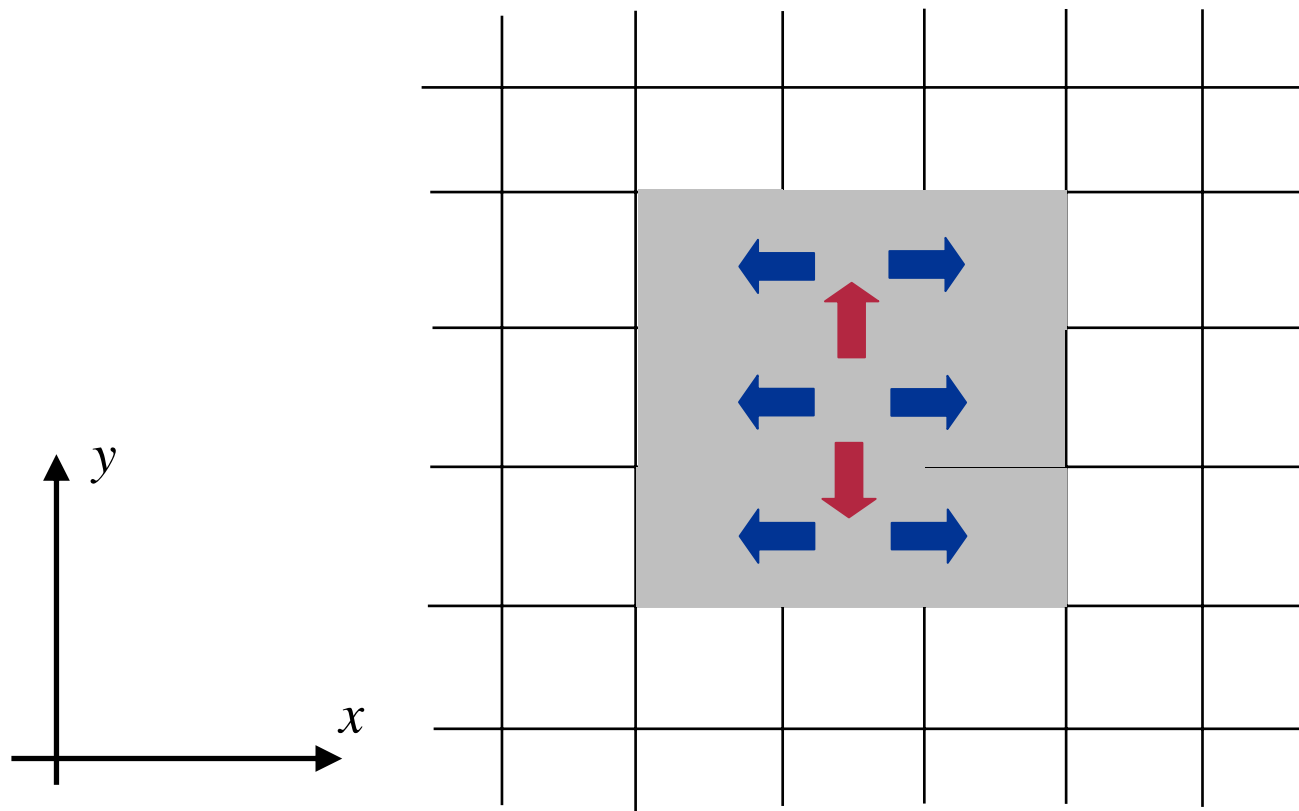


$$\mathbf{P}_y \square \mathbf{P}_x$$



The tensor product case

*Domain of influence of product
derivative operators*

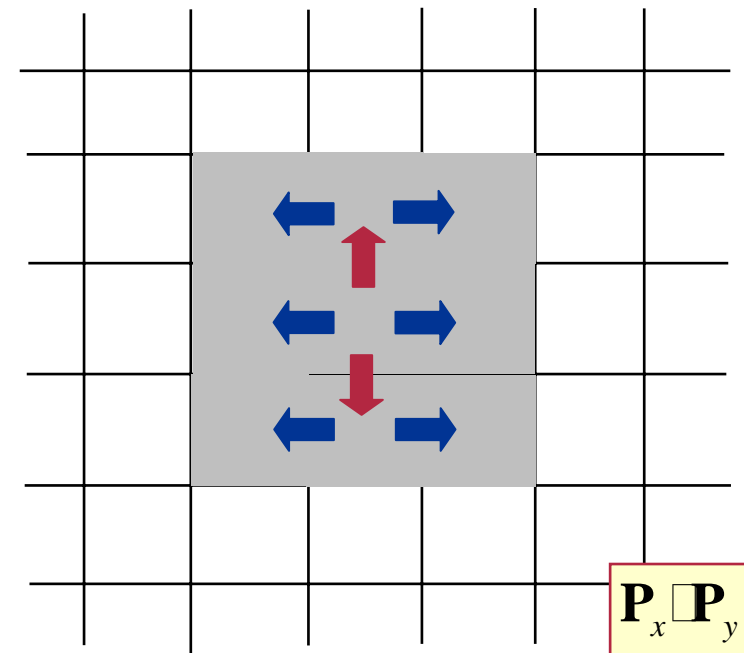
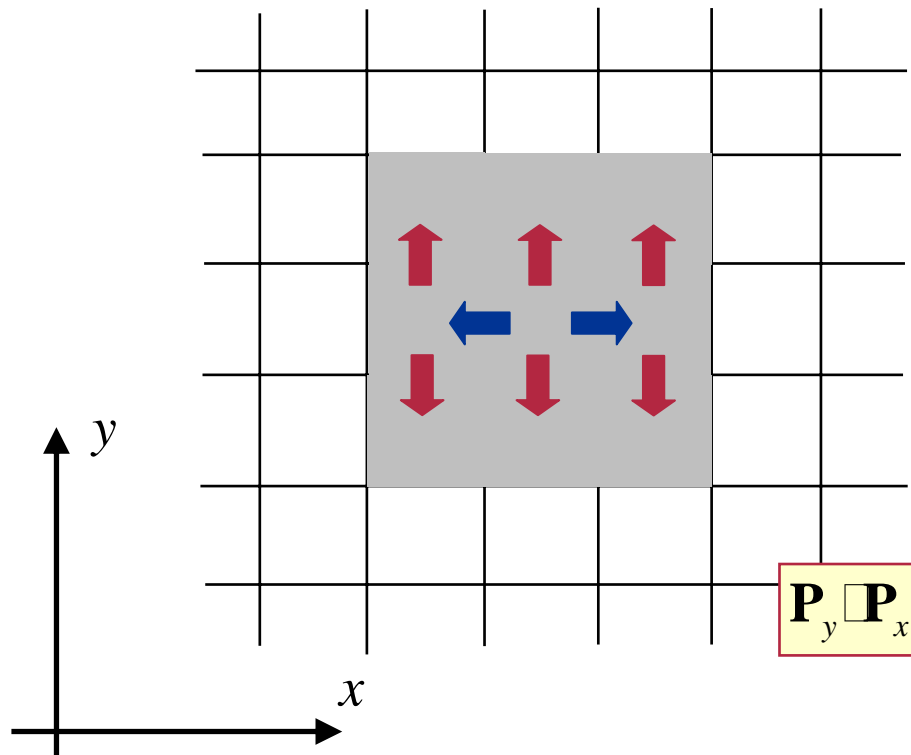


$$\mathbf{P}_x \square \mathbf{P}_y$$



The tensor product case

Domain of influence of product derivative operators



Conservation of discrete charges on regular grids (PIC).

Gjonaj, Lau, Weiland, ICEAA 2007



Example of a long-distance PIC simulation with DG-FEM (later...)

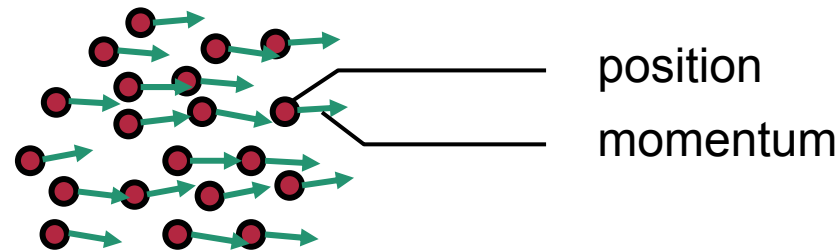
Current work on PIC codes at TEMF

1. Application for the PITZ injector
2. Development of moving grid algorithms (S. Schnepf)
3. Combined (hp-) grid / order refinement
4. Dynamic parallel partitioning for higher order

- Basic principle

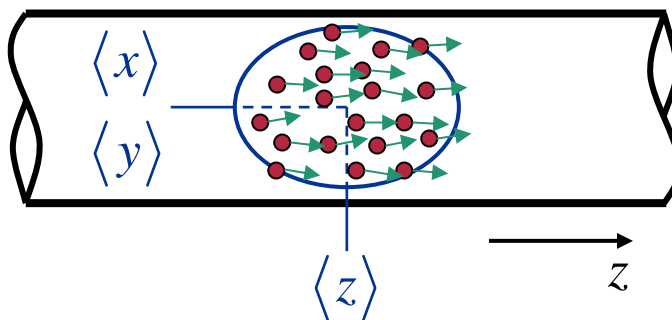
Description of the particle distribution by moments

Distribution:



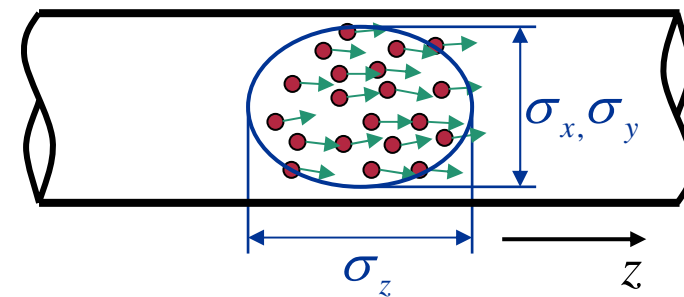
First order moments:

$$\langle x \rangle = \int x f \, d\vec{r} d\vec{p}$$



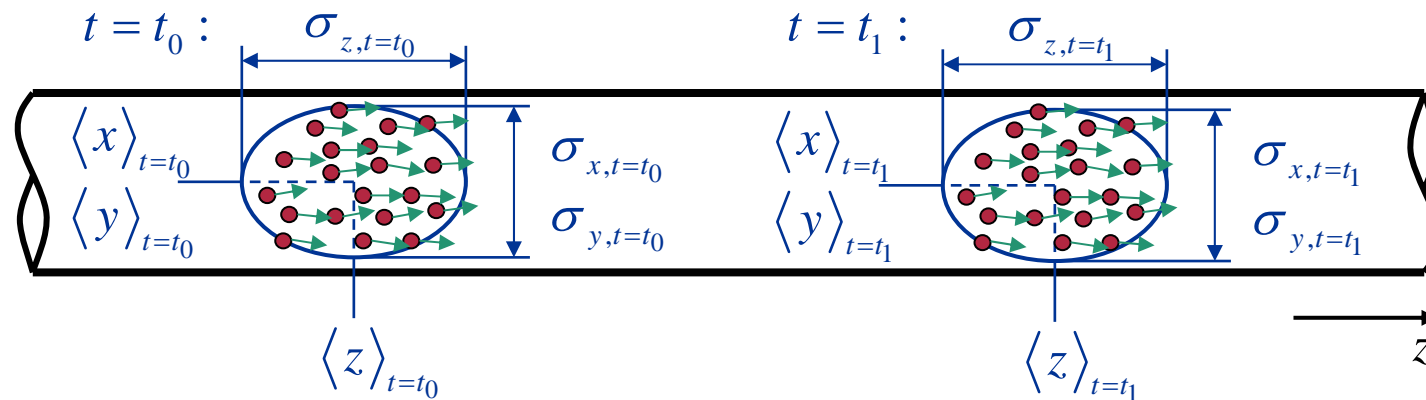
Second order moments:

$$\sigma_x^2 = \int (x - \langle x \rangle)^2 f \, d\vec{r} d\vec{p}$$

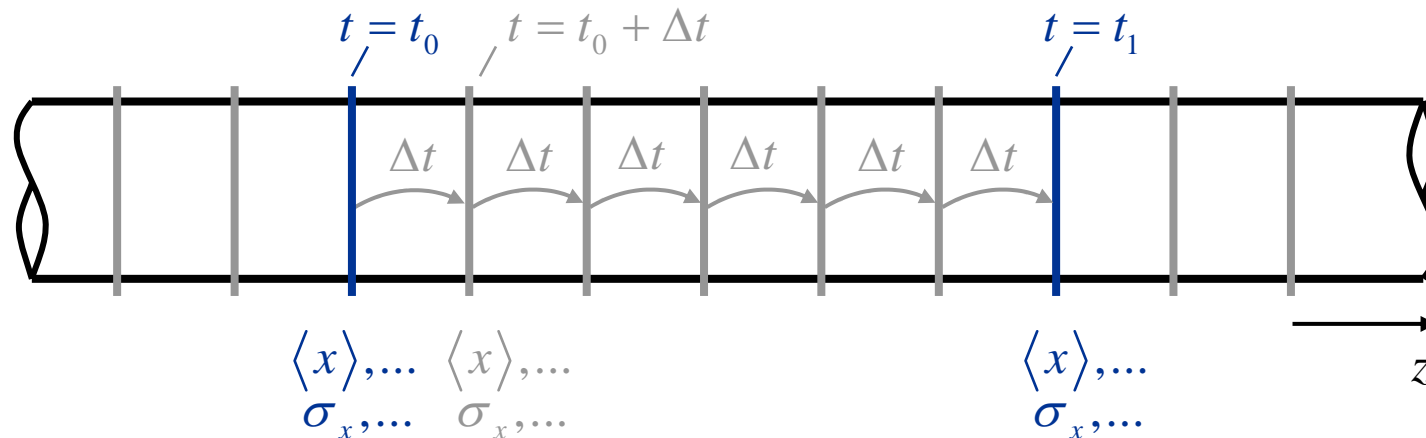


- Evolution of the moments in time

Bunch parameter at different time instants



Simplified description





- Possible ensemble parameter (1)

Raw moments

$$\mu_{ijk}(x, y, z) = \langle x^i \cdot y^j \cdot z^k \rangle$$

$$\langle \mu \rangle = \int \mu \cdot f \, d\vec{r} d\vec{p}$$

Order 0: $\mu_{000} = 1$

Order 1: $\mu_{100} = \langle x \rangle, \mu_{010} = \langle y \rangle, \mu_{001} = \langle z \rangle$

Order 2: $\mu_{200} = \langle x^2 \rangle, \mu_{020} = \langle y^2 \rangle, \mu_{002} = \langle z^2 \rangle$

$\mu_{110} = \langle xy \rangle, \mu_{101} = \langle xz \rangle, \mu_{011} = \langle yz \rangle$

Order 3: ...

Property

$$\mu_{ijk}(x-a, y-b, z-c) \neq \mu_{ijk}(x, y, z)$$

(not translatory invariant)



- Possible ensemble parameter (2)

Centralized moments

$$\sigma_{ijk}(x, y, z) = \left\langle \left(x - \langle x \rangle \right)^i \cdot \left(y - \langle y \rangle \right)^j \cdot \left(z - \langle z \rangle \right)^k \right\rangle$$

$$\langle \mu \rangle = \int \mu \cdot f \, d\vec{r} d\vec{p}$$

Order 0: $\sigma_{000} = 1$

Order 1: $\sigma_{100} = 0, \quad \sigma_{010} = 0, \quad \sigma_{001} = 0$

Order 2: $\sigma_{200} = \sigma_x^2, \quad \sigma_{020} = \sigma_y^2, \quad \sigma_{002} = \sigma_z^2$ (variance)

$\sigma_{110} = \sigma_{xy}, \quad \sigma_{101} = \sigma_{xz}, \quad \sigma_{011} = \sigma_{yz}$ (covariance)

Order 3: ...

Property

$$\sigma_{ijk}(x-a, y-b, z-c) = \sigma_{ijk}(x, y, z) \quad (\text{translatory invariant})$$



- Appropriate moments in 6-D phase space

Order 1: $M_\mu = \langle \mu \rangle \quad \mu \in \{x, y, z, p_x, p_y, p_z\}$

$$(M_x, M_y, M_z, M_{p_x}, M_{p_y}, M_{p_z})$$

$${}^w C_6^1 = \binom{6}{1} = 6$$

$\Sigma 6$

Order 2: $M_{\mu\nu} = \langle (\mu - \langle \mu \rangle) \cdot (\nu - \langle \nu \rangle) \rangle \quad \mu, \nu \in \{x, y, z, p_x, p_y, p_z\}$

$$\begin{pmatrix} M_{xx} & M_{xy} & M_{xz} & M_{xp_x} & M_{xp_y} & M_{xp_z} \\ M_{yx} & M_{yy} & M_{yz} & M_{yp_x} & M_{yp_y} & M_{yp_z} \\ M_{zx} & M_{zy} & M_{zz} & M_{zp_x} & M_{zp_y} & M_{zp_z} \\ M_{p_x x} & M_{p_x y} & M_{p_x z} & M_{p_x p_x} & M_{p_x p_y} & M_{p_x p_z} \\ M_{p_y x} & M_{p_y y} & M_{p_y z} & M_{p_y p_x} & M_{p_y p_y} & M_{p_y p_z} \\ M_{p_z x} & M_{p_z y} & M_{p_z z} & M_{p_z p_x} & M_{p_z p_y} & M_{p_z p_z} \end{pmatrix}$$

$${}^w C_6^2 = \binom{7}{2} = 21$$

$\Sigma 27$

Order 3: ...

$${}^w C_6^3 = \binom{8}{3} = 56$$

$\Sigma 83$

Order 4: ...

$${}^w C_6^4 = \binom{9}{4} = 126$$

$\Sigma 209$



- Number of moments in 6-D phase space

Order	Moments per order	Total number of moments
1	6	6
2	21	27
3	56	83
4	126	209
5	252	461
6	462	923
7	792	1715
8	1287	3002
9	2002	5004
10	3003	8007



- Method to solve the VLASOV equation

- Basic formulation

$$\frac{\partial f}{\partial \tau} + \frac{\partial f}{\partial \vec{r}} \cdot \frac{\vec{p}}{\gamma} + \frac{\partial f}{\partial \vec{p}} \cdot \frac{\vec{F}}{m_0 c^2} = 0 \quad \vec{F} = \text{LORENTZ force}$$

- Moment approach

- Integration over phase space reduces PDE to ODE
 - Approximation: **limited amount of moments** used to describe the particle distribution function

$$\frac{\partial \langle \mu \rangle}{\partial \tau} = \frac{\partial}{\partial \tau} \int_{\infty} \mu f(\tau, \vec{r}, \vec{p}) d\vec{r} d\vec{p} \quad \rightarrow \quad \text{time evolution}$$

- Evolution of raw and centralized moments in time

$$\begin{aligned}
 \frac{\partial \langle \mu \rangle}{\partial \tau} &= \frac{\partial}{\partial \tau} \int \mu f \, d\vec{r} d\vec{p} & \mu \in \left\{ x, y, z, p_x, p_y, p_z, x^2, \dots, (x - \langle x \rangle)^2, \dots \right\} \\
 &= \int \frac{\partial \mu f}{\partial \tau} \, d\vec{r} d\vec{p} = \int \left(f \frac{\partial \mu}{\partial \tau} + \mu \frac{\partial f}{\partial \tau} \right) d\vec{r} d\vec{p} \\
 &= \int f \left(\text{grad}_{\langle \vec{r} \rangle} (\mu) \cdot \frac{\partial \langle \vec{r} \rangle}{\partial \tau} + \text{grad}_{\langle \vec{p} \rangle} (\mu) \cdot \frac{\partial \langle \vec{p} \rangle}{\partial \tau} \right) d\vec{r} d\vec{p} \\
 &\quad - \int \mu \left(\text{grad}_{\vec{r}} (f) \cdot \frac{\vec{p}}{\gamma} + \text{grad}_{\vec{p}} (f) \cdot \frac{\vec{F}}{m_0 c^2} + f \, \text{div}_{\vec{p}} \left(\frac{\vec{F}}{m_0 c^2} \right) \right) d\vec{r} d\vec{p}
 \end{aligned}$$

$$\begin{aligned}
 \frac{\partial \langle \mu \rangle}{\partial \tau} &= \left\langle \text{grad}_{\langle \vec{r} \rangle} (\mu) \right\rangle \cdot \left\langle \frac{\vec{p}}{\gamma} \right\rangle + \left\langle \text{grad}_{\langle \vec{p} \rangle} (\mu) \right\rangle \cdot \left\langle \frac{\vec{F}}{m_0 c^2} \right\rangle \\
 &\quad + \left\langle \text{grad}_{\vec{r}} (\mu) \cdot \frac{\vec{p}}{\gamma} \right\rangle + \left\langle \text{grad}_{\vec{p}} (\mu) \cdot \frac{\vec{F}}{m_0 c^2} \right\rangle
 \end{aligned}$$

$$\tau = c \cdot t$$

$$\lim_{\vec{r}, \vec{p} \rightarrow \infty} (f) = 0$$



- Evolution of raw and centralized moments in time

General form:

$$\begin{aligned} \frac{\partial \langle \mu \rangle}{\partial \tau} = & \left\langle \text{grad}_{\langle \vec{r} \rangle} (\mu) \right\rangle \cdot \left\langle \frac{\vec{p}}{\gamma} \right\rangle + \left\langle \text{grad}_{\langle \vec{p} \rangle} (\mu) \right\rangle \cdot \left\langle \frac{\vec{F}}{m_0 c^2} \right\rangle \\ & + \left\langle \text{grad}_{\vec{r}} (\mu) \cdot \frac{\vec{p}}{\gamma} \right\rangle + \left\langle \text{grad}_{\vec{p}} (\mu) \cdot \frac{\vec{F}}{m_0 c^2} \right\rangle \end{aligned}$$

$$\tau = c \cdot t$$

First component, order 1:

$$\begin{aligned} \frac{\partial \langle x \rangle}{\partial \tau} &= \left\langle \frac{p_x}{\gamma} \right\rangle \\ \frac{\partial \langle p_x \rangle}{\partial \tau} &= \left\langle \frac{F_x}{m_0 c^2} \right\rangle \end{aligned}$$

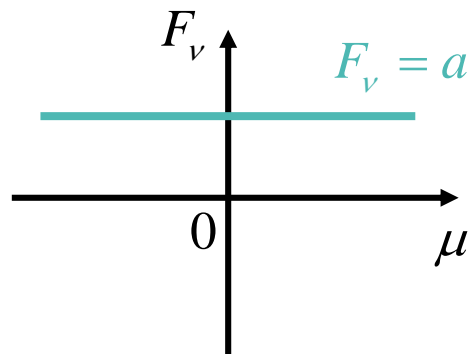
Aim:

Expand all arguments of the right hand side such that the resulting expression can be interpreted as a moment description form

- Incorporation of the influencing forces

TAYLOR series expansion

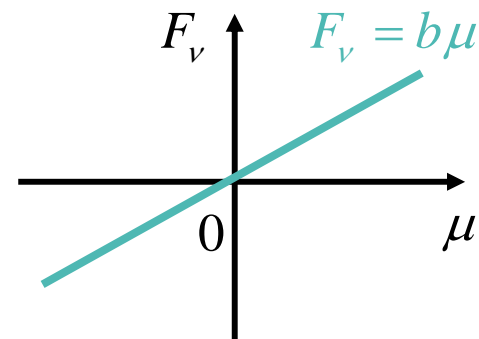
constant



$$\langle F_v \rangle = a$$

$$\langle \mu F_v \rangle = 0$$

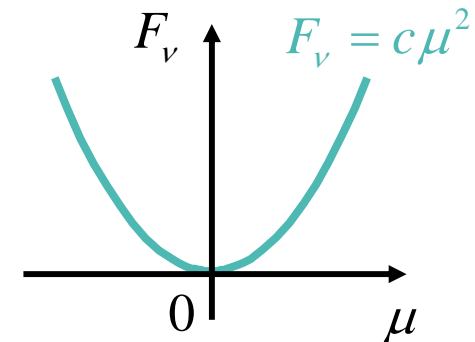
linear



$$\langle F_v \rangle = 0$$

$$\langle \mu F_v \rangle = b M_{\mu\mu}$$

quadratic



$$\langle F_v \rangle = c M_{\mu\mu}$$

$$\langle \mu F_v \rangle = c M_{\mu\mu\mu}$$

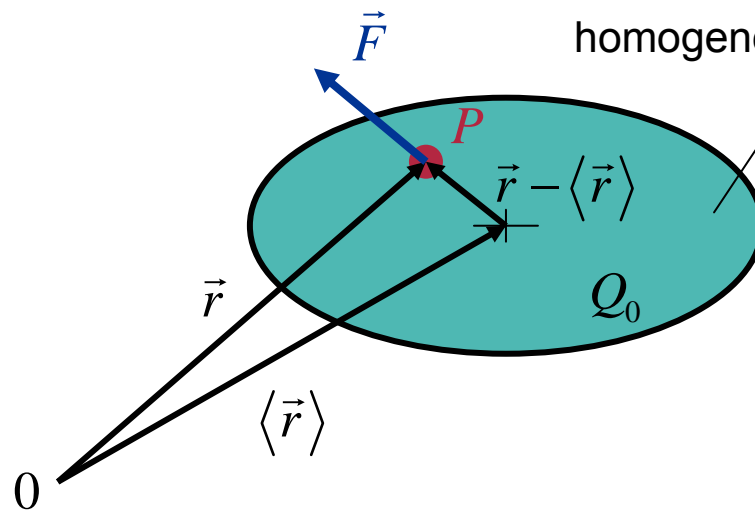
Series expansion of the forces for all beam line elements



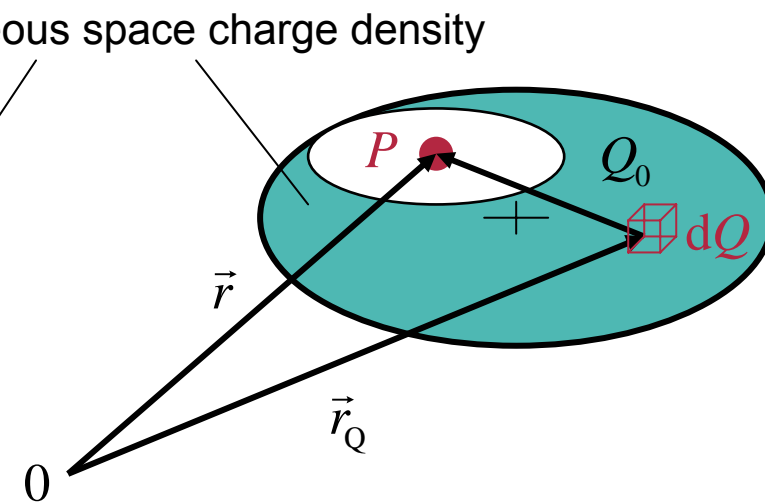
Dipole magnets, quadrupoles, solenoids, resonators, ...

- Linear space charge model

Configuration



Calculation



$$\vec{F}(\vec{r}) \approx G \left(\frac{2\gamma\sigma_z}{\sigma_x + \sigma_y} \right) \cdot \frac{eQ_0}{\gamma^2} \cdot \frac{\vec{r} - \langle \vec{r} \rangle}{V_G}$$

$$G(u) = (1 - \exp(-u)) \cdot \begin{pmatrix} 1 & 0 & 0 \\ 0 & 1 & 0 \\ 0 & 0 & \gamma/u \end{pmatrix}$$



- Implementation using a symbolic algebra program



Mathematica

(sequence of algebraic transformations)

$$\frac{\partial \langle \mu \rangle}{c \partial t} = \langle \text{grad}_{\langle \vec{r} \rangle}(\mu) \rangle \cdot \langle \frac{\vec{p}}{\gamma} \rangle + \langle \text{grad}_{\vec{p}}(\mu) \cdot \frac{\vec{F}}{m_0 c^2} \rangle$$

$$+ \langle \text{grad}_{\langle \vec{p} \rangle}(\mu) \rangle \cdot \langle \frac{\vec{F}}{m_0 c^2} \rangle + \langle \text{grad}_{\vec{r}}(\mu) \cdot \frac{\vec{p}}{\gamma} \rangle$$



Visual.cpp

...



Tracking.cpp



CDipole.cpp

...

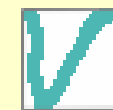


CQuadrupole.cpp



C++ Compiler

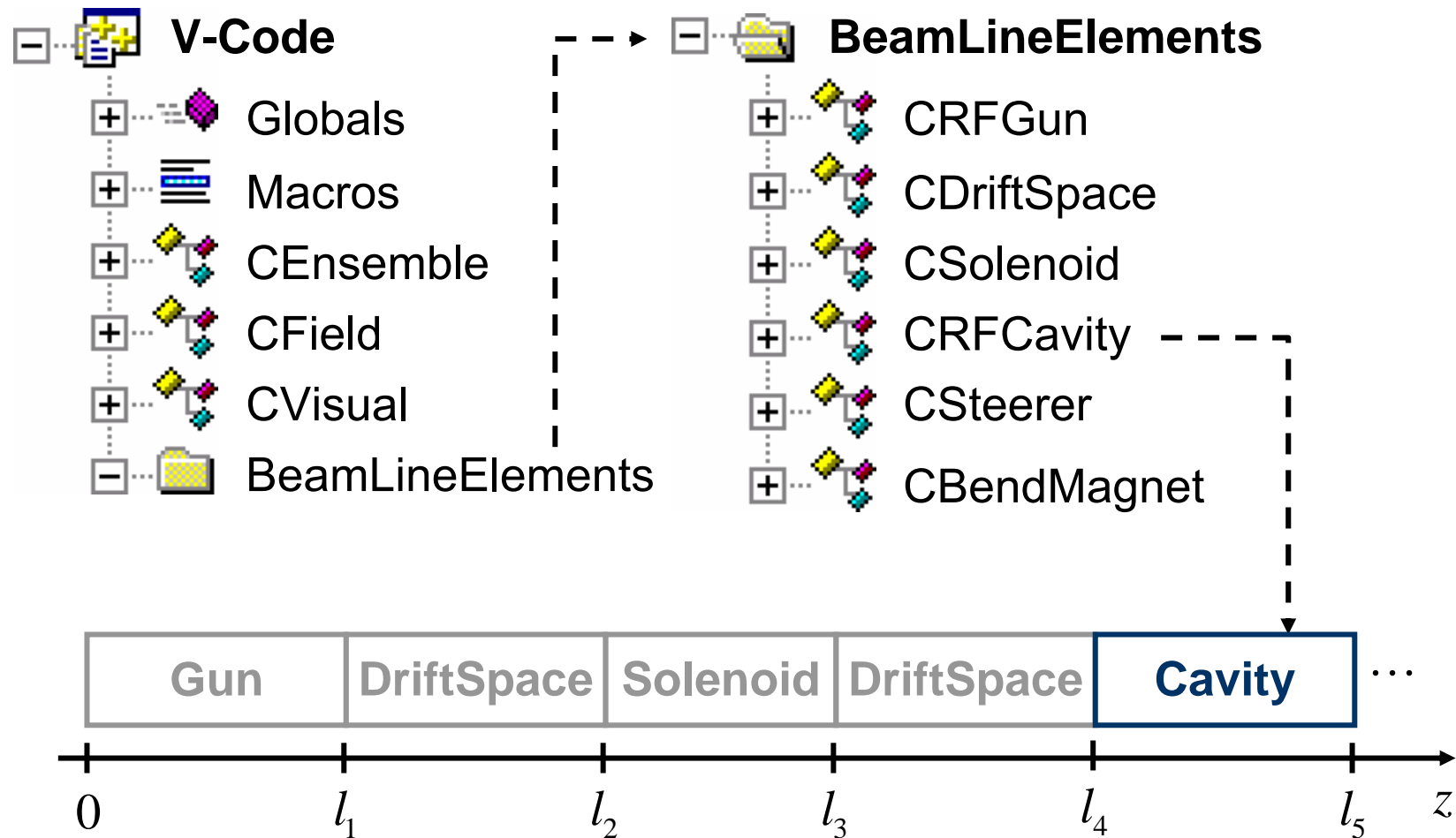
(user interface, time integration, administration of BLE)



V-Code.exe

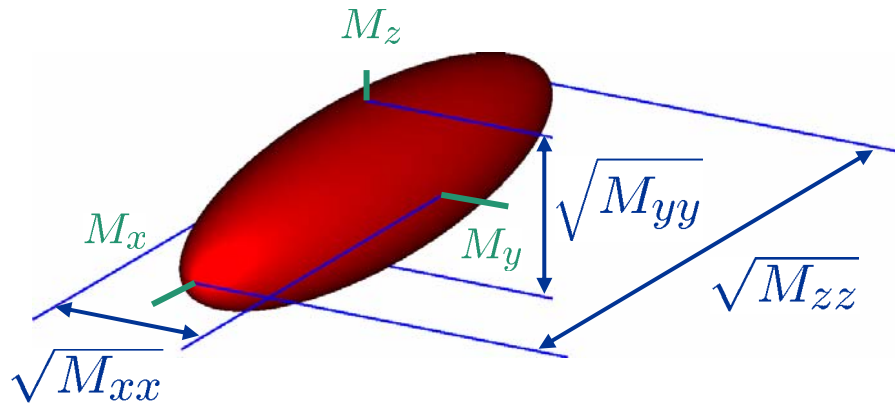


- Decomposition in individual beam line elements



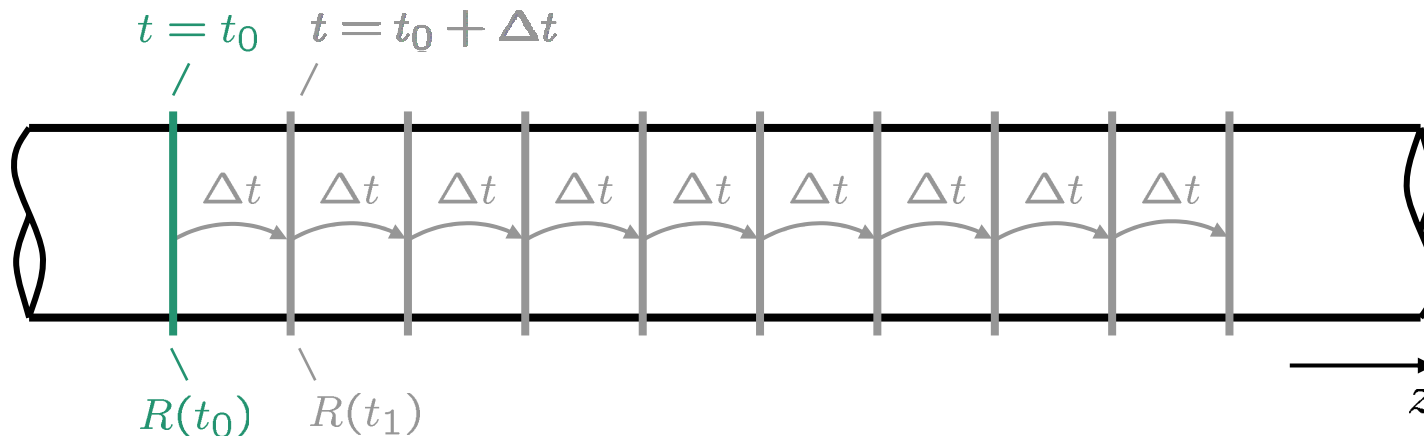
- Solving the assembled moment equations

- Time dependent ensemble parameter



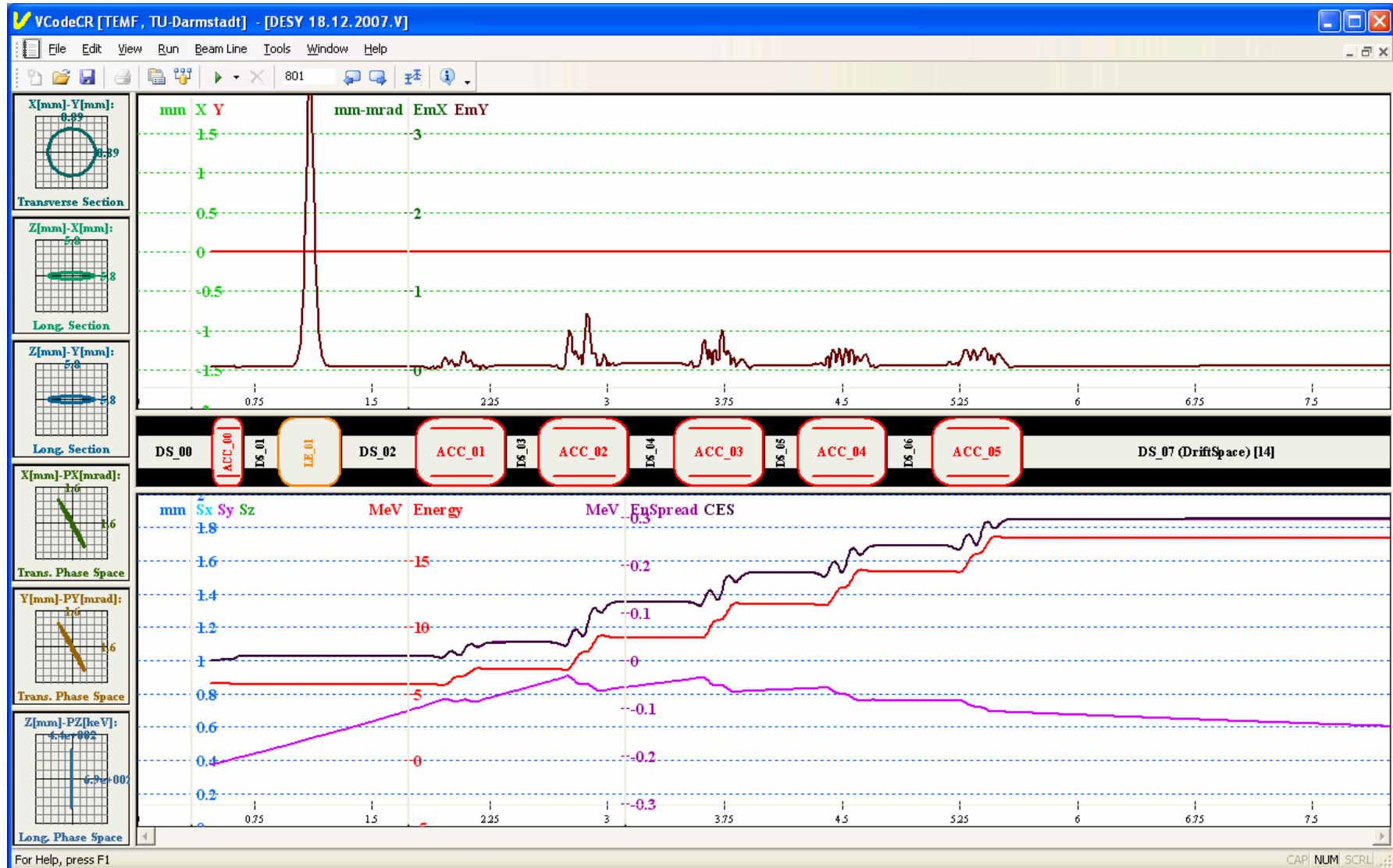
$$R(t) = \begin{pmatrix} M_x \\ M_y \\ M_z \\ M_{px} \\ M_{py} \\ M_{pz} \\ M_{xx} \\ M_{xy} \\ \vdots \end{pmatrix} = \begin{pmatrix} 1 \\ 2 \\ 3 \\ 4 \\ \vdots \end{pmatrix}$$

- Initial condition and time stepping technique





• V-Code user interface



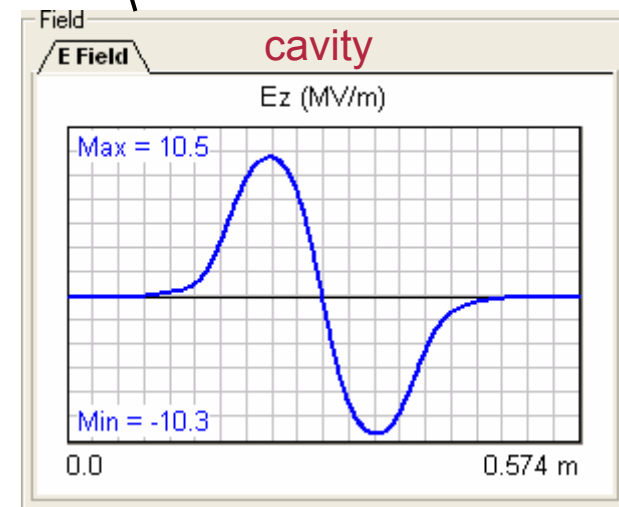
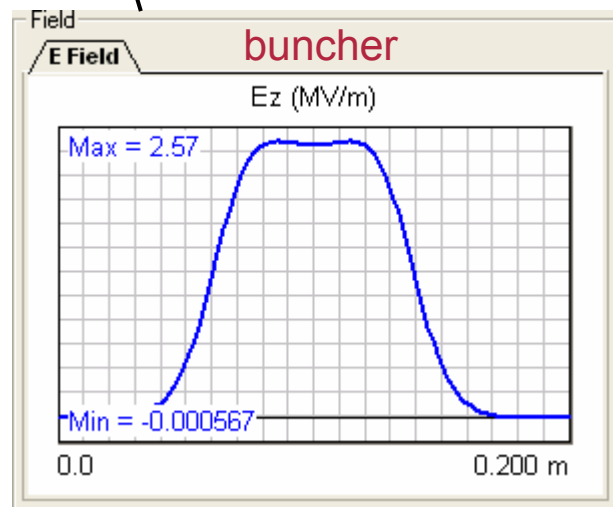
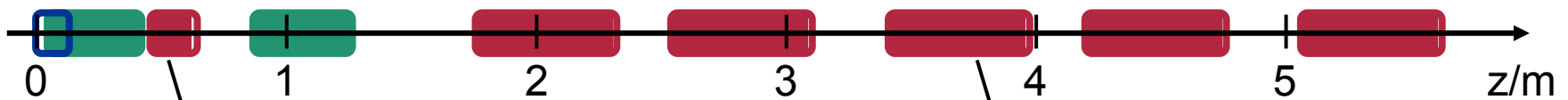
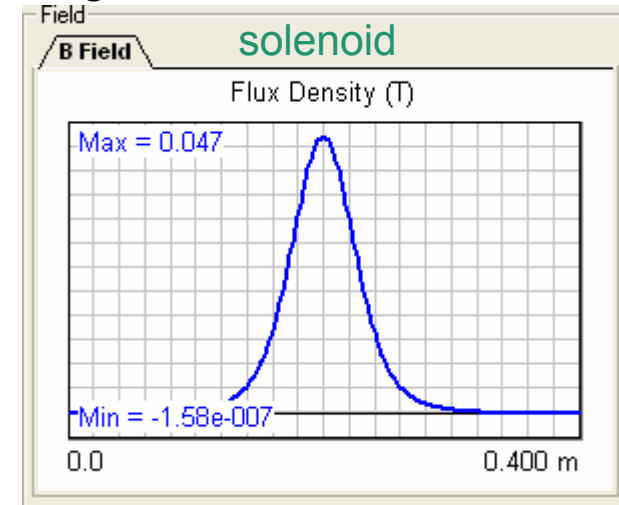
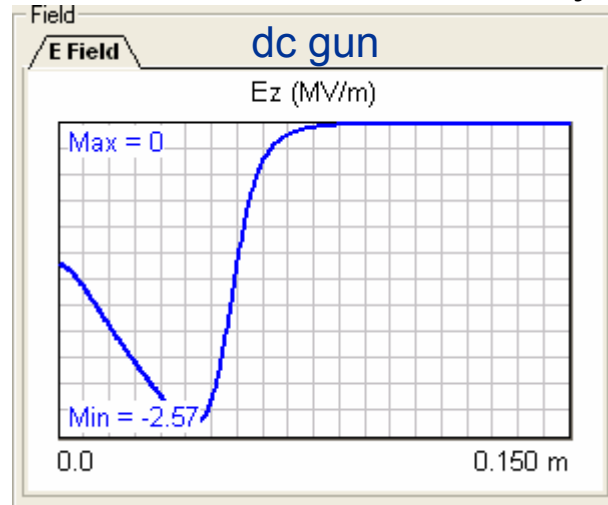


Courtesy: Georg Hofstaetter, Cornell University

- Layout

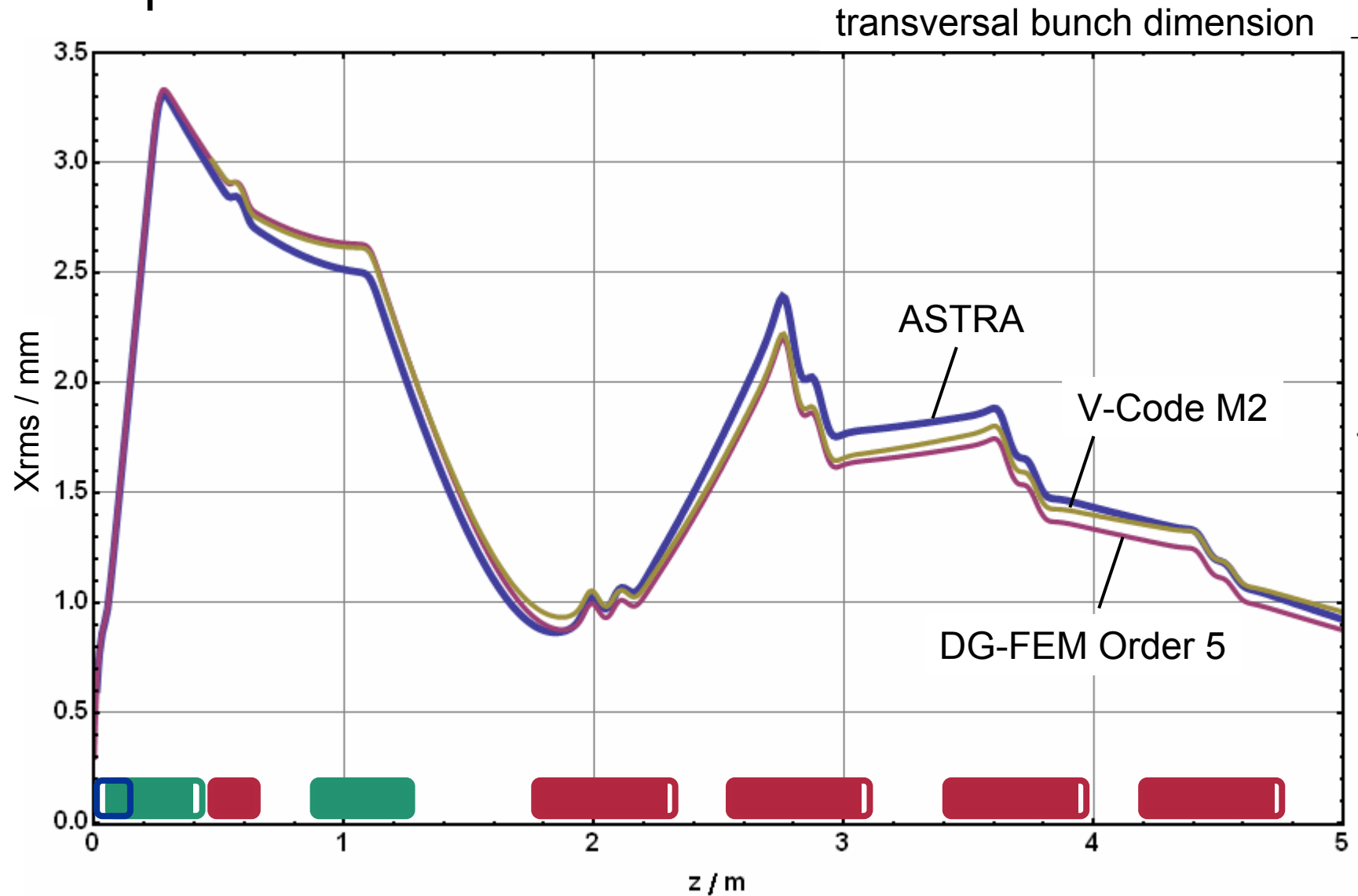
Bunch:

$T_{rms} = 11.146$ ps
 $XY_{rms} = 0.294907$ mm
 $Q_{bunch} = 0.107743$ nC





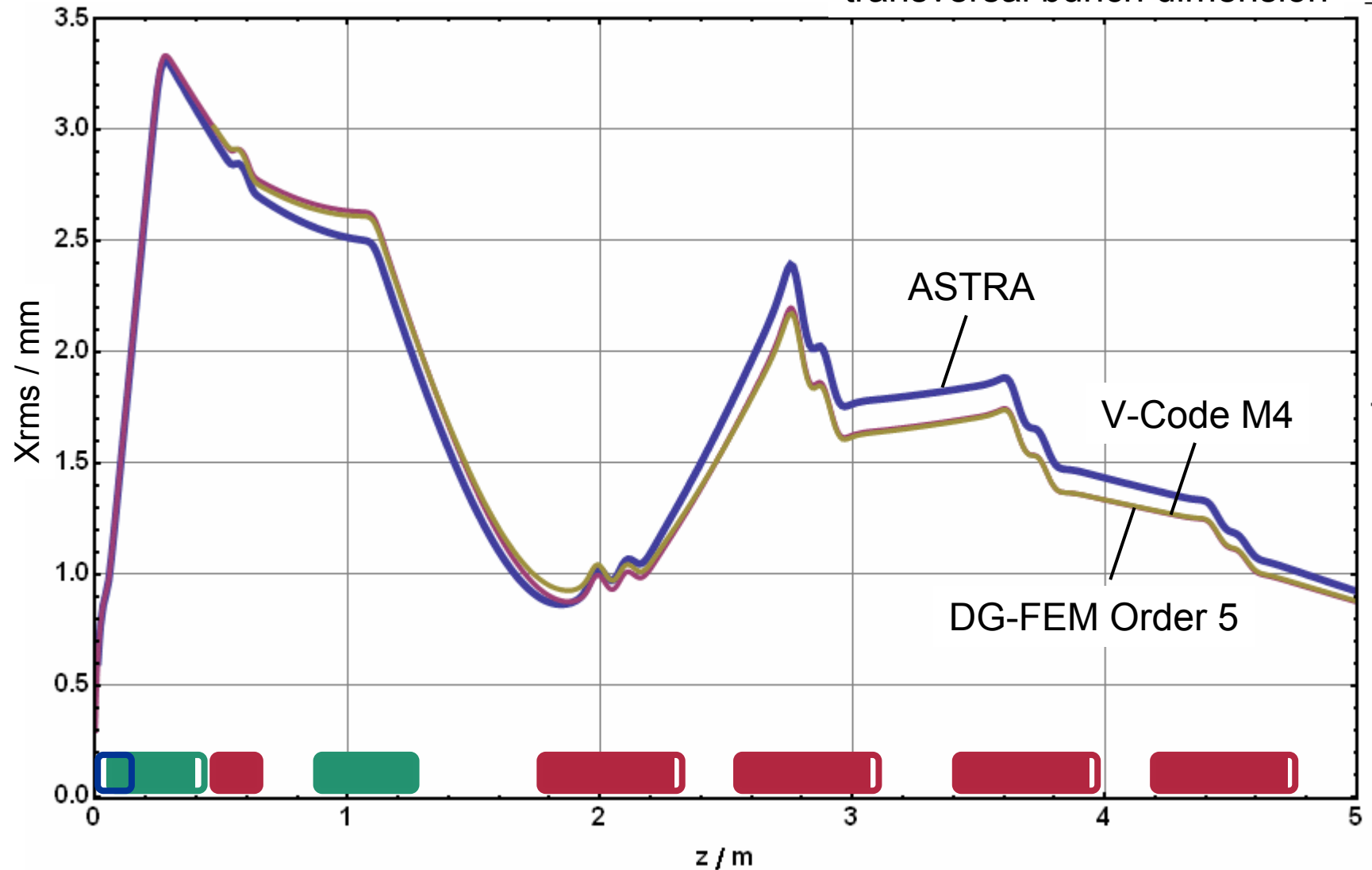
- Comparison





- Comparison

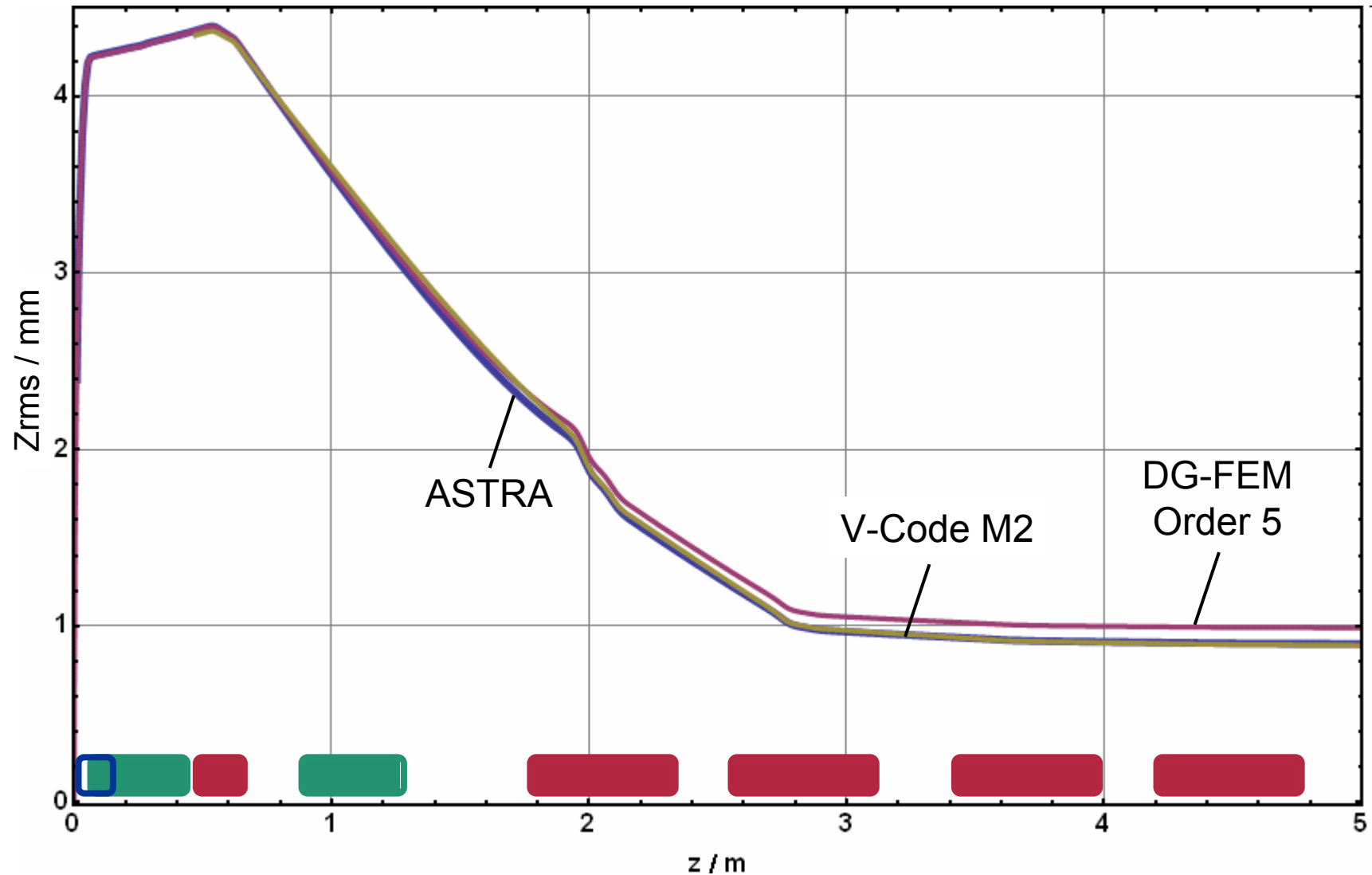
transversal bunch dimension





- Comparison

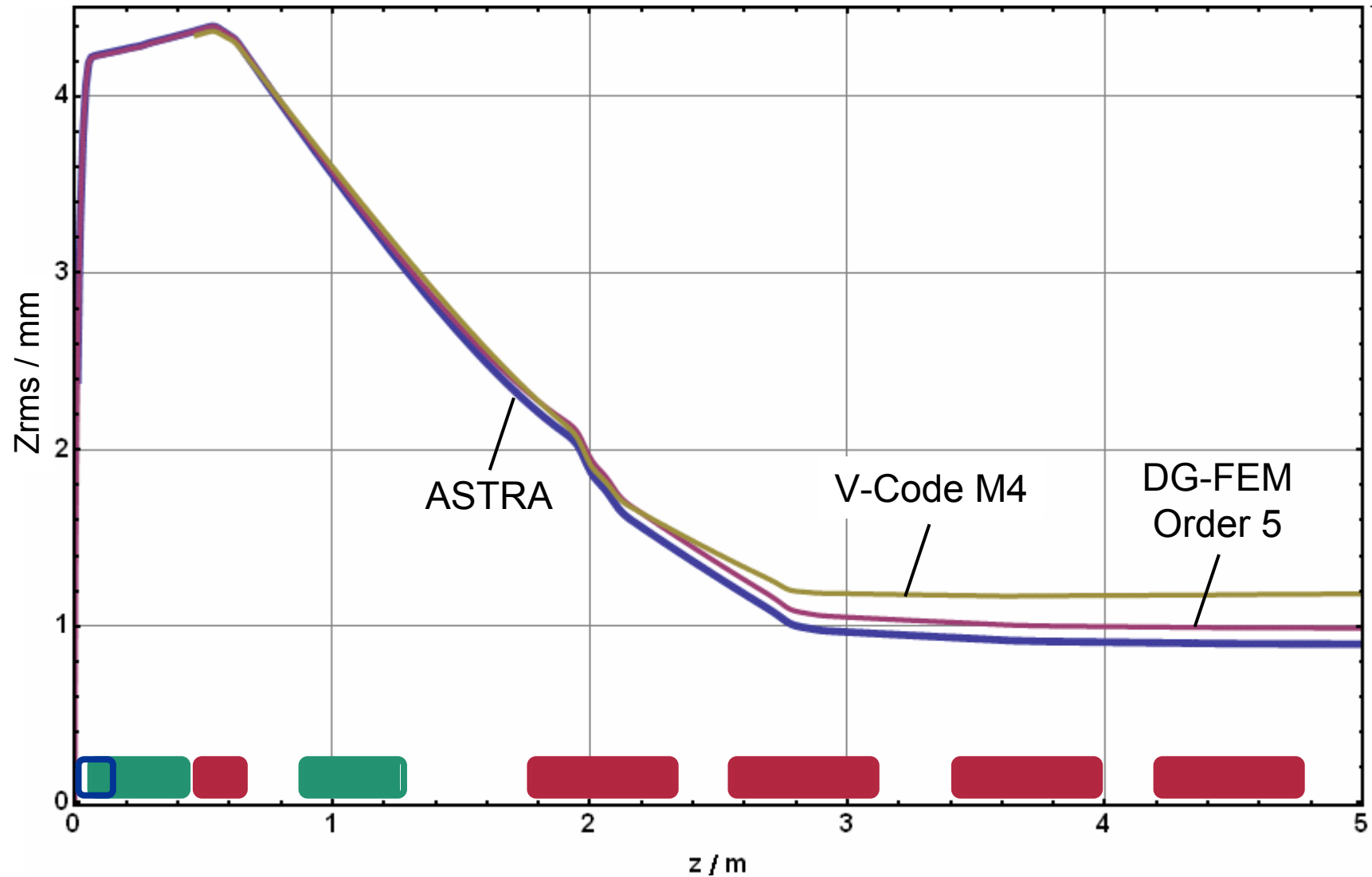
longitudinal bunch dimension





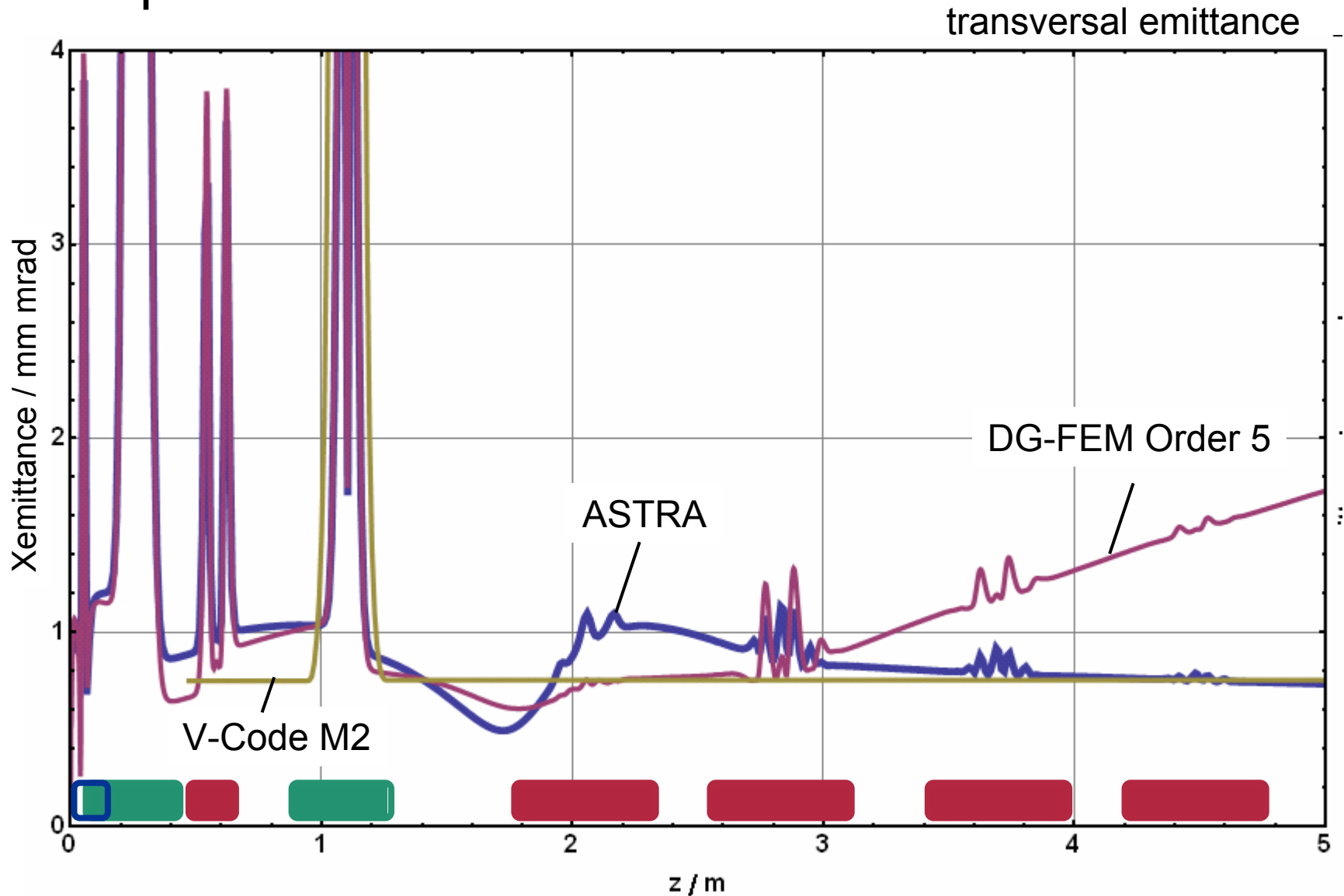
- Comparison

Longitudinal bunch dimension





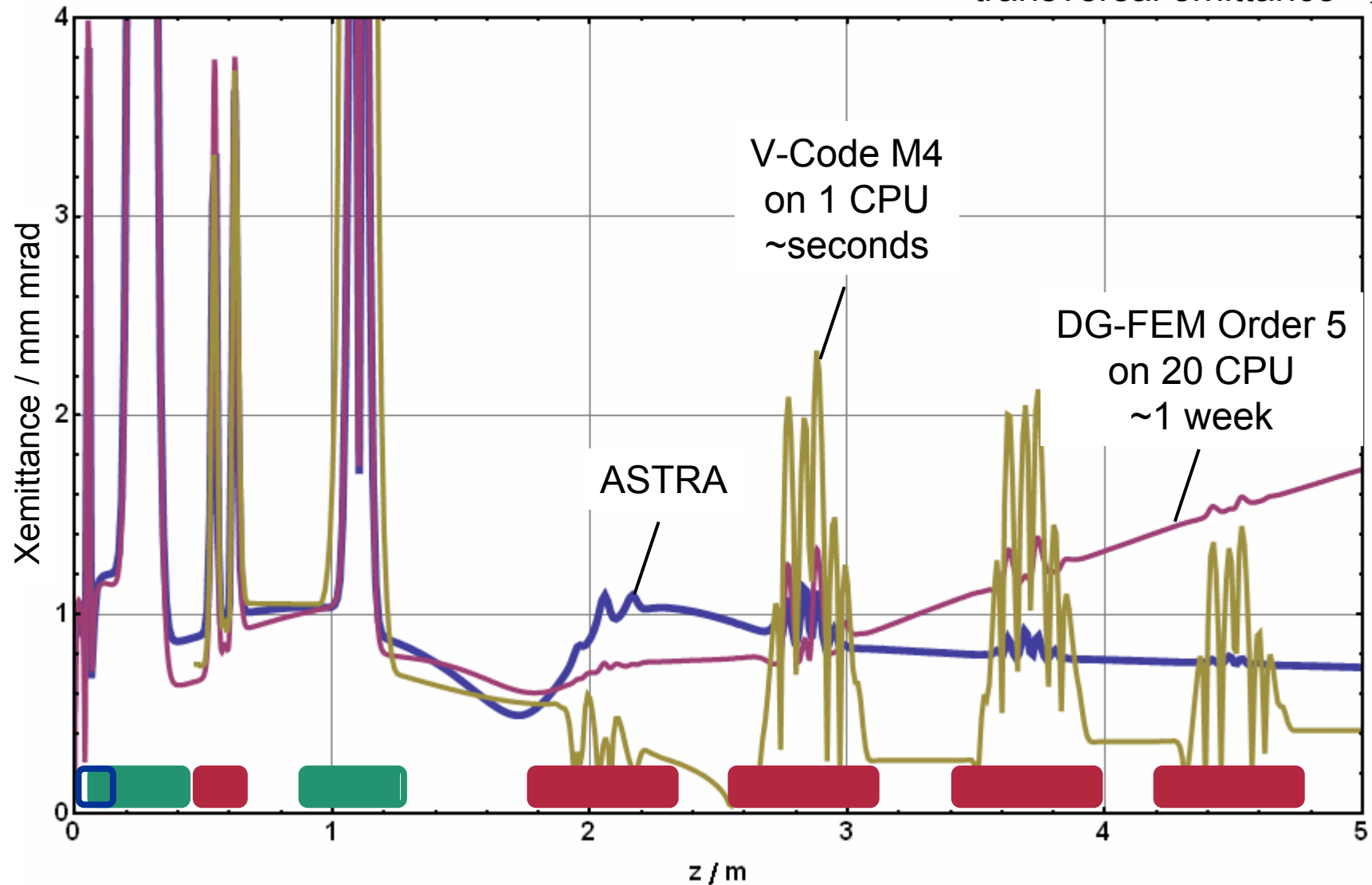
- Comparison





- Comparison

transversal emittance





- Current Work related to V-Code
 - Implementation of multi-ensemble formulation
 - Incorporation of VCode into the control system at the S-DALINAC to assist operation
 - Extension of the BLE library to enable alpha-magnet simulation for the new S-DALINAC injector
- Outlook
 - Improved and consistent space charge model for single and multi-ensemble formulation
 - Automatic ensemble decomposition

